STUDIES ON HEMIN AND COBALT CORRINOIDS IN AQUEOUS SOLUTION

Vivien Mary Campbell

A Thesis submitted to the Faculty of Science,
University of the Witwatersrand, Johannesburg
for the Degree of Doctor of Philosophy

December 1980

Declaration

I hereby declare that the work reported in this thesis was carried out exclusively by myself and that this thesis has not been submitted for a degree at any other university.

V. Campbell.

Vivien Mary Campbell

18th day of December 1980

ACKNOWLEDGMENTS

I would like to sincerely thank the following people for their assistance:

Professor J.M. Pratt, my supervisor, for his guidance and enthusiasm;

Dr D.A. Baldwin for his advice and encouragement;

Professor R. Hasty for his assistance with the simplex optimization;

Mr A.P. Domleo of Glaxo-Allenbury's (S.A.) (Pty) Limited for samples of vitamin B_{12a};

The technical staff in the Department of Chemistry for their helpfulness and cooperation;

Mr E. Batterton for proofreading this thesis;

Mrs I. Warner for typing this thesis;

My colleagues for their advice, friendship and tolerance of thiols.

To my mother and father

ABSTRACT

Reactions of hemin and cobalt corrinoids have been studied in aqueous solution. The equilibria of hemin in aqueous alkaline solution, in the absence of added ligands, showed five distinct types of complexes (monomers, dimers and polymers) whose spectra fell into two types. These equilibria were independent of pH but dependent on the hemin concentration and ionic strength. The dimerization constant (μ = 0,1) was found to be $\geq 10^9\ M^{-1}$. The formation of the monomeric hemin-caffeine adduct was confirmed and the complex shown to contain one OH^- ligand. Some detergents were found to form adducts with the dimer, well below the critical micellar concentration ($K \sim 10^5\ M^{-1}$ per mole detergent bound).

Unstable monomeric and dimeric forms of the aquo complex of hemin in aqueous acid were formed by rapid dilution from pH 8 and the equilibrium between them studied (the dimerization constant was $1,1 \times 10^5\ M^{-1}$). Comparison of the spectrum of the monomer with that of hemin in acidic aqueous ethanol, indicates that it is probably a six-coordinate high spin bis-aquo complex (λmax 397 nm; ε = 120 ± 3 $mM^{-1}\ cm^{-1}$). Since the same spectrum was also observed in very dilute solutions of low ionic strength at ~ pH 7 the pKa for the coordinated water is ≥ 8.

The equilibria between hemin and imidazole analogues included adduct formation and aggregation, in addition to that leading to the formation of the bis-ligand complex, but no significant concentration of any monomeric monoligand complex was observed. Quantitative studies with histidine, histamine and pilocarpate, showed the initial formation of an adduct with the dimer, with one

base bound per dimer. At higher concentrations of ligand, the monomeric bis-ligand complexes were obtained. The variation with pH of the overall equilibria from the alkaline hemin dimer indicated that on coordination, the pKa of the pendant -OH of pilocarpate is reduced from 15 to 10 (with a corresponding change, though slight, in the spectrum above and below pH 10) and that of the pendant $-NH_2$ of histidine and histamine from ~9,5 to < 8, which was ascribed to relative stabilization of the conjugate base by the residual positive charge on the iron.

The reduction of both B_{12a} and bis-histidine hemin by dithiothreitol occurred via an inner sphere electron transfer. The marked difference in rates between the dithiol, dithiothreitol and the monothiols, mercaptoethanol and cysteine where reduction rather than coordination was rate limiting, together with the requirement of a second thiol for the reduction of B_{12a} by cysteine, was ascribed to a one electron reduction of the metal, assisted by the second thiol to give the disulphide radical anion or its conjugate acid.

In the oxidation of thiols by O_2 catalysed by cobalt corrinoids and bis-histidine hemin it was shown that reduction of the metal was rate determining, the rate of O_2 uptake was faster than the rate of reduction of B_{12a} and bis-histidine hemin by the thiol under N_2, and that the disulphide radical anion is a likely reducing agent in the presence of O_2 (where additional paths for its formation are present). The cobalt corrinoids were found to model the suppression of H_2O_2 formation as well as the high turnover number characteristic of cytochrome c oxidase.

The kinetics of the bis-histidine hemin catalysed reactions were complex.

The relevance of these results to the hemoproteins were discussed.

TABLE OF CONTENTS

LIST OF TABLES

LIST OF FIGURES

CHAPTER 1 - INTRODUCTION

Hemin (figure 1.1) is the main, but not only, prosthetic group in hemoproteins[1-3] and hence, in order to understand the role of the protein in modulating the reactions of the iron porphyrin, the reactions of the protein-free species must be understood.

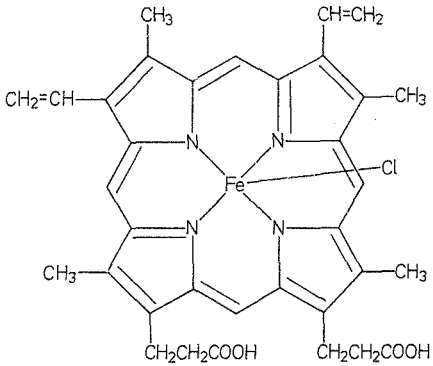

Figure 1.1 Hemin chloride (Fe(III)) protophoryrin IX chloride

The hemoproteins are involved in a variety of reactions[1-3]. Myoglobin and hemoglobin reversibly bind O_2 to store or transport it. The cytochromes transfer electrons. The terminal oxidases

such as cytochrome c oxidase reduce O_2 to H_2O. The mono-oxygenases, such as cytochrome P-450, hydroxylate hydrocarbons (to aid their excretion) by activating O_2. The dioxgenases also do this but add two oxygen atoms. Peroxidase and catalase reduce and disproportionate H_2O_2 respectively. Such diversity and specificity of the reactions carried out by hemoproteins, emphasizes the important role of the protein in controlling and modifying the reactions.

Axial ligands to the iron in hemoproteins so far established include: two histidines (cytochrome b_5)[4], one histidine and one methionine (cytochrome c)[5], one histidine and one vacant site (or occupied by H_2O/OH^-) (hemoglobin, myoglobin,[6] cytochrome c peroxidase)[7]. *It is also generally agreed that cytochrome P-450* has one cysteine coordinated and probably one H_2O (or a vacant site).[8]

Although a particular hemoprotein may contain more than one iron porphyrin (e.g. four in hemoglobin, catalase) there is no evidence that they are ever present except as discrete monomeric complexes.

Although the porphyrin ring is apparently always held in a hydrophobic cleft in the protein[4-7], at least the "vacant" coordination site (i.e. unoccupied by a protein amino acid residue) is accessible to solvent and to hydrophilic reagents, i.e. at least the iron functions in a protic environment while the protein as a whole is found in an aqueous environment (unless membrane bound).

Hence the mechanism of action of the hemin and the role of the protein, can only be understood with reference to the coordination chemistry of monomeric hemin complexes with ligands such as

H_2O, OH^-, histidine, cysteine and methionine in an aqueous or protic environment.

Yet in spite of the importance of hemin as a co-factor, relatively little is known about its simple coordination chemistry in aqueous solution, in contrast to the extensive study of the coordination chemistry of vitamin B_{12}.[9]

Most studies with hemin have been done in non-aqueous solvents, as have many studies on the synthetic iron porphyrins such as iron, α, β, γ, δ-tetraphenyl porphin (FeTPP), to avoid the problems of aggregation which occur in aqueous solution.

The major problems in studying hemin in aqueous solution are:

1) Hemin will only dissolve in aqueous solution at high pH.

2) At pH > 8, it exists mainly as a dimer corresponding to $(FeOH)_2$[10]. However, a monomeric adduct with caffeine has been reported[12] but the axial ligand(s) not identified, and monomeric hemin in detergent micelles have been reported.[13-15]

3) Hemin forms aggregates and precipitates on reducing the pH below 8[10]. The net result of this is that the coordination chemistry of hemin is limited to pHs above 8. At high pH, OH^- competes with added ligands for the coordination site and the dimeric hydroxo complex is the product.[10] For the ligands studied, this limited the study to pH ≤ 11.

4) Hemin readily forms adducts through hydrogen bonding, hydrophobic interactions or charge transfer interactions, so that observed changes in the spectrum on adding a potential ligand do not automatically denote coordination of that

reagent. A classic case of this is pyridine. [16]

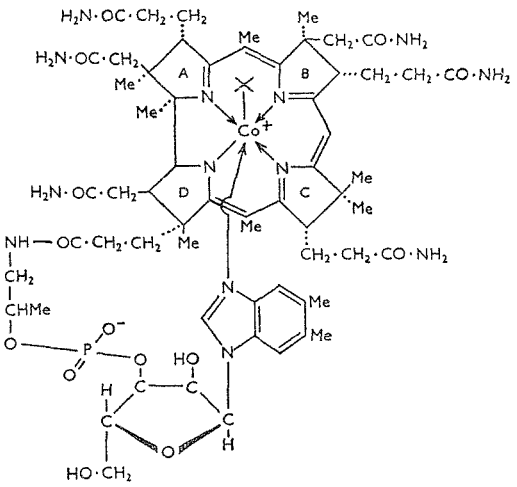

Figure 1,2 Cobalamins: X = H_2O aquocobalamin (B_{12a});
X = OH^- hydroxocobalamin; X = RS^- thiolatocobalamin;
X = CN^- cyanocobalamin (vitamin B_{12}).

5) The vinyl side chains are fairly readily oxidised [17] which results in changes in the aggregation properties and hence in non-reproducibility of results. This could be overcome by using fresh solutions or by the storing of the solution at ~18°C under N_2 (see chapter 2).

1.2 Aims

The broad aim of this thesis is to increase our knowledge of the coordination chemistry of monomeric hemin complexes in aqueous solution with particular emphasis on the complexes containing the ligands H_2O, HO^-; imidazole, histidine and analogues; cysteine and other thiols. The structures, equilibria, redox and catalytic reactions will be investigated with the aim of providing possible answers to the questions concerning the role of the protein in controlling and modifying the equilibria and kinetic (especially redox) properties of these hemin complexes.

Our approach to overcoming some of the above problems are based on three strategies:

1) to establish the nature of the monomeric caffeine adduct, and then to use this as a "stock" monomer in aqueous solution.

2) to investigate the region below pH 8 by stopped flow spectrophotometry.

3) to use B_{12a} as a model for the mono-histidine complexes present in some hemoproteins [9].

The existence of some interesting parallels between the iron and cobalt complexes is emphasized by the formation of a functionally active O_2-carrying "coboglobin" by substituting the Fe(II) porphyrin by the Co(II) analogue in hemoglobin, which retains

the cooperative interaction between the four polypeptide [18] subunits. It is known that the Co(II) derivative of B_{12a} reversibly binds O_2 at low temperatures. The use of B_{12a} and other cobalt corrinoids [19] allows the reactions to be studied in an aqueous environment from pH < 0 to pH > 13, [9] and may provide useful pointers to reactions which are experimentally difficult or impossible to study with the protein-free hemin complexes.

The more specific aims are thus to build up our knowledge of the coordination chemistry of hemin (and to a lesser extent the cobalt corrinoids) in aqueous solution by studies in the following four areas which form a progression from equilibria through redox reactions to catalytic activity:

1) the structures and equilibria shown by hemin in the absence of added ligands, with particular emphasis on identifying monomeric complexes with H_2O and OH^- as the only axial ligands (chapters 3 and 4).
2) the structures and equilibria shown by hemin with imidazole, histidine and analogues (chapter 5).
3) the reduction of B_{12a} (chapter 6) and monomeric hemin complexes (chapter 7) by thiols.
4) the catalytic activity of B_{12a} and other corrinoids (chapter 8) and of the bis-histidine hemin complex (chapter 9) in the reduction of O_2 by thiols.

All studies have been done in aqueous solution and most have been done on the Fe(III) complexes. The main techniques used were UV-visible spectrophotometry (ordinary and stopped flow) and kinetic measurements on a Clark type oxygen electrode.

The results will be summarised in chapter 10 and their relevance to the equilibria and reactions of hemoproteins discussed.

1.3 Nomenclature

Hemin consists of iron(III) coordinated to the porphyrin protoporphyrin IX.[20] The proto-prefix indicates that the side chains in the 2,4 positions are vinyl groups (other so-called natural porphyrins have other groups in these positions), while IX indicates the particular structural isomer. Figure 1.1 shows the structure of hemin or iron(III) protoporphyrin IX.

If the oxidation state of the iron is not specified, iron(III) is implied. Heme will be used to denote the Fe(II) protoporphyrin IX.

Ligands can only coordinate in the axial positions and the iron porphyrin can be five or six coordinate. The name reflects the number and nature of the ligands but not the position as the two are not distinguishable, e.g bis-imidazole iron(III) protoporphyrin IX. However, if the solvent provides the ligand, the ligand is often not included in the name.

Certain cobalt corrinoids are used in this study. The major one used is B_{12a} or aquocyanocobalamin (figure 1.2). Also used is diaquocobinamide. Cobinamides differ from the cobalamins in that the benzimidazole base has been removed by hydrolysis of the phosphate linkage.[9]

1.4 Literature Survey

1.4.1 Spin state and coordination numbers

Iron(III) has five d electrons which can either give a high spin complex in which case all five are unpaired or a low spin complex

in which case only one is unpaired. [1] Many iron(III) complexes are high spin except those coordinated to strong field ligands such as CN^-. [21] However, the coordination of porphyrin to iron(III), enables both high and low spin complexes to be formed [1,2] depending on the axial ligands. Ligands such as pyridine, imidazole and of course cyanide, give low spin complexes while weaker field ligands such as OH^-, Cl^- give high spin complexes. [1]

Until recently it was believed that all the high spin complexes were five coordinate with the iron out of the ring plane while the low spin complexes were six coordinate with the iron in the ring plane. [2] However, a crystal structure of a six coordinate high spin complex in which iron is in the ring plane has been reported, [22] where the ligands are weak field ones such as H_2O, dimethylsulphoxide (DMSO) and DMF. This was also shown to be the case by NMR. [23] Hence although the low spin complexes are six coordinate, the high spin ones can be five or six coordinate.

The cobalt corrinoids have six d electrons in Co(III) and five in Co(II). Both oxidation states are low spin. [9] The Co(III) corrinoids are generally six coordinate while the Co(II) ones are generally five coordinate. [9]

1.4.2 Aqueous solution chemistry of iron porphyrins

As mentioned previously, aggregation is a major problem in studying the aqueous solution chemistry of hemin.

Before discussing the factors affecting the aggregation of hemin in aqueous solution, the forces holding the iron porphyrins in dimers in aggregates will be briefly discussed.

The interactions responsible can be broken into two groups: [24]

a) coordination to the iron

b) interactions between the rings to give ring-ring dimers.

Two types of dimers held together by coordination to the iron have been proposed. It was suggested that one propionate side chain of one hemin may coordinate to the iron of another [25] but no evidence supporting this has been found. [24]

The other coordination dimer, the μ-oxo dimer in which O^{2-} bridges two high spin Fe(III) porphyrins, resulting in antiferromagnetic coupling has been well established, [24,26] but UV-visible, [26] Moessbauer [27], IR [26] and EPR [26] spectra as well as the magnetic susceptibility [28] indicate that hemin in aqueous alkaline solutions where it is dimeric, does not have a μ-oxo linkage.

The ring-ring dimers may be hydrophobically bonded [29] or may form Π-Π donor-acceptor complexes [29,30] and both may be present simultaneously.

Hydrophobic bonding has been found with both the 2,4 disubstituted deuterohemins [31] and the 2,4-disubstituted deuteroporphyrins in aqueous solution. [32] Evidence for Π-Π donor-acceptor interactions between the rings of the 2,4 disubstituted deuterohemins has been found at low temperatures in non-aqueous solvents by NMR. [33]

Various factors are known to affect the aggregation of hemin in aqueous solution. Decreasing the pH to less than 8, results in aggregation. [10,24] High concentrations of electrolytes are known to favour aggregation. [34-36] In a 1.2M NaCl alkaline solution, the aggregates apparently contain an average of forty-eight hemin units. [36] Adding electrolytes decreased the Soret intensity [34] (by lifting degeneracies or possibly because of optical

heterogeneity) [37] and the magnetic susceptibility [35] (ascribed to the formation of μ-oxo linkages).

Micellar detergents have been shown to dissociate the dimers of natural iron porphyrins [13-15], but not the synthetic ones [28] (which have μ-oxo linkages).

The donor, caffeine, has been shown to split the dimer [12] and other donors and acceptors have been shown to interact with porphyrins [37-39] and iron porphyrins [39-41].

1.4.3 Imidazole complexes (and analogues) of hemin

Histidine residues, which coordinate through the imidazole ring, are found coordinated to hemin in several hemoproteins (see earlier).

Equilibrium studies have been carried out in non-aqueous solvents [42,43] as well as in aqueous, mixed aqueous and detergent solutions, mainly using UV-visible spectrophotometry, but NMR has also been used. [43] Except at low ligand concentrations [42] and with sterically hindered imidazoles, [42] where coordination has not been established, the bis-imidazole complex was obtained with no sign of the mono-imidazole complex [42-49], i.e. the binding constant for the first imidazole (K_1) is less than that for the second (K_2), because of a spin change on binding the second. X-ray studies [50] provide further evidence in addition to the EPR [51] and UV-visible [42,44-49] spectra for the bis-imidazole product. Tailed porphyrins, i.e. those in which imidazole is covalently linked to the porphyrin ring via an organic chain of a suitable length to permit coordination of the imidazole, have been synthesized [52] to overcome this problem, but in most cases there is no clear-cut evidence for the imidazole being coordinated to

Fe(III) in the absence of other ligands.

Hydrogen bonding is important in these complexes both in solution [53,54] and in the solid [50,55] state and evidence for a π complex between imidazole and the porphyrin has been presented. [56]

1.4.4 Reduction of hemin and cobalt corrinoids by thiols

Reduction of Fe(III) to Fe(II) occurs in the reaction pathway of many hemoproteins, in particular the cytochromes and hence an understanding of the reduction of hemin is necessary to understand these hemoproteins.

Reduction studies have been carried out with various reducing agents with iron porphyrins [57], but little work has been done with thiols. [58] Thiols have been studied with hemin but largely in trying to model the spectra of cytochrome P450 [59-61] and in studying the hydroxylation of aniline [62,63]. The kinetics of the reduction of FeTPPCl in toluene solution in the presence of pyridine by alkyl thiols has been studied [58] and two paramagnetic intermediates were found.

A kinetic study of the reaction between B_{12a} and cysteine in aqueous solution has been reported [64], but was largely concerned with coordination. However, it was reported that the reduction step required a second thiol group and that Co(II) cobalamin was the product.

In the literature are reports of pKas of thiols and intermediates found on oxidising them.

Thiols may lose a proton with a pKa of ~9 to give the thiolate, i.e.

$$RSH \rightleftharpoons RS^- + H^+$$

Table 1.1 lists the pKas of the thiols used.

Table 1.1 : pKas of the thiols used in this study

Thiols	pKa	Reference	Structure
ethanethiol	10,6	65	CH_3CH_2SH
cysteine	8,54 ($-NH_3^+$ 8,86)	65	$NH_3^+(COOH)CHCH_2SH$
mercaptoethanol	9,43	65	$HOCH_2CH_2SH$
penicillamine	8,17 ($-NH_3^+$ 8,61)	65	$NH_3^+(COOH)CHC(SH)(CH_3)_2$
dithiothreitol	9,12 ; 10,15	66	$SHCH_2CH(OH)CH(OH)CH_2SH$

E^o values are important to reduction and oxidation reactions. However, there is a paucity of information of the E^o values of thiols. Thiols in any case tend to undergo one electron transfers to give the thiol radicals, [65] and the E^o value for the reaction:

$$RS^- \longrightarrow RS^{\cdot} + e^-$$

would be of greater relevance.

Evidence has been presented showing that the thiol radicals are actually found as $RS\overset{\cdot}{-}SR$ which has a three electron two centred bond [65,67,68] because the rate of the reaction $RS^{\cdot} + RS^- \longrightarrow RS\overset{\cdot}{-}SR$ is rapid ($k \geqslant 10^9\ M^{-1}\ s^{-1}$) [65]. This is apparently more stable than the simple radical.

With a dithiol such as dithiothreitol, this species can be formed intramolecularly. [68] In dithiothreitol this would result in a six membered ring which would confer additional stability. The radical species also has a pKa. It has been reported as being 5,5 [68] and refers to the reaction (1 - 1)

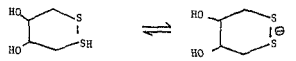

(1 - 1)

These radical species have different second order decay rate constants. For dithiothreitol the neutral radical has a rate constant of $1,7 \times 10^9$ M^{-1} s^{-1} while that for the anionic radical is $1,7 \times 10^8$ M^{-1} s^{-1}. [68] No values have been reported for the other thiols.

1.4.5 Reactions of iron porphyrins and cobalt corrinoids with O_2

Hemoproteins, as mentioned earlier, are involved in a variety of reactions with O_2 and its reactions with the prosthetic group, heme and models is of interest.

Some studies on the oxidation of Fe(II) porphyrins by O_2 have been reported. [69] The reactions are generally first order in O_2 and apparently both inner and outer sphere mechanisms occur.

Similarly, O_2 is known to oxidise cobalt(II) corrinoids. [9] Reducing agents such as quinols and thiols have been shown to accelerate this reaction, by facilating the more favourable two electron reduction of bound O_2. [70]

A few studies have been carried out on the catalysed autoxidations. These include aquocyanocobinamide with various thiols, [71] a Co(II) phthalocyanine with cysteine, [72] and Fe(III) with cysteine. [73]

Molecular oxygen is reduced to water by the transfer of four electrons. Figure 1.3 [74] shows the reduction potentials for O_2 reduction. The four and two electron transfers are thermodynami-

cally favourable but the one electron reduction of O_2 is not. This may no longer be the case when the oxygen species are bound to a metal, [2] but at least for the uncoordinated species, a mechanism which involves two electron transfers would be favoured over one involving one electron transfer.

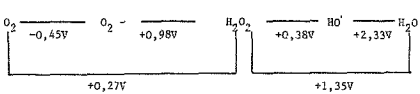

Figure 1.3 The reduction potentials for the one and two electron reductions of O_2 at pH 7. [74]

In addition to the free superoxide, peroxide and hydroxyl radicals, the coordinated species may be present but the competition between the metal complex and H^+ may destabilize some (the pKas of superoxide and peroxide are 4,9 [75] and 11,62 [76] respectively). Iron porphyrin species found in non-aqueous solvents include the μ-peroxo dimer [77] and the $Fe(IV)O^{2-}$ [78] species, the latter being stabilized by the coordination of a base. The cobalt corrinoids may form μ-peroxo dimers [79] but steric hindrance makes it unlikely.[69]

CHAPTER 2 - MATERIALS AND METHODS

2.1 Materials

Protohemin was supplied by BDH; mesohemin was prepared by a literature method[20]; cytochrome b_5, prepared by a literature method [80], was kindly supplied by Dr D. Baldwin; B_{12a} was supplied by Mr A.P. Domleo of Glaxo-Allenbury (Pty) Limited; diaquocobinamide was kindly supplied by Mr E. Betterton.

Water was purified by the Millipore Milliro 40 H_2O system. Other solvents used were 96% ethanol (National Chemical Products), methanol (Merck AR), DMSO (Merck AR) (only from freshly opened bottles), formamide (Merck).

The following AR grade reagents were used: CH_3COOH (Merck), $NaHCO_3$ (Hopkins and Williams), borax (Merck), glycine (Merck), potassium hydrogen phthalate (Merck), HNO_3 (nitric acid), NaH_2PO_4 (Merck), Na_2HPO_4 (Merck), $NaNO_3$ (Merck), KNO_3 (Merck), NaCl (Protea), KCN (BDH), L-arginine (Merck), L-tyrosine (Merck), 1,10 phenanthroline (Merck), methyl viologen (Merck), urea (Merck), sucrose (Merck), $CuSO_4$ (Merck), imidazole (BDH), N-methyl imidazole (Merck), 2-methyl imidazole (Merck), L-histidine, histamine dihydrochloride (BDH), pilocarpinium nitrate (Merck), L-cysteine hydrochloride (BDH), D(-)-penicillamine (Aldrich).

Other reagents used were NaOH (Protea, > 97%), lithium nitrate (Merck), cetyl trimethyl ammonium bromide (BDH), triton X-100 (BDH), sodium lauryl sulphate (BDH), caffeine (Merck), adenine (Merck), theophylline (Merck), guanidine hydrochloride (BDH), sodium silicate (BDH), dithiothreitol (BDH, > 98%), ethanethiol (Merck), 2-mercaptoethanol (Schuchardt; > 95%, redistilled under vacuum just prior to use), sodium dithionite (Hopkins and Williams), superoxide dismutase

from beef erythrocytes (supplied as a powder by Miles Research Laboratories), catalase from bovine liver (supplied by Miles as a crystalline suspension in a phosphate buffer at pH 5,7 containing 565109 units per millilitre (one unit of activity is that amount of enzyme catalysing the decomposition of 1 μ mole of H_2O_2 per minute at 25°C), N_2 was deoxygenated by passing it through a V^{2+} solution. [81]

2.2 Instrumentation

Ultraviolet-visible absorption spectra were recorded on a Jasco Uvidec -1 spectrophotometer, which was calibrated with holmium glass as a standard. Unless otherwise stated, quartz cells of pathlength 10 mm were used and thermostatted at 25°C (± 0,5°C).

The kinetics of faster reactions and the determination of certain pKas (see later) were studied using a Durrum D-110 stopped flow system connected to a Datalab DL 901 Transient recorder and an Apple microcomputer which was programmed to accept the data points, subtract out the value at infinite time, plot the semilog plot and carry out a least squares fit. If required, the program converted the voltage output into absorbance. The solutions were thermostatted at 25°C (± 0,2). The rate of O_2 uptake was studied using a Clark type oxygen electrode made by Rank Bros, Cambridge, England (Figure 2.1) connected to a Servogor recorder. The maximum recorder deflection was set manually using O_2 saturated or air saturated water (where applicable) as standards. The zero setting was set using water depleted of O_2 by the addition of sodium dithionite. Sodium dithionite was also used to check the membrane; a good membrane shows depletion of most of the O_2 (i.e.> 90%) in

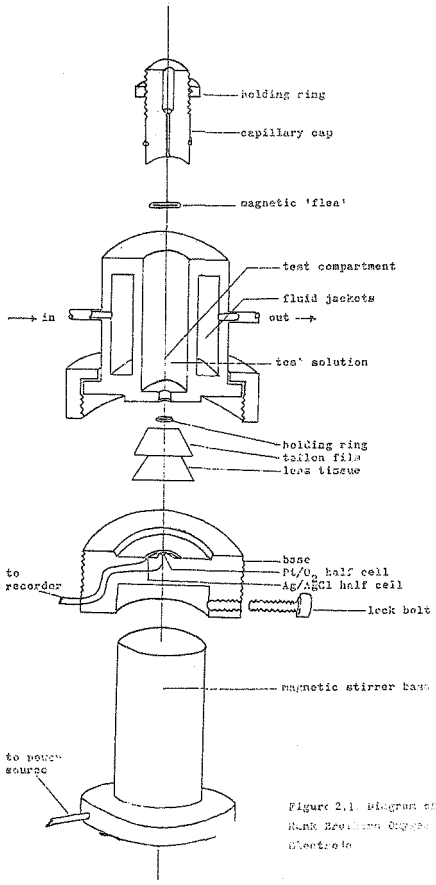

Figure 2.1 Diagram of Rank Brothers Oxygen Electrode

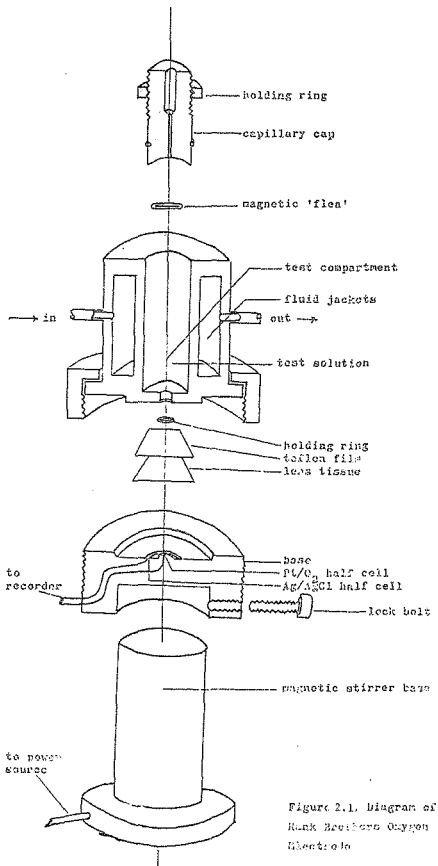

Figure 2.1. Diagram of Rank Brothers Oxygen Electrode

solution within ten seconds after adding dithionite, while a leaky one does not and was discarded. The O_2 content in air and O_2 saturated water was determined by titrating the O_2 with glucose in the presence of the enzyme glucose oxidase, using the oxygen electrode. The O_2 saturated solution (obtained by passing pure O_2 through the solution for at least ten minutes) was found to have $8,7 \times 10^{-4}$M O_2 while the air saturated solution was found to have $2,2 \times 10^{-4}$M O_2.

The oxygen electrode consists of three sections (see figure 2.1), the test solution compartment (and capillary cap), the base section containing the Pt/O_2 and Ag/AgCl half cells connected by a saturated KCl solution and the stirrer base. The dissolved O_2 in the test solution diffuses through the teflon film (500 microns thick) onto the polarised Pt electrode where it becomes reduced (equations (2.1);(2,2)) consuming four Faradays per mole of O_2.

$$O_2 + 2e^- + 2H^+ \longrightarrow H_2O_2 \qquad (2.1)$$

$$H_2O_2 + 2e^- + 2H^+ \longrightarrow 2H_2O \qquad (2.2)$$

The current produced causes the recorder to deflect and is proportional to the oxygen concentration in the solution (as is the deflection).

The test compartment was sealed from the atmosphere by the capillary cap which, however, allows injection of samples into the system. It was surrounded by a water jacket through which water at 25°C was pumped. The solution was kept well mixed by a small magnetic stirrer.

In all cases, the reaction was initiated by injecting the thiol solution, through the capillary opening in the cap. In some cases the cobalt corrinoid or iron porphyrin was added before the thiol, while in others it was added after (this enabled the uncatalysed

rate to be determined). Care was taken to exclude all air bubbles from the test compartment when the cap was inserted as these cause erratic results and to ensure that the capillary tube was filled with solution to avoid O_2 from the atmosphere entering. The stirring speed was made sufficient to avoid problems with rate limiting mass transport. If injection of reagents was done too rapidly or too near the base, a sudden decrease in the readout occurred due to a rapid depletion of O_2 at the base of the cell and this caused problems in measuring the initial slope. Hence care was taken in injection of the reagents.

The pH of solutions was measured with a Metrohm digital E 532 pH meter and a Metrohm glass electrode or for recording of small samples, a Metrohm glass microelectrode. The reference electrolyte was 3M potassium chloride. The pH meter was standardised using BDH standard buffers at pH 7,0 ± 0,1 (phosphate) and pH 4,0 ± 0,1 (phthalate).

2.3 Methods

2.3.1 Preparation of solutions

Hemin in solution is slowly attacked by air[17]. To minimise this, hemin was dissolved in a 0,1M sodium hydroxide solution which had been thoroughly flushed with N_2 and the solution kept under N_2. It was found that hemin stored under N_2 and kept at ~18°C was stable (i.e. < 3% change in absorbance) for at least two weeks. The hemin solutions were calibrated by measuring the absorbance at 385 nm in 0,1M NaOH (the position of the Soret band of the dimeric alkaline hemin) and using the extinction coefficient of 58 mM^{-1} Fe.

Buffers were prepared according to the instructions in "Biochemist's Handbook".[82] In all cases, the ionic strength con-

tribution from the buffer was 0,1. In general HNO_3 + $NaNO_3$ was used for pHs 1 - 2; glycine + HNO_3 for pHs 2,2 - 3,4; acetic acid + NaOH for pHs 3,6 - 5,8; NaH_2PO_4 + NaOH for pHs 6,0 - 7,8 and $NaHCO_3$ + NaOH for pHs 8,0 - 11,0; Na_2HPO_4 + NaOH for pHs 11,0-12,0; NaOH for pHs ≥ 12,0. Phthalate buffers gave unreliable results when used in the determination of the pKas of hemin as they decreased the Soret intensity, perhaps due to aggregation or donor-acceptor complex formation; hence they were avoided.

Caffeine is hydrolysed in basic solution.[83] By following the decrease in the band at 273 nm, the rate of decomposition could be followed. At pH 13, 8% of the caffeine had decomposed after two hours while at pH ≤ 12,3, less than 1% decomposition had occurred after three hours. Hence to avoid problems with hydrolysis, only freshly made up solutions with pH ≤ 12,3 were used and used within three hours.

Fairly high concentrations of histidine, histamine and pilocarpate were necessary for complete formation of the bis ligand hemin complex. As these species are charged, they contribute to the ionic strength (it was assumed, however, that the zwitterion does not), and for this reason these solutions had fairly high ionic strengths. For consistency, they were all made 0,5 by adding $NaNO_3$ where necessary.

Histidine goes yellow with age, presumably undergoing a photo-oxidation reaction.[84] To minimise this, solutions were used within two hours when the yellow colour was negligible or were well-protected from light. This yellow species did not affect the equilibrium constant determinations but resulted in scattered reduction and O_2 uptake kinetic results.

The lactone ring of pilocarpine can be hydrolysed within a few minutes in 0,1M NaOH.[85] The solutions of pilocarpate were therefore made up by dissolving pilocarpine in 0,1M NaOH and leaving to stand for at least an hour before the pH was adjusted to the required value.

As thiols are air-sensitive, they were made up in solutions which had been deaerated by thorough flushing with N_2 and were kept under N_2.

2.3.2 Determination of equilibrium constants

With the exception of the determination of pKas of hemin, equilibrium constants were determined by following the change in absorbance with a change in ligand concentration or with a change in the hemin concentration (Shack and Clark dilution studies).[10]

When a sufficiently concentrated stock solution of ligand could be made up, the concentration of ligand was increased by adding aliquots of the stock solution, as in titrations with caffeine, detergent and pilocarpate. This method could not be used, however, if side reactions occurred (as with histamine) or if the ligand had limited solubility (as with histidine); in these cases, each ligand solution required was made up separately.

In most cases the hemin concentration was varied by adding aliquots of the stock hemin solution to the ligand solution, taking care not to change the total volume and hence the ligand concentration by more than 3%. With histamine this was not possible, and each hemin solution required was made up separately.

The results were analysed using the equations derived in appendix 1.

The titration at low ligand concentrations (where the ligands

were histidine, histamine and pilocarpate) were carried out at 590 nm (the position of an isosbestic point between the intermediate and bis-ligand complex) by adding aliquots of the stock ligand solution (in this case the intermediate hemin-histamine complex is stable). Fairly high hemin concentrations ($\sim 1 \times 10^{-4}$M) were used to give sufficiently large absorbance changes.

2.3.3 Determination of the pKas of hemin and hemin-caffeine by stopped-flow UV-visible spectrophotometry

Hemin and the hemin-caffeine adduct aggregate rapidly on acidification and stopped flow UV-visible spectrophotometry was used to determine the absorbance at a particular pH after acidification (proton transfers are rapid) but before aggregation.

One barrel of the stopped flow contained approximately 5×10^{-6}M hemin (plus caffeine where relevant) (unbuffered, pH was ~9) while the other contained buffer such that when it was diluted twofold, it gave the required pH and ionic strength (0.1) (i.e. used double concentrations of the buffer components).

Aggregation was evident by a decrease in the Soret band (all runs were done at or near the Soret maximum) and the absorbance was taken prior to the decrease. Only in slightly acid solutions did the decrease start shortly after the mixing time (1 ms). (At other pHs the decrease, where it occurred, occurred more slowly.)

In the absence of caffeine, hemin tended to adsorb onto the syringe surfaces. Certain runs were repeated throughout the experiment to enable the correction of absorbances for the change in concentration.

Absorbances were determined at a fixed wavelength (402 nm in the presence of caffeine; 397 nm in the absence of caffeine) at

varying pHs and the results treated using the equations derived in appendix 1 to give the pKas.

The spectrum of the transient intermediates was built up by determining the absorbance by stopped flow spectrophotometry at various wavelengths (re-zeroing at each) in the Soret region.

CHAPTER 3 - STUDIES OF HEMIN IN AQUEOUS ALKALINE SOLUTION

3.1 Introduction

As hemoproteins operate in aqueous solution it would be useful to study the prosthetic group, hemin, in aqueous solution, particularly as pH effects for instance are only meaningful in aqueous solution.

Most aqueous solution studies of hemin have been done at pH > 8 because of aggregation and precipitation below this pH. It is generally agreed that the main species in aqueous alkali is a dimeric species in which all the propionic acid side chains are ionised and in which each iron has one OH^- (or its equivalent) coordinated.

There is evidence for the formation of high molecular weight aggregates at high hemin concentrations [10,36] and in solutions of high ionic strength.[36] Blauer and Zvilichovsky[36] found that 4×10^{-4} M hemin in 1,2 M sodium chloride at pH 11-12, aggregates and the species formed contained as many of fifty hemin units. However, in the absence of NaCl, hemin did not sediment in the ultra centrifuge[36] and hence it will be assumed that at fairly low concentrations of hemin and in solutions of moderate ionic strength, hemin is dimeric. Certainly it behaves as a dimer.[10]

It is well known that aqueous alkaline solutions of hemin may show surprising variations in the UV-visible spectra and magnetic susceptibilities, and monomers,[12,13-15] dimers and[10] polymers[10,36] have all been identified.

However, there are gaps in our knowledge. Caffeine is known to split the alkaline hemin dimer to give the monomer[12] but the pH dependence has not been studied and hence the product has not

been fully identified.

Sucrose is known to affect the magnetic susceptibility[85] but the effect of sucrose on the spectrum has not been studied.

It is known that salts affect the aggregation of hemin[34-36] but the effectiveness of different anions and cations compared to their ability to order water is not known.

The aims of this chapter are to improve our understanding of the nature of the complexes and equilibria observed in aqueous alkali as well as to investigate the conditions required for monomer formation in aqueous alkaline solution, in order to model hemoproteins which usually contain isolated hemin. To this end quantitative studies on caffeine and detergents as well as qualitative studies on salts, sucrose and donors/acceptors have been carried out.

Studies in aqueous acid will be reported in Chapter 4.

The following abbreviations will be used in this chapter:

M for monomer

D for dimer

P for polymer

Each of these may have a subscript A or B. These refer to spectral types, the A type spectrum being the typical high spin spectra[87] while the B type being analogous to the μ-oxo spectrum.[26]

3.2 Results

3.2.1 Beer's law plot of hemin

The Soret band for hemin in 0,1M NaOH is at 385 nm. Hence this wavelength was chosen to see if any deviations from Beers law at low hemin concentrations occur, as this would indicate the formation of the monomer.

A plot of absorbance versus hemin concentration (in 0,1M NaOH to eliminate any ionisations of groups on the hemin) was linear down to 1 x 10^{-7}M hemin (on a per mole iron basis) (figure 3.1)

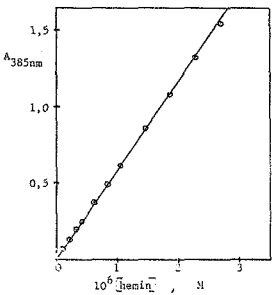

Figure 3.1 Beer's law plot of hemin in 0,1M NaOH; ℓ = 10 cm, 25°C

The slope was 5,8 x $10^5 M^{-1}$. As the pathlength was 10 cm, the extinction coefficient was 58 x 10^3 M^{-1} cm^{-1} (per mole Fe). This is in agreement with earlier results [34] (62 x 10^3 M^{-1} cm^{-1} at 385 nm) at low ionic strength.

The linearity of the plot indicates that monomerization is not occurring to any extent down to at least 1 x 10^{-7}M. At 1,2 x 10^{-7} M hemin the absorbance at 385 nm was 0,069 ± 0,003. Taking this error into account, the monomer concentration is $\leq$ 7 x 10^{-9} M.

Hence the equilibrium constant for the equation (3 - 1),

$$2M \rightleftharpoons D \qquad (3 - 1)$$

K_D, is $\geq 1 \times 10^9\ M^{-1}$. It must be pointed out that K_D will vary with ionic strength.

It is difficult to compare this value with that previously reported (4,5)[31a] as the latter equilibrium involved the loss of a proton on dimerization.

However using the value reported for the pK_a of the dimer (7,5),[31a] K_D is calculated to be $1,4 \times 10^8\ M^{-1}$. The discrepancy between these values may be a consequence of this latter study being largely carried out at pHs near the precipitation point where higher aggregates are probably present,[34] and hence may be the equilibrium constant for polymerization.

These values are greater than that of $3,1 \times 10^6\ M^{-1}$ reported for protoporphyrin,[32] showing that the presence of Fe(III) in the ring enhances dimerization.

3.2.2 Effect of salts and sucrose

It has been reported that the addition of electrolytes to hemin results in a decrease in the Soret band as well as the development of a band around 580 nm.[34] These changes have been correlated with aggregation of hemin[36] and are pH independent between pH 9 and 13.

Figure 3.2 shows the change in spectrum quite clearly (i.e. the A type spectrum is converted to a B type) and confirms the effect of ionic strength, in causing these changes.

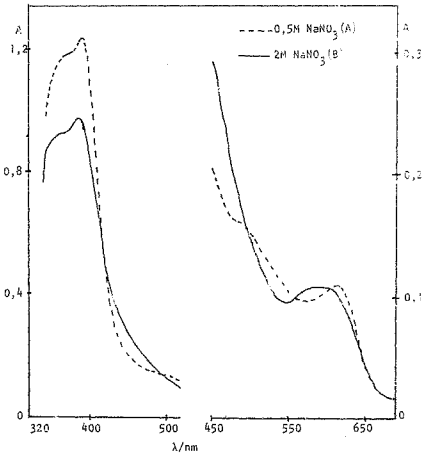

Figure 3.2 Effect of the ionic strength on the spectrum of hemin at pH12; 2,26 x 10^{-5} M hemin; 25°C; ℓ = 1 cm.

The formation of the 580 nm band increases with hemin concentration (figure 3.3) which supports the proposal that aggregation occurs.

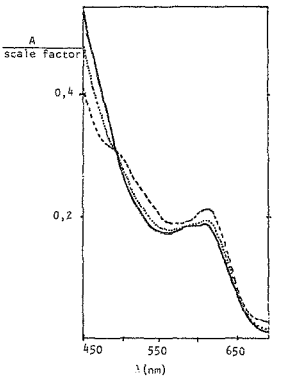

Figure 3.3 Effect of the hemin concentration on the visible spectrum at pH12; 0,5M $NaNO_3$; 25°C; ℓ = 1 cm. ---- 22,6 μM hemin (2 x scale); ···· 90,4 μM hemin (0,5 x scale); —— 181 μM hemin (0,25 x scale).

Different salts affect the spectrum to different extents. This is shown in figure 3.4.

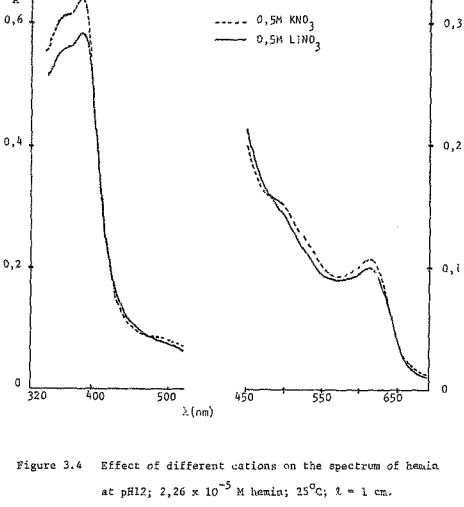

Figure 3.4 Effect of different cations on the spectrum of hemin at pH12; $2{,}26 \times 10^{-5}$ M hemin; 25°C; ℓ = 1 cm.

Li^+ is more effective than K^+ in decreasing the Soret and visible region.

Table 3.1 shows the effect of different salts and different ionic strengths on the Soret intensity.

Table 3.1 : Effect of different salts on the Soret band of hemin in alkaline aqueous solution

System	Soret λmax/nm (ε/(mMFe)$^{-1}$cm^{-1})	
10^{-4} M NaOH	387	(61,3)
10^{-2} M NaOH	385	(58,6)
10^{-1} M NaOH	385	(58,0)
0,5M $LiNO_3$; 10^{-2}M NaOH	385	(52,1)
0,5M $NaNO_3$; 10^{-2}M NaOH	385	(56,8)
0,5M KNO_3; 10^{-2}M NaOH	385	(57,4)
2M $NaNO_3$; 10^{-2}M NaOH	385	(45,0)
0,5M NaCl	385	(56,2)

In agreement with figure 3.2, the decrease in the Soret intensity (but not position) increases with ionic strength. There is a shift in the Soret position at very low ionic strength which is reproducible and may be the consequence of a change in the dimer structure because the carboxylates are no longer shielded from each other. It can also be seen that the order of effectiveness of ions in decreasing the Soret is $Li^+ > Na^+ > K^+$ and $NO_3^- > Cl^-$. This is also the order of the abilities of these ions to increase the structure of water[88] and hence the order of increasing hydrophobic bonding to minimise the unfavourable entropy of solvation. This suggests that the further aggregation shown earlier,[34-36] results at least in part, from hydrophobic interactions.

Sucrose has been shown to increase the magnetic moment of high concentrations of hemin in alkaline solution from 3,6 to

5,6 B M,[86] but its effect on the spectrum has not been reported. It was found that 30% sucrose added to hemin in 2M $NaNO_3$ at pH12, converted the B type spectrum to an A type, i.e. a μ-oxo type to a typical high spin type. Hence sucrose counteracts the electrolytes and displaces the equilibrium in favour of the dimer (equation 3 - 2)

$$n\ D_A \underset{\text{sucrose}}{\overset{\text{electrolytes}}{\rightleftharpoons}} P_B \qquad (3 - 2)$$

This shift in equilibrium explains the effect of sucrose on magnetic susceptibility particularly as A type species have high magnetic moments while B type species have low magnetic moments. (See later.)

The effect of electrolytes in promoting aggregation can be attributed to their shielding like charges from each other in the formation of the aggregate. The effect of sucrose may reverse the formation of the aggregate by disrupting the structure of water and thus disfavouring hydrophobic interactions.

3.2.3 Effect of caffeine

Caffeine is the heterocyclic compound shown in figure 3.5. It has no pK_as in the alkaline region (it has one of <1).[83]

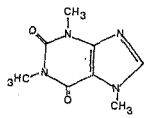

Figure 3.5 Caffeine

Figure 3.6 shows the spectral changes occurring on adding caffeine to hemin at pH12,3.

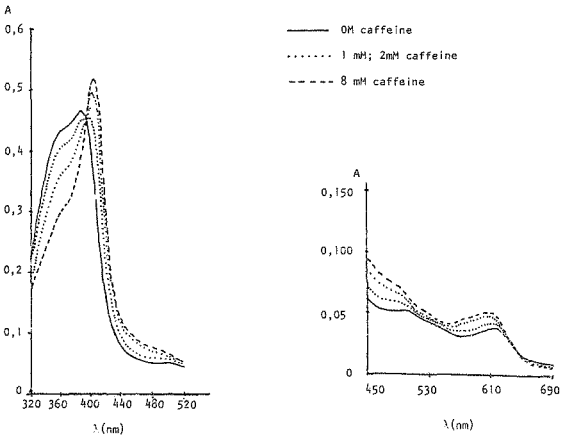

Figure 3.6 Spectral changes occurring on titrating hemin with caffeine; $8{,}28 \times 10^{-6}$ M hemin; pH12,3; 25°C.

The major changes are shifts in the Soret band to 402 nm and the visible band to 606 nm, with isosbestic points at 392 nm and 642 nm, which indicates an equilibrium between two species. Both initial and final spectra are A types. The same spectral changes were observed by Gallagher and Elliott.

3.2.3.1 Quantitative studies

The quantitative studies were limited to pHs between 8 and 12,3. Below pH8, hemin aggregates, while above 12,3 caffeine is hydrolysed (see Chapter 2). Changes in the absorbance at 400 nm were monitored when the caffeine concentration and hemin concentration were independently changed. All experiments were carried out at 25°C.

Experiments in which the caffeine concentration was varied (at a constant hemin concentration), were performed at pH 8,50 and pH 12,00. Gallai and Elliott[12] showed that reaction (3 - 3) was occurr

$$D + 2\,ca... \rightleftharpoons 2M\text{-caffeine}\ (K_c) \qquad (3-3)$$

It can be shown (see appendix 1) that if this reaction is occurring then a plot of

$$\log \frac{(A - A_o)^2}{A_\infty - A} \quad \text{vs} \quad \frac{2\,[Fe]_{TOT}}{A_\infty - A_o}$$

versus log [caffeine]free should be linear with a slope of two (A, A_o, A_∞ are absorbances at a particular caffeine concentration; in the absence of caffeine; for the fully formed hemin-caffeine adduct respectively; $[Fe]_{TOT}$ is the total hemin concentration (on a per mole iron basis)).

This was found to be the case at both pHs (see figures 3.7a and b; tables 1a, b in appendix 2).

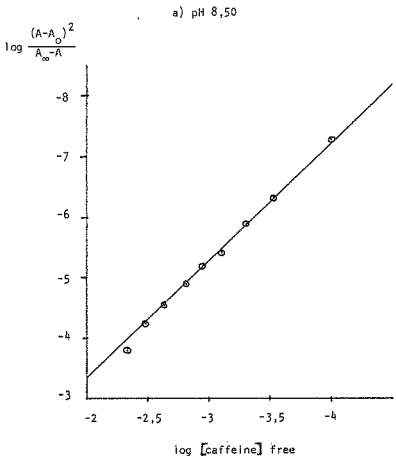

Figure 3.7a Analysis of the titration of hemin with caffeine results at pH 8,50 and 12,0; 1 x 10^{-5} M hemin; u = 0,1; 25°C

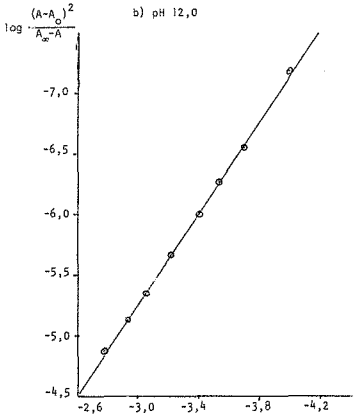

Figure 3.7b Analysis of the titration of hemin with caffeine results at pH 8,50 and 12,0; 1×10^{-5} M hemin; $\mu = 0,1$; 25°C.

The equilibrium constant, K_c, for this reaction was found to be 5,4 M^{-1} and 6,1 M^{-1} at pH 8,50 and pH 12,00 respectively.

Experiments in which the hemin concentration was varied (at a constant caffeine concentration) were carried out at pH 8,50; pH 10,00 and pH 12,00. If reaction (3 - 3) is occurring then a plot of $\log \alpha [Fe]_{TOT}$ versus $\log (1 - \alpha) [Fe]_{TOT}$ should be linear with a slope of 0,5 (see derivation in appendix 1) (where α is the fraction of th.. hemin which has reacted; $[Fe]_{TOT}$ is the total

hemin concentration (on a per mole iron basis)). This was in fact true for all pHs as long as the hemin concentration did not exceed 2×10^{-5} M. (See table 2a, b, c in appendix 2; Figures 3,8 a, b, c.) The equilibrium constant for this reaction, K_C, was found to be 5,1 M^{-1}; 5,8 M^{-1}; 5,7 M^{-1} at pH 8,50; pH 10,00; pH 12,30 respectively.

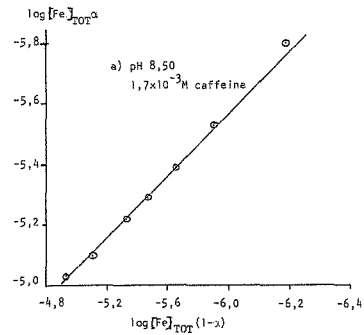

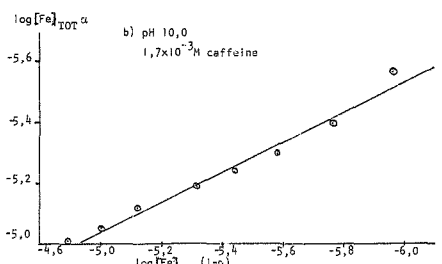

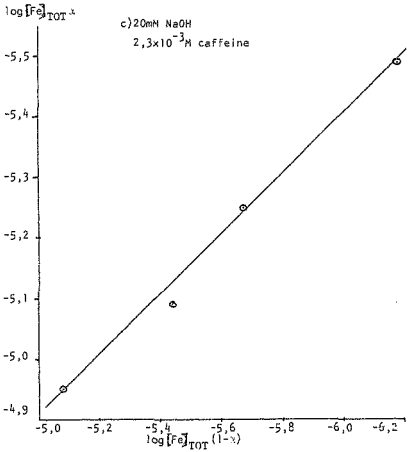

Figure 3.8 Analysis of data obtained by varying the hemin concentration at a constant caffeine concentration, at pH 8,50; 10,00 and 12,30; μ = 0,1; 25°C.

It can be seen that the equilibrium constant, K_C, calculated from experiments where the caffeine concentration and hemin concentration are varied, are the same within experimental error.

More interesting, the equilibrium constant doesn't vary with pH between pH 8,5 and 12,3. As the starting species contained one OH^- per iron, the final monomeric hemin-caffeine adduct must

as well.

Gallagher and Elliott ascribed the relatively low ΔG and high ΔS they found for the dissociation of the hemin-caffeine adduct to hydrophobic bonding between the hemin and caffeine.[12] As caffeine has been shown to form a donor-acceptor complex with hemin in $CDCl_3$,[41] it is probably fair to assume that this type of interaction occurs in aqueous solution as well.

The average value of the equilibrium constant in reaction (3 - 3) is 5,6 M^{-1} (25°C) which compares well with that found at 28° (6,25 M^{-1}) by Gallagher and Elliott.[12]

Reaction (3 - 3) can be formally separated into two steps, splitting the monomer (3 - 4) and binding caffeine (3 - 5).

$$D \rightleftharpoons 2M \qquad K_D^{-1} \qquad (3 - 4)$$

$$M + \text{caffeine} \rightleftharpoons M\text{-caffeine} \quad K_{caff} \qquad (3 - 5)$$

i.e. $K_C = K_D^{-1} (K_{caff})^2$

Using the values of 5,6 M^{-1} for K_C and $\geq 10^9\ M^{-1}$ for K_D (3.2.1), K_{caff} was found to be $\geq 7{,}5 \times 10^4\ M^{-1}$. This value is at least forty times greater than that found for the reaction between caffeine and monomeric hematoporphyrin.[38] This difference is similar to that found for K_D' (reaction 3 - 6) for proto- and hematohemin.

$$2M \longrightarrow D + H^+ \qquad K_D' \qquad (3 - 6)$$

K_D''s were found to be 4,5[31a] and $1{,}0 \times 10^{-2}$ [31f] respectively at about pH 7. This suggests that similar types of interactions occur in both the dimer and the caffeine adducts. As discussed above these are likely to include hydrophobic as well as Π-Π interactions. The more extended Π system as well as the greater

hydrophobicity of vinyl in protohemin compared with hydroxyethyl in hematoporphyrin would then be responsible for the greater binding constant of caffeine to hemin. Hydrogen bonding can be excluded as a major interaction as this would be greater with hematoporphyrin than with hemin.

3.2.3.2 Analogous systems to caffeine

Within experimental error, there was no change in the spectrum of bis-cyanohemin on adding caffeine, showing that if caffeine does bind, the spectral changes observed in figure 3.6 largely arise from splitting the dimer (bis-cyanohemin is monomeric [10]).

Only slight changes in the intensities, but not positions of the UV-visible bands, observed on adding caffeine to monomeric hemin in ethanol, formamide and DMSO, also show that the major spectral change results from splitting the dimer.

Similar spectral changes to those observed with hemin (figure 3.6) were found on titrating mesohemin with caffeine, under analogous conditions. Hence, the vinyl group is not essential for this interaction.

Most donors/acceptors added to hemin decreased and shifted the Soret to the red. These include adenine (λmax. 400 nm), o-phenanthroline (λmax. 406 nm), methyl viologen, arginine at pH 8,5 (λmax. 390 nm), theophylline (λmax. 408 nm). Tyrosine (at pH 8,5) however, shifted the Soret to 374 nm and increased its intensity slightly while guanidine split the Soret into two bands of roughly equal intensity at 356 nm and 394 nm, and decreased its intensity.

With the exception of phenanthroline and methyl viologen which gave B type spectra, there was little change in the visible region

on adding the above species.

These effects are varied and could be reflecting the relative contributions of hydrophobic, donor-acceptor and possibly hydrogen bonding interactions. The effects of phenanthroline and in the visible region, methyl viologen (which absorbs in the Soret region) are similar to those observed with pyridinium salts. It must be pointed out that arginine and tyrosine do not bind at pH 13 but do at pH 8,5 which is below the pK_a of the amino group.[82] This could indicate a coulombic effect as found by Mohr and Scheler[89] and attributed to an interaction between the cation and the propionates.

The effects of caffeine, adenine and theophylline are contrary to the report that these have no effect on hemin.[40]

3.2.3.3 Effect of the hemin concentration on the hemin-caffeine adduct.

It was observed that the reaction (3 - 3) could not explain the results if the hemin concentration exceeded 2×10^{-5} M, and calculating the extinction coefficient at 402 nm from Gallagher and Elliott's spectra[12], gave values between 74 and 80 x 10^3 M^{-1} cm^{-1}, with the value decreasing with hemin concentration. Hence, the spectra of hemin in an excess of caffeine, with increasing concentrations of hemin were determined (see figure 3.9).

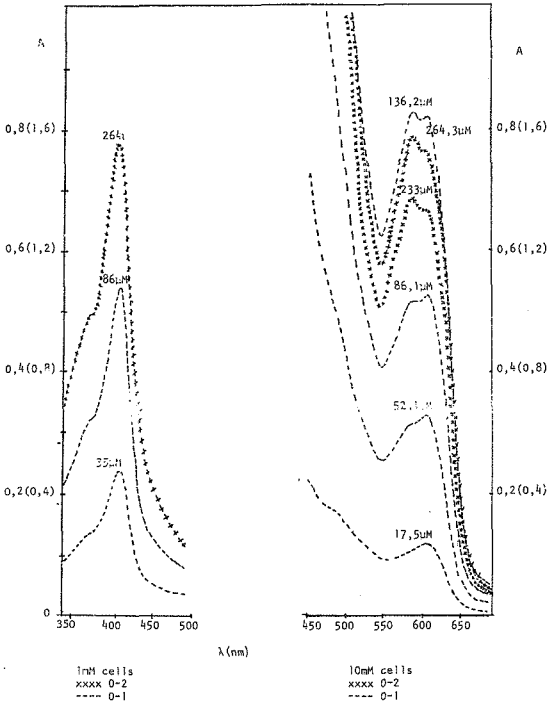

Figure 3.9 Variation in the spectrum of hemin in 0,1 M caffeine with hemin concentration; pH 10,0; μ = 0,1; 25°C.

The changes in the visible region are most marked with the appearance of the band at 575 nm which becomes relatively more intense as the hemin concentration increases. At high concentrations of hemin there are bands at 575 nm, 600 nm and shoulders at ~560 nm and 620 nm. These are likely to be vibrational overtones.[87] There is no change in shape or position of the Soret although the extinction coefficient does decrease.

Beer's law at 402 nm was not obeyed above $1,5 \times 10^{-5}$ M hemin (figure 3.10).

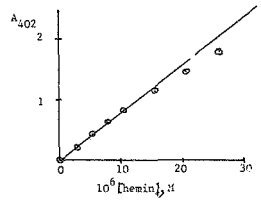

Figure 3.10 A Beers law plot of hemin-caffeine at 402 nm; 0,1 M caffeine; pH 12,0; 25°C; μ = 0,1.

To avoid this further reaction, (which is some kind of aggregation or dimerization of the monomeric hemin-caffeine adduct, as it depends on the hemin concentration) experiments were generally done with $\leq 1,5 \times 10^{-5}$ M hemin. At low hemin concentrations ε_{402} was found to be $81,1 \times 10^3$ M^{-1} cm^{-1} for hemin caffeine.

The Beer's law plot at 575 nm showed a positive deviation while that at 600 nm showed a negative deviation above

$1,5 \times 10^{-4}$ M hemin. The respective extinction coefficients at low hemin concentrations are $6,0 \times 10^{3}$ M^{-1} cm^{-1} and $6,8 \times 10^{3}$ M^{-1} cm^{-1}.

Unfortunately, a stage is not reached where the extinction coefficients become constant at high hemin concentrations, so this equilibrium cannot be quantitatively studied.

3.2.4 Effect of detergents

3.2.4.1 Qualitative studies

Simplicio and co-workers showed, using equilibrium and kinetic studies, that micellar detergents split the dimer to give monomers intercalated within the detergent micelle.[13,14] They showed that as the detergent concentration was increased, the absorbance of the detergent monomer Soret increased until a limiting value was reached. This was found to be reproducible using the detergent cetyltetramethyl ammonium bromide (CTMAB) in 0,1 M NaOH at 400 nm. However, following the alkaline hemin dimer Soret (385 nm) a decrease in the absorbance followed by an increase was observed, with signs of a limiting value being approached. (See Figure 3.11.)

The minimum in absorbance occurred at about 1×10^{-4} M CTMAB. By comparison, the critical micellar concentration (cmc) of CTMAB in water is 1×10^{-3} M.[90] The fairly similar values suggest that the increase occurs because of incorporation of the hemin monomer into the micelle, bearing in mind that salts generally decrease the cmc and that micelles are found below the cmc which is an average value. The decrease suggests a different kind of interaction with the detergent and has been studied quantitatively. (See later.)

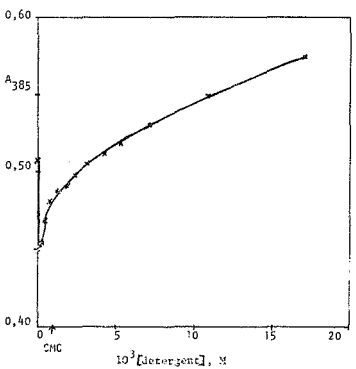

Figure 3.11 Change in the λmax of the alkaline hemin dimer with detergent concentration.

It was found that at low detergent concentrations a limiting spectrum was found, and this enabled the quantitative study to be carried out. The limiting spectra in low and high concentrations of CTMAB are shown in Figure 3.12a.

Both low and high concentrations gave B type spectra with the major differences being in the Soret region.

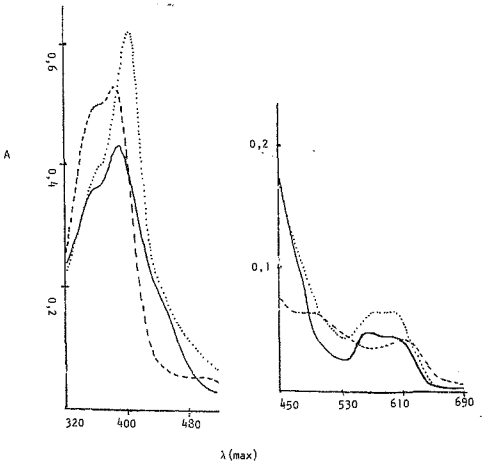

Figure 13.2a Spectra of hemin in low and high concentrations of CTMAB; 0,1 M NaOH; 25°C; 8,65 x 10^{-5} M hemin
---- 0M CTMAB; —— 3 x 10^{-5} M CTMAB;
···· 3% (0,082 M) CTMAB.

The UV-visible bands obtained at high and low CTMAB concentrations are reported in table 3.2 together with those of the μ-oxo dimer in benzene for comparison.[26]

Table 3.2 Extinction coefficients* for the UV-visible bands of hemin in a) 30 x 10^{-6} M CTMAB; b) 4% CTMAB (0,11 M) c) μ-oxo dimer [26]

Band	30 x 10^{-6}M CTMAB λmax (εmM λmax)	4% CTMAB (=0,11 M) λmax (εmM|max)	μ-oxo dimer λmax (εmM λmax)
Soret	390 nm (49,8)	399 nm (66)	397 nm (58)
β	568 nm (6,8)	573 nm (8,4)	573 nm (7,0)
α	600 nm (5,9)	597 nm (8,5)	599 nm (6,9)

* expressed on a per mole iron basis.

There are similarities in these spectra. The low detergent species could be a μ-oxo dimer but not the high detergent species as this is monomeric .

Similar spectral changes were observed for triton X-100 (TX) but not sodium lauryl sulphate (SLS) (see figure 3.12b). . Hence SLS gives an A type spectrum while CTMAB and TX both give a B type spectrum at both low and high concentrations.

At high detergent concentrations, the absorbance of the Soret band of the detergent monomer decreas d with time. This was found to some extent at all pHs with SL[illegible] [illegible]B, TX Tween 80, lauryl pyridinium chloride s [illegible] TX and mesohemin. It could not be reversed by t [illegible]ion of KCN which indicates decomposition rather than dimerization. Ways in which this effect could be minimised were by working at low detergent concentrations, high hemin concentrations where the relative

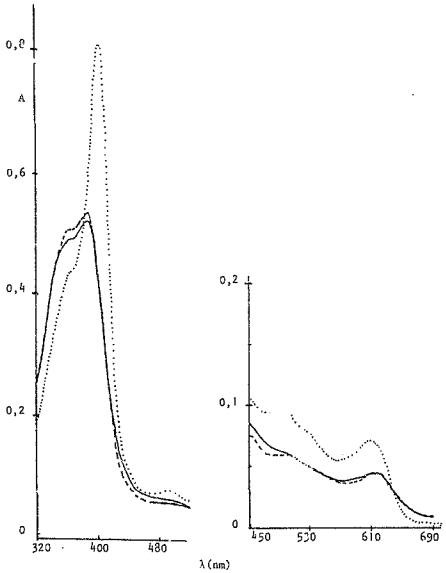

Figure 3.12b Spectra of hemin in low and high concentrations of SLS; 0,1 M NaOH; 25°C; 8,65 x 10^{-5} M hemin.
--- 0M SLS; 1,2 x 10^{-4} M SLS; ••• 4% (0,14 M) SLS

change in absorbance was small or running spectra as soon as possible after mixing.

3.2.4.2. Quantitative studies

The titration of hemin with CTMAB, TX and SLS to give the low detergent species, showed isosbestic points (figure 3.13).

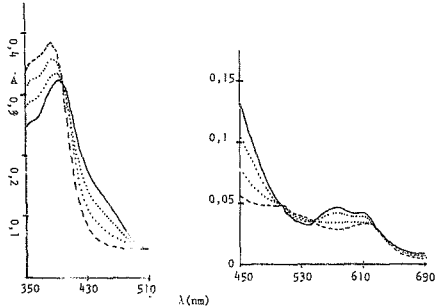

Figure 3.13 Spectral changes on titrating hemin with low concentrations of CTMAB; 6.80 x 10^{-6} M hemin; 0,1 M NaOH; 25°C.
--- 0 M CTMAB; ··· 1,8 and 6,0 x 10^{-6} M CTMAB;
—— 21 x 10^{-6} M CTMAB.

The titration data in each case were shown to fit reaction (3 - 7) but not reaction (3 - 8).

$$D + nL \rightleftharpoons DL_n \qquad (3 - 7)$$

$$D + 2nL \rightleftharpoons 2nL_n \qquad (3 - 8)$$

If reaction (3 - 7) is occurring then a plot of $\log \frac{A - A_o}{A_\infty - A}$ against log [detergent] should be linear with a slope of n. In addition a plot of log $[Fe]_{TOT}$ α versus log $(1 - \alpha)$ $[Fe]_{TOT}$ should be linear with a slope of one. (See appendix 1).

With CTMAB, figure 3.14 a) shows that the former is true, with a slope of two, while figure 3.14 b) shows that the latter is also true. (Data tables in appendix 2, tables 5a, i, ii, iii.)

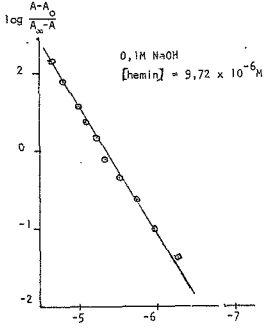

Figure 3.14a Analysis of the data for the titration of hemin by CTMAB.

The log K values were as follows:

At pH 8,5 : 10,6 ± 0,3 (varying CTMAB) (M^{-2})

In 0,1M NaOH : 10,56 ± 0,03 (varying CTMAB) (M^{-2})

10,7 ± 0,3 (varying hemin) (M^{-2})

Figure 3.14b Analysis of the data for the titration of hemin by CTMAB; 0,1M NaOH; $1,5 \times 10^{-5}$M CTMAB; 25°C

Hence this reaction is pH independent between pH 8,5 and 13, which implies that each iron still has OH^- or its equivalent coordinated.

With SLS, only one detergent is bound and log K at pH 13 was found to be 5,3 ± 0,2 (M^{-1}) (see figure 3.15).

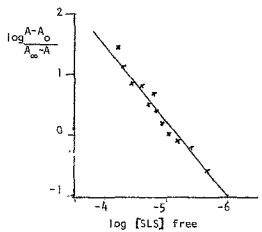

Figure 3.15 Analysis of the data for the titration of hemin by SLS in 0,1 M NaOH; 25°C; 1,12 x 10^{-5} M hemin.

The titration with TX showed a curved plot which could be resolved into the binding of one detergent at low concentrations and two detergents at higher concentrations (see figure 3.16a).

The log of the binding constant for one detergent was 4,8 ± 0,2 (M^{-1}) while that for two was 9,5 ± 0,1 (M^{-2}). TX thus has a lower affinity for hemin than do CTMAB and SLS.

These results may be a consequence of differing hydrophobicities as well as coulombic interactions with the porphyrin core (which has a +1 charge) and the propionate side chains with the different detergents.

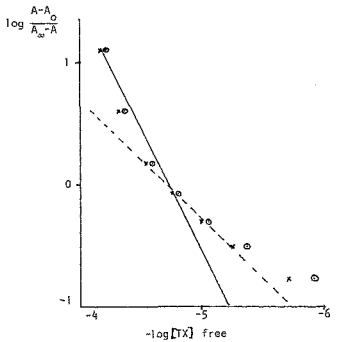

Figure 3.16a) Analysis of the data for the titration of hemin by TX in 0,1 M NaOH; 10,0 x 10^{-6} M hemin; 25°C;
x---x solved assuming one detergent bound
Θ—Θ solved assuming two detergents bound

In spite of the two overlapping equilibria with TX (figure 3.16 b), isosbestic points were still present, indicating that the first detergent binding causes the major spectral changes.

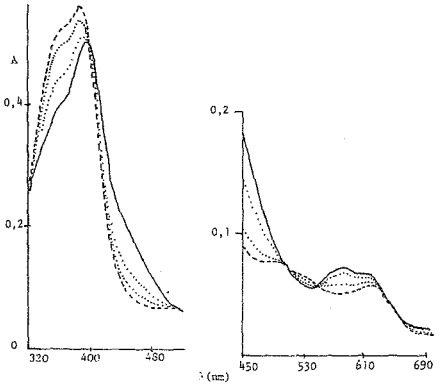

Figure 3.16 b) Corresponding spectral changes (conditions as in figure 3.16a).

3.2.5 Spectra

UV-visible spectra have been recorded under various conditions. Table 3.3 lists the positions and intensities of the Soret and visible bands of hemin in various alkaline solutions.

There is a reasonable comparison between the results of this study and those of other workers, particularly as many of the quoted figures for the latter have been read off from reported spectra.

Table 3.3 λ_{max} (and $\varepsilon_M(\lambda_{max})$) for the Soret and visible bands of hemin in alkaline solutions

	System	Soret λ_{max}[a] (ε_M)[b]	Visible λ_{max}[a] (ε_M)[b]	Type[c]	Ref.
1.	Aqueous solution; 25°C				
1.1.	low ionic strength				
	1×10^{-3}; pH 9,5	387 (91)	494(6,3); 530*(5,3); 612(4,7)	A'(D)	this study
	pH 11,0	383 (62)	495(6,3); 533*(5,4); 619(4,7)	A'(D)	34[d]
1.2.	moderate ionic strength				
	μ = 0,1; pH 9 - 13	385 (58)	496(6,2); 535(5,1); 612(4,4)	A'(D)	this study
	pH 11, 3	-	480*(6,0); 530*(6,2); 612(5,9)	A'(D)	1[d]
1.3.	high ionic strength				
	2M $NaNO_3$; 22×10^{-6}M hemin; pH12	385 (45)	525 - 603 (4,7)	B (P)	this study
	4M $NaClO_4$; pH13; 65×10^{-6}M hemin	-	578(4,4); 603(4,3)	B (P)	this study
	1,9M NaCl; pH11; 50×10^{-6}M hemin	385 (41)	580(5,0); 600*(4,7)	B (P)	34[d]
	2,4M KOH	-	565 - 600 (5,1)	B (P)	47
1.4.	plus caffeine				
	0,05M caffeine; μ=0,1; 15×10^{-6}M;				
	pH 9,5 - 12,3	402 (78)	490*(10,4); 604(7,7)	A (M)	this study
	excess of caffeine; 5×10^{-6}M hemin;				
	20mM NaOH	402 (80)	498(10,4); 604(7,8)	A (M)	12[d]
	0,1M caffeine; μ=0,1; 69,2M hemin;				
	pH 10 and 12	400 (57)	542(3,0)	B (D)	this study
	0,1M caffeine; 20mM NaOH;				
	38×10^{-6}M hemin	-	585(4,8); 604(4,7)	B (D)	12[d]
1.5.	Detergents				
1.5.1.	low (detergent)				
	30×10^{-6}M CTMAB; pH9,6-12,3; μ=0,1	390 (50)	568-6,8); 600(5,9)	B (M)	this study
	$1,2\times10^{-6}$M TX; 0,2M NaOH	392 (52)	574-6,2); 603(5,5)	B (D)	this study
	$1,2\times10^{-6}$M SLS; 0,2M NaOH	386 (53)	611(3,3)	A'(D)	this study
1.5.2.	high (detergent)				
	3% CTMAB; 0,1M NaOH	401 (86)	573(6,4); 600(6,1)	B (M)	this study
	3% CTMAB; pH9,5; μ=0,1	400 (67)	572(3,8); 596(5,7)	B (M)	14[d]
	4% TX; 0,1M NaOH	400 (63)	574(6,3); 598(6,1)	B (M)	this study
	4% TX; pH9,5; μ=0,1	400 (62)	573(6,3); 597(6,2)	B (M)	14[d]
	4% SLS; 0,1M NaOH	402 (90)	588(9,6); 617*(7,7); 604(7,1)	A (M)	this study
	4% SLS; pH9,0; μ=0,1	400 (82)	600(6,3)	A (M)	13[d]
2.	Mixed aqueous solvents				
	44% aqueous ethanol; 20mM NaOH	-	482(9,7); 600(7,1)	A (M)	this study
	44% aqueous ethanol; pH9,0	399 (108)	482*(11,5); 600(7,6)	A (M)	47[d]
	66% aqueous ethylene glycol;				
	20mM NaOH	-	488(8,4); 530*(6,4); 603(6,0)	A	this study
	0,771 mole fraction water in				
	DMSO; 5mM OH^-	-	580(7,0); 600(6,1)	B	91[d]
	65% aqueous DMSO; pH9-9	396 (110)	540(?10); 590(?10)	B (D)	92
	65% aqueous DMSO; pH9-9 + NaClO_4/KClO_4	397 (55)	580 - 600	B	92
3.	Non-aqueous solvents - μ-oxo dimer				
	benzene	397 (57)	573(7,0); 598(5,9)	B (D)	26
	pyridin	397 (60)	572(7,0); 597(11,6)	B (D)	26

[a] in nm [b] in $(mM\ Fe)^{-1}\ cm^{-1}$ [c] see text and figure 3.17 [d] read off spectrum * shoulder

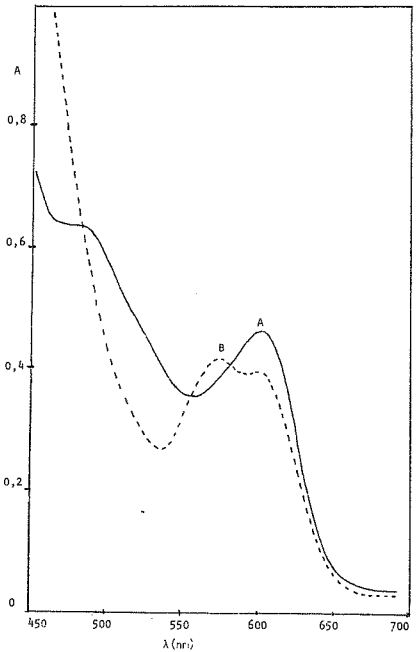

Figure 3.17 Types of hemin spectra in alkaline solution
—— (A): $6{,}55 \times 10^{-5}$M hemin in 44% aqueous ethanol containing 20mM NaOH
--- (B): $6{,}55 \times 10^{-5}$M hemin in 3% (0,082M) CTMAB containing 0,1M NaOH.

(a) Visible region

There are quite distinctly two types of visible bands as represented in figure 3.17. The A type spectrum is a typical high spin[87] spectrum while the B type spectrum is analogous to that of the μ-oxo dimer.[26] (A' is still an A type with the bands shifted slightly to the red.) Curiously, these changes in the visible region are not paralleled in the Soret region.

The B type spectra may in many cases be due to a μ-oxo dimer (e.g. at low (detergent), high (hemin) in caffeine) where dimers have been established or seem likely, or may be due to μ-oxo linkages present in an aggregate (high ionic strengths). There are cases, however, where the hemin is monomeric but still has a B-type spectrum (e.g. micellar CTMAB and TX). This suggests that there is some common feature.

It has been proposed[87] that although the bands in the UV-visible spectrum of hemin are largely due to $\Pi \rightarrow \Pi^*$ transitions, varying amounts of mixing can occur with $\Pi \rightarrow d$ charge transfer transitions, particularly in high spin complexes. If there is little mixing of the low energy $\Pi \rightarrow \Pi^*$ transition with the high energy charge transfer transitions, then a relatively weak band at $\lesssim$ 476 nm and a band at ~588 nm (εmM~10) (with vibrational progressions) would be expected. A characteristic of the B type spectrum is a band at ~580 nm (εmM 5-7) with a nearby band at ~600 nm. There is also a slight shoulder at $\lesssim$476 nm in all the B type spectra, including the μ-oxo dimer (see for example figures 13a and 16b).

Hence the primary difference between A and B type species could depend on whether there is mixing of the low energy $\Pi \rightarrow \Pi^*$

transition with the high energy $\pi \rightarrow d$ charge transfer transition or not.

(b) Soret band

The changes in the Soret band do not parallel those found in the visible region, which indicates that different factors determine the positions and intensities of the bands in these two regions.

The Soret intensity decreases as the degree of aggregation increases i.e. the extinction coefficient decreases in the order M > D > P. The monomers tend to have their λmax at ~400 nm while the dimers and higher aggregates tend to have their λmax at 385 - 390 nm. The exception to this are the μ-oxo dimers which have their max at 397 nm. These changes on dimerization and aggregation must result from interactions between the hemin units. The μ-oxo dimer may differ perhaps because of a different type of interaction or a lack of $\pi - \pi$ interaction.

3.3 Discussion

On the basis that the hemin species in alkaline solution of moderate ionic strength is dimeric, the existence of equilibria between monomers, dimers and higher polymeric forms have been found in aqueous alkaline solution. These equilibria are pH independent (pH > 8).

The visible spectra of the species studied here as well as others in alkaline non-aqueous and mixed aqueous organic solvents show that they all fall into two series characterised as follows:

A series with bands at about 610 nm and between 480 and 500 nm as expected for high spin Fe(III).

B series with bands at 570 - 600 nm (most likely being vibrational overtones) with no obvious bands at about 500 nm. These are not

quite those expected for a low spin Fe(III) which have bands between 530 and 580 nm.[87,93]

The changes in the Soret region showed no correlation with those in the αβ region.

A type spectra have been found for monomers and dimers (hence labelled M_A and D_A) while B type spectra have been found for monomers, dimers and polymers (hence labelled M_B, D_B, P_B).

Hence the following equilibria exist between the five types of hemin found in aqueous alkaline solution:

monomers		dimers		polymers
M_A		D_A		
⇅	⇄	⇅	⇄	P_B
M_B		D_B		

The equilibria are all pH-independent but obviously depend on the hemin concentration and the different forms are stabilized by conditions as follows:

M_A : observed in aqueous alcohols and in aqueous solution in the presence of caffeine and micellar SLS.[13]

M_B : observed in TX, CTMAB detergent micelles in aqueous solution.[14]

D_A : observed in aqueous solution, where it is stabilized by sucrose and at low concentrations of SLS.

D_B : observed in DMSO,[92] in aqueous solution at low concentrations of TX and CTMAB, with pyridine and pyridinium salts[89] and with caffeine.

P_B : observed in aqueous solution containing high concentrations of electrolytes.[34]

Correlations between the spectral types and magnetic susceptibility exist. The species giving A type spectra have magnetic susceptibilities of around 5,9 BM which is what is expected for the high spin species which would have five unpaired electrons. For example, hemin in aqueous alkali gives a value of 5,8 as long as the hemin concentration is not greater than 2×10^{-4} M [28] or if 30% sucrose is present. [86]

The species giving B type spectra which have been measured, give values around two BM which may arise either from the low spin species (with one unpaired electron) or from antiferromagnetic coupling of two high Fe(III)s via an oxo bridge. For example hemin in the presence of high concentrations (~2M) of electrolytes gave values of 2,6-2,9 BM.[35] Hemin in 20% pyridine containing 0,2M NaOH gave a value of 1,97 and the μ-oxo dimer gave a value of 2,4 BM at room temperature decreasing with temperature. [26] Unfortunately determinations have not been carried out on M_A and M_B so it is not certain that M_A is high spin and M_B is low spin although the former is probably true. It is not clear that the B type species are necessarily low spin or antiferromagnetically coupled. A high spin species, in which mixing of $\Pi \rightarrow \Pi^*$ and charge transfer transitions is unfavourable because of symmetry or energy differences, is a possibility. An equilibrium has been found between high spin and low spin ferrihemoglobin and ferrimyoglobin containing H_2O, HO^-, N_3^-, imidazole, NCS^- and NO_2^- as ligands (together with the protein histidine). [93] Even cyanocatalase is 50% high spin. [87] So a mixture of high spin and low spin is also a possibility for the B type species. These equilibrium mixtures demonstrate the ease of high spin to low spin conversion.

Whether or not the conversion of an A species to a B species involves a high spin-low spin equilibrium or a change in mixing of transitions, the metal ligand bond length as well as the distance of the metal from the ring plane are likely to be significant.

In considering possible structures for the species found, the nature and number of ligands as well as the spin state must be considered. In aqueous alkali, possible ligands are H_2O, OH^- and bridging O^{2-}. The complexes could be five or six coordinate but in practice as the sixth ligand would be H_2O these two cannot be distinguished. As discussed above, both high spin and low spin (or even a mixture) are possible. In addition the dimers and polymers may be held together by a μ-oxo bridge, by coordination of carboxylate from another hemin, by hydrophobic interactions or by donor-acceptor interactions. As no evidence has been found for carboxylate dimerization,[24] this will be ignored. Hydrophobic and donor-acceptor interactions give rise to interactions between the porphyrin rings and will result in ring-ring dimers.

As the equilibria were all pH independent, all the species have OH^- or its equivalent coordinated. In each case H_2O may be an additional ligand.

Hence the monomeric species can be Fe - OH and H_2O-Fe-OH.

The dimeric species may be Fe-O-Fe; H_2O-Fe-O-Fe-OH_2; $(Fe\text{-}OH)_2$; $(H_2O\text{-}Fe\text{-}OH)_2$ (for the μ-oxo dimers and ring-ring dimers respectively).

Coordination of H_2O may alter the metal-ligand bond length as well as the distance between the metal and ring plane and enable the transition between A and B to be effected at least in the case of the monomers and the ring-ring dimers. The μ-oxo

dimer is unlikely to change its spin state on coordination of H_2O as antiferromagnetic coupling generally predominates over ferromagnetic coupling in μ-oxo dimers.[94]

Hence M_A is likely to be Fe-OH while M_B could be H_2O-Fe-OH. D_A is likely to be $(Fe-OH)_2$ while D_B could be Fe-O-Fe or $(H_2O-Fe-OH)_2$. P_B could contain D_B units held together by cations and possibly involving ring-ring interactions between these units, because evidence for hydrophobic bonding was found from the effectiveness of different ions.

The formation of an M_B type species in some detergent micelles is rather puzzling, as A type species are found in their absence. Possibly the low dielectric constant in the micelle interior, by preventing charge delocalisation, induces a short Fe-O bond which enables the transition to occur. SLS may differ perhaps because more solvent is included in the micelle interior.

Hence this study has provided further information on the nature of species and the equilibria exhibited by hemin in alkaline aqueous solution. Five different types of complexes (including monomers, dimers and polymers) were found to be in pH independent equilibria. The species found demonstrate a complex interplay of coulombic, hydrophobic, donor-acceptor and possibly hydrogen bonding interactions.

This provides a framework for further studies on the nature of the equilibria and physical properties of the individual complexes

Monomeric hemin in a predominantly aqueous environment at pH > 8 can be obtained in the presence of caffeine or in micellar detergents. These are superior to mixed aqueous solvents as pH still has its normal meaning.

CHAPTER 4 : HEMIN IN AQUEOUS ACID SOLUTION

4.1 Introduction

The previous chapter dealt with hemin in aqueous alkali (above the pKas of the coordinated hydroxide and propionic acid side chains) where hemin is soluble and hence true thermodynamic equilibria can be studied. Only five types of complexes were found!

By contrast the acid and neutral region (pH<8) is complicated not only by these pKas but also by the insolubility of hemin, with all solutions being metastable (see later).

Hence a study in this region presents the problem of how to get the hemin into solution as well as how to study it.

Three approaches can be used to get hemin dissolved in aqueous acid, dilution into aqueous acid from hemin dissolved in aqueous alkali or organic solvents (e.g. from pure DMSO to 0,1% aqueous DMSO)[92], and from hemoproteins (e.g. hamoglobin) dissolved in water, can all be used.

Previous work on equilibria in acid has shown two pKas, one at about 2[92,96] and the other at about 7,5.[10,31a,34,92,96] These probably refer to dimers or possibly even higher aggregates in the slightly acid region and the number of protons and the nature of the species has not been identified.

To improve the conditions for study, either the rate of aggregation reactions must be slowed down, as reported earlier in the presence of silicate,[11] or else a rapid method of study must be used, such as stopped flow. When using stopped flow pH jumps (i.e. rapidly mixing unbuffered hemin at about pH9 with a buffer of the required pH), it must be borne in mind that any observed pKa may not be a true equilibrium between metastable species but

may include the pH dependence of an irreversible aggregation reaction.

The aims of this chapter are to improve the understanding of the nature of the complexes and equilibria observed in neutral and acid aqueous solution with particular emphasis on identifying the simple monomeric aquo complex and determining at least an approximate pKa for the coordinated water.

4.2 Results

4.2.1 Aqueous solution alone

4.2.1.1. Moderate ionic strength (μ = 0,1)

Preliminary experiments in which equal volumes of hemin in dilute (10^{-4}-10^{-5}M) NaOH and double strength buffers were mixed to give a final concentration of $\sim 2 \times 10^{-6}$M hemin gave a fairly stable species (i.e. < 2% decrease in the Soret intensity in one minute) and this enabled it to be studied by ordinary spectrophotometry. The changes in the Soret absorbance were rapid in the pH range 3 - 6 and hence this region was studied by stopped flow spectrophotometry.

Spectra at pH1 of the Soret region (350 nm to 450 nm) were obtained by adding typically 1µl of a $8,8 \times 10^{-3}$M hemin stock solution in 0,1M NaOH to 10 ml of water followed by the addition of 10 ml double strength pH 1,1 buffer to give a final hemin concentration of $4,4 \times 10^{-7}$M and using a 10 cm pathlength cell. (Addition of the hemin stock directly to the buffer resulted in precipitation.) In all cases the new spectrum appeared within five seconds and showed little change with time (i.e. < 2% decrease in the Soret intensity in two minutes). The spectrum showed a reasonably sharp Soret band and the species is possibly monomeric.

The λmax was at 397 nm with an extinction coefficient of 120 ± 3, the latter being strong support for a monomer. On standing for five hours, however, ε dropped to 80.

As the hemin concentration was increased above 2×10^{-6}M a decrease in the extinction coefficient was observed as well as a more rapid decrease in the Soret absorbance with time (at 2×10^{-5}M hemin a ~10% decrease occurred in a minute). Hence a Beer's law study was carried out to investigate these differences. (At higher hemin concentrations the absorbance found 10s after mixing was used.) Figure 4.1 shows the plot of absorbance at 397 nm (the Soret λmax) against the hemin concentration. (The data are given in appendix 3 table 1a.)

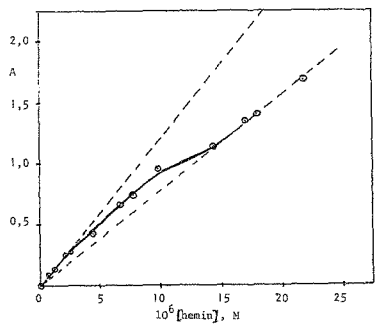

Figure 4.1 Beer's law plot of hemin at pH 1,1; μ = 0,1
ℓ = 1 cm; 25°C.

This shows a marked deviation from linearity. It could be shown (appendix 3 table 1b) that this deviation was due to the equilibrium (4 - 1)

$$2M \rightleftharpoons D \qquad (4-1)$$

and the equilibrium constant was found to be $1,1 \times 10^5\ M^{-1}$. This is considerably less than that found for the alkaline dimer ($K_D > 10^9$) indicating a different type of dimer, with weaker interactions.

The spectra of both the monomer and dimer have the Soret maximum at 397 nm but the dimer has a lower extinction coefficient as well as a shoulder at about 360 nm. (See figure 4.2 and table 4.2.)

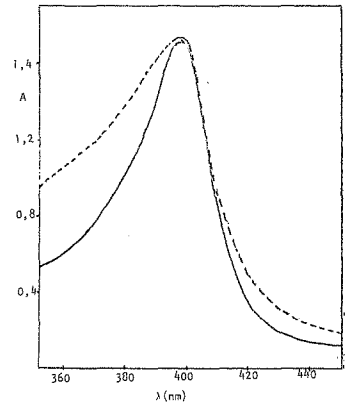

Figure 4.2 Spectra of hemin at high and low concentrations at pH 1,1 (Soret region) $\mu = 0,1$; $25^{\circ}C$
—— $1,4 \times 10^{-6}$M hemin; $\ell = 10$ cm
---- $2,2 \times 10^{-5}$M hemin; $\ell = 1$ cm

In the stopped flow experiments, equal volumes of $4,30 \times 10^{-6}$ M hemin in 10^{-6}M NaOH and double strength buffers from pH 1,1 to 11,0 were mixed to give a final concentration of $2,15 \times 10^{-6}$M hemin. The change in absorbance (where evident in the time scale used) was monitored at 397 nm.

No changes in absorbance with time were observed between pH 7,8 and 11,0. Below pH 3, the traces showed the end of a rapid rise in absorbance (extending for approximately 1 m s (the mixing time of the instrument is 1 m s)) which then remained steady for at least 100 m s. The absorbance at pH 1 - 2 (0,515) corresponds to an extinction coefficient (at 397 nm) of 120×10^3 M^{-1} cm^{-1} ($\lambda \approx 2$ cm) in agreement with the results of the Beers law plot at low hemin concentrations.

Between pH 3 and 7 the traces showed an initial rapid rise to a maximum (which usually occurred at approximately 2 m s after mixing) followed by a slower fall. The maximum values are recorded in table 2 appendix 3 together with the steady values in the other pH regions. The variation of these is shown in figure 4.3a. This shows the occurrence of two apparent pKas at pH 2,8 and pH 6,4. The data were evaluated in terms of various equations involving interconversions of monomers and dimers, dimers and dimers and monomers and monomers with the involvement of one or more protons, but unfortunately the data were not good enough to distinguish between the various possibilities. This is probably due to a significant amount of an aggregated species or dimer in the intermediate pH region which would invalidate the equations used to treat the data.

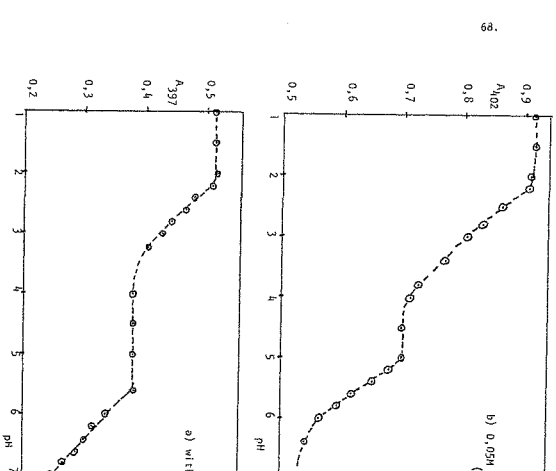

Figure 4.3 Variation in absorbance of the Soret with pH in the absence and presence of caffeine; 25°C; μ = 0,1

However, further experiments varying the hemin concentrations at pH 6,4 (see table 4.1) showed that the pKa in this region apparently involves the conversion of a dimer at high pH to a monomer at low pH.

Table 4.1 : Variation of [hemin] at pH 6,4. ($25^{o}C$; μ = 0,1)

(Fe)	A_{397}(pH6,4) (≡ A)	A_{397}(pH11,0) (≡ A_{∞})	A_{397}(pH5,0)[a] (≡ A_{o})	$-\log K_a$[b]
$16x10^{-6}$M	1,720	1,518	3,078	6,59
$8x10^{-6}$M	0,8[illegible]	0,746	1,512	6,69
$4x10^{-6}$M	0,478	0,383	0,774	6,59
$2x10^{-6}$M	0,267	0,203	0,383	6,69

a ~ calculated using ε_{397}(pH5,0) = $96x10^{3}$ M^{-1} (on a permole Fe basis) (see later).

A plot of $\log \frac{(A_{\infty}-A)^2}{(A-A_o)(A_{\infty}-A_o)}$ vs $\log [Fe]_{TOT}$ (see derivation in appendix 1b) gave R_2 = 0,98; slope = -1,08 (Sd = 0,10)

intercept = +6,89 (Sd = 0,51) $\Longrightarrow$

pK_a[b] = 6,64 ± 0,05

b K_a refers to the equation $2M \rightarrow D + 2H^{+}$

The spectra of the intermediate at pH 5 over the range 340 - 450 nm, determined by stopped flow spectrophotometry at several wavelengths, shows a maximum at 397 nm (ε = $96x10^{3}$ M^{-1} cm^{-1}) with a shoulder at about 360 nm. With the exception of the extinction coefficient of the λmax this is similar to that of the dimer found at pH 1,1 (figure 4.2b) and may represent a mixture of acid

monomer and acid dimer. The spectrum of the pH 1,1 species is identical to that found by ordinary spectrophotometry at low hemin concentrations (λmax at 397 nm, ε_{397} = 120 M^{-1} cm^{-1}) and because of the fairly high extinction coefficient probably represents a monomer.

The similarity in the spectra between the pH 1 dimer and the pH 5 stopped flow species, as well as between the pH 1 monomer and the pH 5,5 - 7 species at very low ionic strength (see later) suggests that these are variants of similar species. Hence the first pKa at 2,8 is likely to correspond to the deprotonation of the carboxylic acids as these would not be expected to have a marked effect on the spectra while the second at 6,6 corresponds to the deprotonation of coordinated water which should have a marked effect on the spectra.

Unsuccessful attempts were also made to pH jump from the monomeric forms at pH 2 and in neutral water (see low ionic strength studies) by stopped flow. In the case of the neutral water the concentrations necessary were too low for meaningful differences to be detected while in the pH2 case, the stock solutions decomposed too fast to enable a sufficient number of quantitative experiments to be made.

4.2.1.2. Low ionic strength

Spectra in the Soret region at low concentrations of hemin ($0,8 \times 10^{-6}$ M) in very low ionic strength solutions ($\mu \sim 10^{-5}$) at pH 7 show a sharp band at 398 with an extinction coefficient of $(122 \pm 3) \times 10^{3}$ M^{-1} cm^{-1}, [97] which is very similar to that found at pH 1,1 (section 4.2.1.1). This species obeys Beer's law up to $4,1 \times 10^{-6}$ M and shows second order decomposition to give a new

species with λmax 398 nm ($\varepsilon \approx 73\ M^{-1}\ cm^{-1}$) (i.e. *similar to* the pH 1,1 dimer).[97] The addition of buffers or salts transformed this low ionic strength species at pH 7 (before decomposition) into an aggregate (broad flat bands were found).[97]

In this study 1μl of a $9{,}18 \times 10^{-3}$ M hemin solution, dissolved in 0,1M NaOH, was added to 25 ml of water to give a final concentration of $0{,}367 \times 10^{-6}$ M hemin. The pH was varied by adding traces of HNO_3 or NaOH, *and was measured with a* pH meter immediately after recording the absorbance (ℓ = 10 cm). Between pH 5,5 and 7, ε_{398} was found to be 122 ± 3, and the absorbance was found to decrease fairly slowly (<4% fall in a minute). Above pH 7, the extinction coefficient was lower, while at pH 10, the alkaline dimer was found (λmax 387 nm and $\varepsilon_{387} = 61{,}3 \times 10^{3}\ M^{-1}\ cm^{-1}$) (the slight shift compared to the spectrum in moderate ionic *strength alkaline presumably* reflecting a slight change in structure because of poor shielding of the carboxylates at low ionic strength). The approximate pKa is ~8. Below pH 5,5 the absorbance at 397 nm rapidly decreased, probably due to the protonation of the carboxylates which would decrease the solubility. Hence this species with a fairly sharp Soret can only be obtained over a fairly narrow range of pH (5,5 - 7) at low ionic strength and is very likely the aquohemin monomer with dissociated carboxylates, which converts slowly to the aquohemin dimer.

4.2.2 Aqueous solution studies in the presence of caffeine

The aqueous solution study of hemin in the presence of caffeine consisted of a stopped flow pH study, analogous to that carried out for the hemin dimer, as well as a qualitative study in the

presence of silicate which slows down aggregation.

The stopped flow pH study in the presence of caffeine was carried out at 402 nm, the Soret maximum of the alkaline monomeric hemin-caffeine adduct (3.2.3) and the final . min concentration was $3,09 \times 10^{-6}$ M. The variation of $A_{402\ nm}$ with pH is shown in figure 4.3b. (The experimental data are presented in table 3 appendix 3.)

Plots of $\log \frac{A-A_o}{A_\infty-A}$ versus pH between pH 2,5 and pH 3,8 for the first pKa and between pH 5,2 and pH 6,0 for the second were linear (figure 4.4) as would be expected for a monomer-monomer conversion (see derivation in appendix 1b). The slopes and intercepts were as follows:

1st pKa : slope = 1,04 (Sd = 0,06)
intercept = -3,13 (Sd = 0,19)
R = 0,99
(A_∞ = 0,700; A_o = 0,915)

2nd pKa : slope = 1,90 (Sd = 0,08)
intercept = -10,66 (Sd = 0,44)
R = 0,99
(A_∞ = 0,530; A_o = 0,700)

(Carbonate buffers were found to decrease A_{402} by 4% relative to phosphate buffers (see table 3 appendix 3 and figure 4.3b) which may be due to some specific interaction of the carbonate. As the absorbances were constant between pH 7,8 and 11,0 using carbonate buffers, the absorbance at pH 7,8 in a phosphate buffer was taken as A_∞ for the second pKa.)

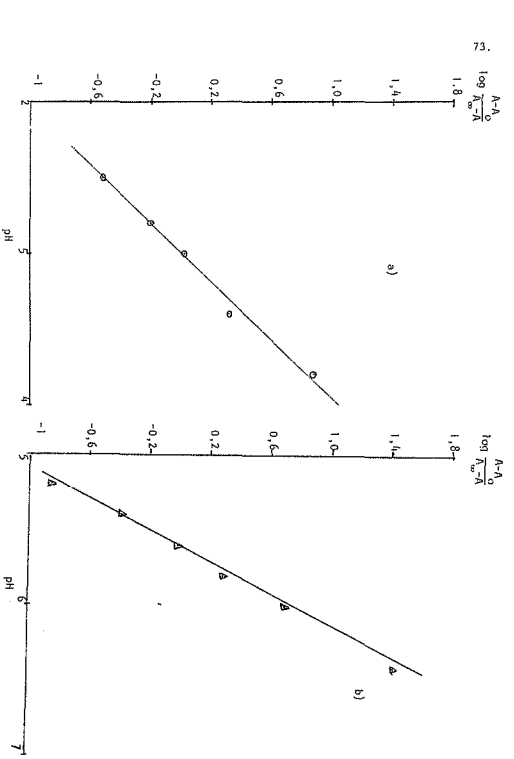

Figure 4.4 Plot for determining the pKas for hemin-caffeine

$3{,}09 \times 10^{-6}$M hemin; 0,05M caffeine; 25°C; μ = 0,1

The *fact that good linear plots* were obtained indicates that unlike in the alkaline dimer system, negligible amounts of dimers and higher aggregates were present up to 20 ms and the equations used were valid.

Hence both pKas corresponded to a monomer-monomer equilibrium. The first pKa had a slope of one which indicates the involvement of one proton (reaction 4 - 2) while the second had a slope of two indicating two protons (reaction 4 - 3).

$$M \rightarrow M' + H^+ \quad (Ka_1) \quad (4-2)$$

$$M' \rightarrow M'' + 2H^+ \quad (Ka_2) \quad (4-3)$$

To enable compariaons to be made more readily, the second pKa can be formally split into two reactions both involving one proton loss (reactions 4 - 4 a & b) and with the same pKa (Ka_2')

$$M' \rightarrow M''' + H^+ \qquad (4-4a)$$

$$M''' \rightarrow M'' + H^+ \qquad (4-4b)$$

It can be seen that $Ka_2' = (Ka_2)^{\frac{1}{2}}$

The derivation (appendix 1b) shows that the pKas for reactions (4 - 2) and (4 - 3) are given by (- intercept) of the plot of $\log \frac{A-A_0}{A_\infty-A}$ versus pH. Hence

$$pKa_1 \approx 3,1$$

$$pKa_2 \approx 10,7 \Longrightarrow pKa_2 = 5,3$$

Hence the first pKa involves deprotonation of one group with a pKa of 3,1 while the second pKa involves the deprotonation of two groups both with pKas of 5,3. The assignment of pKas to $Fe\text{-}OH_2$+Fe-OH (one) and -COOH+COO^- (two) can be made in two ways:

a) the two carboxylates have a pKa of 5,3 while the $Fe\text{-}OH_2$ has a pKa of 3,1 which is much lower than previous pKas reported[10,92,96] and the corresponding pKa in the alkaline dimer (~7) (the

pKas of the carboxylates being normal).[98]

b) A cooperative interaction between Fe-CH_2 and one carboxylic acid which results in them having a common pKa at 5,3 while the second carboxylic acid has a pKa at 3,1. (Only one pKa (7,6) for hemin in 40-80% DMSO was found and this was explained as being due to cooperative interactions between the ionisable groups.)[92]

Certainly the hydrophobic character of caffeine would favour the neutral (ignoring side chains) hydroxohemin over the aquohemin which has a +1 charge and hence may account for the pKa of 3,1. Caffeine cannot be acting as a strong donor[30] as this would tend to favour the aquo complex.

The spectra of the acid species at pH 1 and 4,6 over the range 340 - 450 nm were determined by stopped flow spectrophotometry at several wavelengths. Both species had λmax at 402 nm while the respective extinction coefficients were 151 and 94 x 10^3 M^{-1} cm^{-1}. Comparisons of the Soret of the corresponding species in the absence of caffeine show that caffeine is bound in both cases (by a shift in the λmax and in the case of the pH 1 species by an increase in intensity).

Silicate was added to hemin-caffeine to prevent its aggregation in acid solution.[11] Figure 4.5 shows the effect of pH when 0,74g/100 ml silicate was added to hemin-caffeine and the pH varied.

These changes are reversible and show approximate isosbestic points. The pKas were ∿7 and ∿3. The sharpness of the Soret and the reversibility shows that silicate has in fact prevented aggregation. This is a kinetic effect as silicate did not reverse the aggregation in a partially aggregated hemin-caffeine solution.

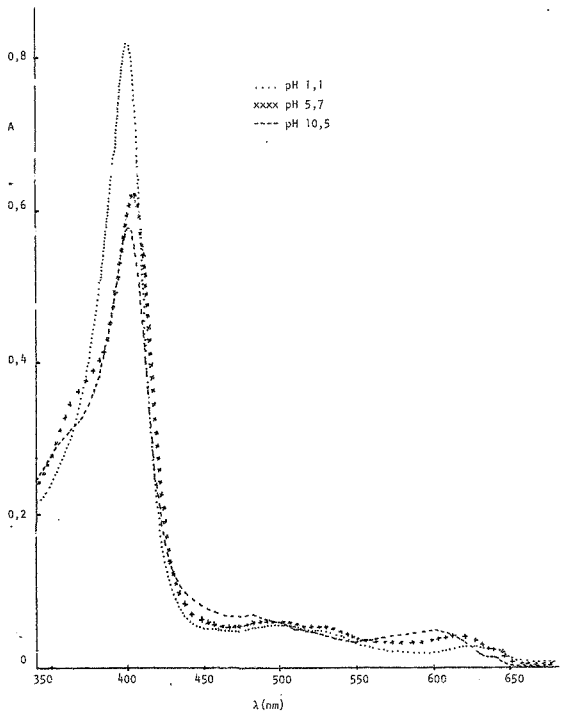

Figure 4.5 Spectra of hemin caffeine in the presence of sodium silicate at various pHs; $7,95 \times 10^{-6}$M he... ..; 0,07M caffeine; 0,74g/10(sodium silicate

In contrast, silicate did not prevent the aggregation of hemin in the absence of caffeine on acidification, as seen by the broad flat Soret band obtained. This could be because the rate of aggregation of hemin in the absence of caffeine is much faster than in the presence of caffeine and hence the viscosity of silicate is less effective in the former case. This ties in well with the stopped flow studies where further reactions after the pH jump of the alkaline dimers prevented pKas from being calculated.

The λmax and ε for the Soret in the presence of caffeine with and without silicate are similar at pH ∿5 but not at pH 1. The latter discrepancy may result from interactions between the charged hemin species at pH 1 and the silicate/silicic acid (a weak acid).

4.2.3 Comparison with other published spectra

A number of other spectra in neutral and acid aqueous solutions which are similar to those found above have been reported and are collected in table 4.2.

Table 4.2 : Spectra of hemin complexes in acid in the Soret region

Conditions	λ /nm	ε /10^3 M^{-1} cm^{-1}	Reference
a) Monomers			
pH1,1-2;<2x10^{-6}M hemin;u=0,1 (stopped flow and ordinary spectrophotometry)	397	120	this study
pH5,5-7;0,4x10^{-6}M hemin;μ∿10^{-5}	398	122±3	this study
pH6,8;<1x10^{-6}M hemin (obeys Beer's law up to 4,1x10^{-6}M) μ∿10^{-5}	398	122±3	97
pH6,8; 1,23x10^{-6}M hemin, water	398	∿120	95

Conditions	λ /nm	ε /10^3 M^{-1} cm^{-1}	Reference
Hemin plus albumin, peroxidase, hemoglobin, myoglobin, catalase; pH ∿ 1	397	130	99
Hemoglobin; $3x10^{-6}$M plus 0,02M HCl; pH2,06	398	∿120	95
50% aqueous ethanol pH 1	398	134	96
0,05M caffeine, pH 1,1	402	151	this study
ditto plus 0,74g/100ml Nasilicate	399	102	this study
0,05M caffeine pH 1,6	402	94	this study
ditto plus 0,74g/100ml Nasilicate (pH 5,7)	402	94	this study
b) Dimers		(per Fe)	
pH 1,1;⩾1,$5x10^{-5}$M hemin;μ=0,1	397	78	this study
pH5;μ=0,1;2,$15x10^{-5}$M hemin(stopped flow)(probably at least partly dimeric)	397	96	this study
pH6,8;μ≥10^{-5};$1x10^{-6}$M hemin on standing(second order formation)	∿398	73	97
Hemoglobin($3x10^{-6}$M) at pH2,06 on standing(second order formation)	∿393	⩾80	95

Conditions	λ /nm	ε /$10^3 M^{-1}$ cm^{-1} (per Fe)	Reference
Hemin; pH ∿ 1	397	81	99
Hemin in 0,01% DMSO containing 0,5M H_2SO_4; ∿$7x10^{-6}$M	396	∿80	92
Hemin (≤10^{-7}M) at pH6,98; μ=0,1	394	≥65	31a

In the absence of caffeine, the monomers obtained under various conditions are remarkably similar, as are most of the dimers. Caffeine shifts the Soret slightly to the red and at pH 1,1 increases its intensity. The presence of sodium silicate has no effect on the spectrum of hemin-caffeine at pH ∿5 but does at pH 1,1.

4.3 Discussion

4.3.1 In the absence of caffeine

Table 4.2 shows that the same spectrum with λmax 397 nm (ε = $120x10^3$ M^{-1} cm^{-1}) can be observed under a variety of conditions from pH 1 - 7. The fairly sharp Soret and relatively high extinction coefficient (figure 4.2) support the proposal that these species are monomeric.

This table also shows that a second type of spectrum, attributed to the dimer, with λmax 397 nm (ε = $80x10^3$ M^{-1} cm^{-1}) can also be observed from pH 1 - 7. This study has shown that these two species are related by a simple monomer-dimer equilibrium at pH 1. (K_D = 1,1 x 10^5 M^{-1}).

We conclude that, the monomer is the monomeric aquo complex and the dimer is the dimeric aquo complex because of the difference from the alkaline hydroxy dimer. Other species with broad Soret bands at about 365 nm reported in the region pH 2 - 8,[92,96] must be higher aggregates.

The ionisation of the carboxylic acid groups, which normally have a pKa of about 5,[98] has no significant effect on the spectra of either complex, at least in the Soret region, which is consistent with the negligible effect on the spectrum of esterification.[24] Their pKa is about 3. (Previous values reported at ~1,5 [92,96] probably involve dimers and polymers.) This lowering of the pKa may not be genuine because of the probable significant concentration of the acid dimer in the intermediate pH range, but if it is genuine this may reflect specific hydrogen bonding of water to the carboxylates, as found in the crystal structure,[50] which would stabilize the carboxylates relative to the carboxylic acid groups. It is possible that only one carboxylate is ionised at this pKa, although the results do suggest that two are involved.

Although ionisation of the carboxylic acid groups does not affect the spectrum significantly, qualitative observations indicate that it does have a marked effect on the rate of aggregation which is greatest in the region pH 3 - 7 (see stopped flow results). One would expect aggregation to occur most readily with the uncharged complex (e.g. Fe-OH_2 with one carboxylic acid ionised) whose concentration would probably be at a maximum at ~ pH 5. It is interesting to note that similar dimer spectra are found at pH1 (μ=0,1) and pH7 ($\mu \gtrsim 10^{-5}$) where the carboxylates are protonated and ionised respectively. This suggests similar dimer species at

these two pHs which may, of course, be a consequence of the ionic strength as well as ionisation. (At low ionic strength, the repulsion of the carboxylates must be minimised by placing them as far from each other as possible.)

The pKa for the coordinated water involves a monomer-dimer equilibrium at ∿7 (which corrected for the alkaline monomer-dimer equilibrium is ∿8) at moderate ionic strength, but ∿8 (uncorrected) at low ionic strength. By comparison the pKa of hemin in 44% aqueous ethanol (which is a monomer-monomer equilibrium involving one proton) is 6,5 - 6,6.[46] Other pKas reported at ∿7 probably involve acid dimers and polymers.[10,31a,34,92,96]

The monomeric species in 50% aqueous ethanol is high spin (μ = 5,41 BM)[96] and because of the similar spectral characteristics, the monomeric species in the absence of ethanol probably is as well and may be the same species as H_2O is a better ligand than ethanol. It is not certain whether this species is five or six-coordinate (a high spin bis aquo iron porphyrin (FeTPP) has been reported)[22] but as five coordinate species appear to have a broader and less intense Soret than the six coordinate species,[22] we may tentatively conclude this is the high spin bis-aquo complex.

It is curious, that in both the stopped flow studies and at low ionic strength, a dimer initially splits to give monomers, which then form new dimers. The different dimerization constants of the acid and alkaline dimers indicates that they have different structures. Presumably formation of one type from the other proceeds most readily via the monomer.

4.3.2 In the presence of caffeine

It has been shown that caffeine forms an adduct with the aquo and

hydroxo hemin, both of which are monomeric. Hemin-caffeine shows two pKas both involving monomer-monomer conversions. The one of 3,1 involves one proton while the other at 5,3 involves two, thus accounting for all three protons required. There is a problem in assigning these pKas to particular groups. The pKa of coordinated water may be lowered to 3,1 (compared with that in 44% aqueous ethanol which is 6,5-6,6) by the hydrophobicity of the caffeine which would favour the hydroxo species. The two carboxylic acids would then have normal pKas. The other possibility requires cooperative interactions between the coordinated aquo/hydroxo and one carboxylic acid/carboxylate for these groups to have the same pKa of 5,3 (this must be the case in 60% DMSO where only one pKa was found)[82] as well as a decrease in the pKa of one carboxylate to 3,1, which was also required in the absence of caffeine and could result from specific hydrogen bonding interactions of water between the carboxylic acid/carboxylate groups.[50]

In the absence of caffeine, ionisation of the carboxylates did not have a marked effect on the spectra, but in the presence of caffeine they do, whatever assignment is chosen. Possibly caffeine could hydrogen bond to the carboxylic acids,[89] (but not carboxylates of course) in such a way as to affect the steric properties of the porphyrin ring and hence its electronic properties, for example by affecting the degree of doming or core expansion.[100]

The fairly sharp Soret band at pH 1,1 may, as in the absence of caffeine, indicate the bis-aquo hemin.

The presence of silicate prevented the aggregation of the hemin-caffeine adduct in acid aqueous solution but not the

hemin dimer in the absence of caffeine. Reversible changes and isosbestic points were found. Approximate pKas were ~3 and ~7, not too different from those in the absence of silicate. The spectra all showed bands at >610 nm which indicated high spin Fe(III). The Soret spectra were not affected by the presence of silicate except at pH 1, where the charged aquo hemin may be interacting with the silicic acid.

CHAPTER 5 - HEMIN COMPLEXES WITH IMIDAZOLE AND ANALOGUES

5.1 Introduction

The aqueous solution chemistry of the imidazole/histidine monomeric complexes of hemin is of interest because these complexes are models for hemoglobin, myoglobin and peroxidase (if one histidine is coordinated) and cytochrome b_5 (if two histidines are coordinated).

A lot of work has been done on imidazole and analogues in non-aqueous solvents,[42,43,51] where the iron porphyrins are monomeric. These studies show that K_1 (i.e. the equilibrium constant for binding the first ligand) is less than K_2 (for the binding of the second ligand) and hence the mono-imidazole complex is not normally observed. Because of the insolubility of histidine in non-aqueous solvents, no work has been done on it, but histamine has been studied.[42]

Some work on imidazole and analogues with hemin in aqueous solution has been done.[16,44] This includes a quantitative study on the binding of N-methyl and N-ethyl imidazole,[44a] which is reportedly simple, i.e. isosbestic points were found and the monomeric bis-imidazole complex which absorbs at 412 nm was the product, but as will be seen below, this is not the whole story. Imidazole also gives an analogous complex which absorbs at 412 nm, but this decomposes to give a second product which has its Soret at 435 nm,[16] beyond that of other Fe(III) complexes (except those with two Soret bands).[59] The nature of this complex is still in doubt. Histidine gives the 412 nm species but not the 435 nm species.[44d] The equilibrium constant has not, however, been quantitatively determined, although some determinations of the

ligand concentration required to half saturate the hemin have been made.

We have therefore undertaken a more detailed study of the coordination of some of its derivatives, in particular histidine, in aqueous solution.

It soon became apparent that several additional minor equilibria, not previously reported, are evident. These may be due to hydrogen bonding or donor-acceptor interactions. Also coordination has interesting effects on the pKas of the side chains and this can be used to model neighbouring acid groups in hèmoproteins. The study was therefore extended to histamine and pilocarpate (figure 5.1).

Figure 5.1 Imidazole and analogues: R = H imidazole;

R = $-CH_2-\underset{\displaystyle NH_2}{\underset{|}{C}}HCOO^-$ histidine; R = $-CH_2-CH_2-NH_2$ histamine;

R = $-CH_2-\underset{\displaystyle CH_2OH}{\underset{|}{C}}H-\underset{\displaystyle COO^-}{\underset{|}{C}}H-CH_2-CH_3$ pilocarpate

The aims of this chapter are:

1. To determine the binding constants for histidine, histamine and pilocarpate and to establish the structure of these complexes from the stoichiometry.
2. To study the effect of coordination on the pKas of neigh-

bouring pendant functional groups.

3. To gather further information on the peculiar 435 nm complex of the parent imidazole.
4. To elucidate the nature of the minor equilibria.
5. To test for the occurrence of mono-imidazole hemin in aqueous solution, starting with monomeric hemin-caffeine.
6. To compare the spectra of cytochrome b_5 and the bis-imidazole complexes in order to see the similarity in electronic structure between the hemoprotein and model complexes.

5.2 Results

5.2.1 Preliminary experiments

Most experiments were done above pH8, to avoid aggregation which occurs below this pH (Chapter 4). Most of the quantitative studies were done up to pH11, because of the high concentrations of ligand (and hence a high ionic strength, which favours aggregation (Chapter 3)), required to overcome the competition from hydroxide.

The addition of imidazole to hemin resulted in the formation of the 435 nm species (figure 5.2) via the 412 nm species with an isosbestic point for the 412 nm to 435 nm conversion at 430 nm. The formation of this species is relatively slow (at 8×10^{-6} M in the presence of 1M imidazole it took about an hour for the equilibrium to be established). High hemin concentrations and low imidazole concentrations, shifted the equilibrium towards the 435 nm species

$$D \rightleftharpoons 412 \text{ nm} \rightleftharpoons 435 \text{ nm}.$$

The 435 nm species shows vibrational overtones at 356 nm and 396 nm.

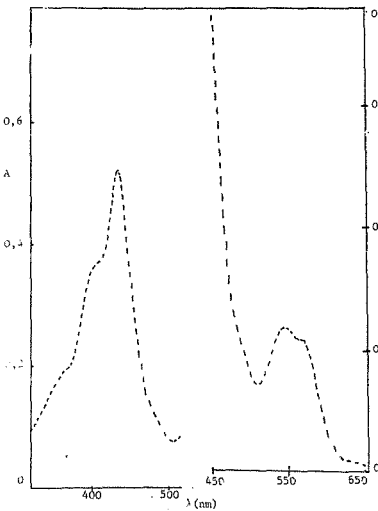

Figure 5.2 Spectrum of the 435 nm species; 7,12 x 10^{-5} M hemin; 1M imidazole; pH12; 25°C; ℓ = 0,1 cm.

Gallagher and Elliott[16] reported that "graphical analysis of the data (for the alkaline dimer to 435 nm species conversion) gave a steep titration curve that approximated to the ideal curve for a reaction in which four molecules of ligand react with the

dimeric hematin without splitting the dimer[11].

The effect of the hemin concentration supports the proposal that this 435 nm species is dimeric. The reversible formation of the 412 nm species on adding more imidazole, supports a dimer rather than an aggregate as the formation of the latter tends to be irreversible. However, the shift in equilibrium towards the normal 412 nm species by an increase in imidazole concentration suggests that the dimer contains less than four ligands.

The addition of low concentrations of detergent ($\sim 10^{-5}$M CTMAB) reversed the formation of this imidazole dimer to give the 412 nm species. This suggests hydrophobic interactions are involved in holding this dimer together, for detergent to have had any effect.

Low concentrations of N-methyl imidazole showed small changes with isosbestic points at 520 nm and 580 nm, while at higher concentrations, the 412 nm species was formed with isosbestic points at 507 and 588 nm (figure 5.3).

The 412 nm species, which has been shown to be the monomeric bis-N-methyl imidazole hemin, [44a] slowly converted to the 435 nm species at $\geq 2 \times 10^{-5}$ M hemin with an isosbestic point at 384 nm, but as found with imidazole, could be suppressed by an excess of ligand. It is possible that this conversion is favoured by ionic strength and this may be the reason why Mohr and Scheler who were working in very low ionic strength solutions apparently did not observe it. The equilibria observed with N-methyl-imidazole are:

D $\rightleftharpoons$ adduct $\rightleftharpoons$ 412 nm (monomeric bis imidazole hemin)

$\Updownarrow$

435 nm (dimeric imidazole hemin)

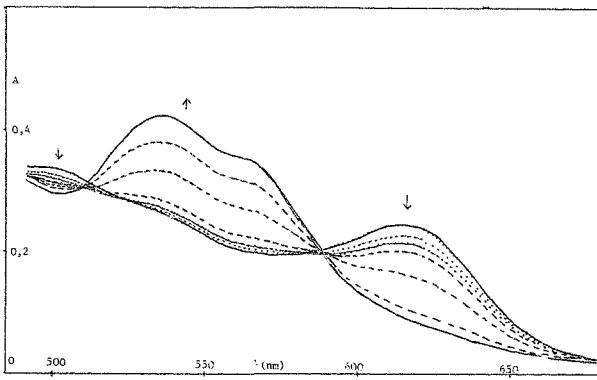

Figure 5.3 Changes in the spectrum of hemin on adding N-methyl imidazole at pH11; $5,6 \times 10^{-6}$M hemin; 25°C; μ = 0,01; ℓ = 10 cm.
—— 0 M; .... 0,025M; 0,038M; ---- 0,063M; 0,10M; 0,14M; —— 0,19M N-methyl-imidazole.

2-methyl-imidazole destabilizes the 412 nm species as shown by its incomplete formation even at concentrations approaching saturation, but forms an adduct at lower concentrations. Figure 5.4 shows the effect on the spectrum in the Soret region at lower concentrations. Little change occurred in the visible region.

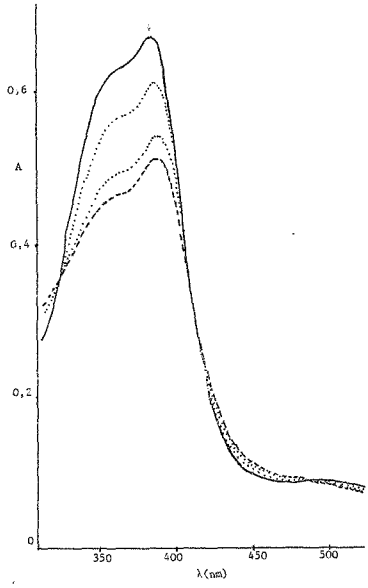

Figure 5.4 Changes in the spectrum of hemin on adding 2-methyl-imidazole; $4,5 \times 10^{-6}$ M hemin; pH12

The spectral changes are similar to those observed on adding adenine and guanidine (Chapter 3), which suggests a donor-acceptor, hydrogen bonded or hydrophobic adduct). No 435 nm species was observed. Steric hindrance to coordination can account for the destabilization of the 412 nm species and perhaps also the 435 nm species.

Histidine, histamine and pilocarpate all show small changes in the spectra at low concentrations, analogous to those observed at low N-methyl imidazole concentrations and at low 2-methyl imidazole concentrations. The isosbestic points were at (400 nm; 610 nm); (401 nm; 502 nm; 614 nm); (392 nm; 498 nm and 590 nm) respectively.

At high ligand concentrations, the 412 nm species was formed with isosbestic points at (392 nm; 500 nm; 585 nm); (394 nm; 502 nm; 582 nm) and (392 nm; 498 nm and 590 nm) respectively. The λmax and $\varepsilon(\lambda max)$ are tabulated in Table 5.1. Histamine shows further changes characterised by an initial increase up to 10 minutes (~2% increase in 1 minute) followed by a slow fall (~16% decrease in ten hours) in the Soret intensity. No 435 nm species was observed with these ligands, presumably because of steric hindrance.

Imidazole and histidine were both added to hemin-caffeine (in alkaline solution). Figure 5.5 shows the spectral changes observed at low ligand concentrations in the visible region. The absorbance at 612 nm decreased while that at ~570 nm increased. In the Soret region the absorbance at 402 nm decreased. These changes are similar to those observed on forming the hemin-caffeine dimer (Chapter 3). For some reason imidazole and

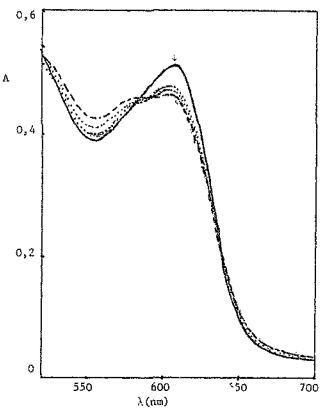

Figure 5.5 Changes in the spectrum of hemin-caffeine on adding low concentrations of imidazole; 7,3 x 10^{-6}M hemin; 0,05M caffeine; —— 0 M; ooo 0,05M; 0,07M; ---- 0,08M imidazole.

histidine may stabilize this dimer. There is no evidence for significant concentrations of the mono-ligand adduct being present (λmax for aquohemoglobin 405 nm; 500 nm; 541 nm (shoulder); 581 nm (shoulder); 629 nm [87]).

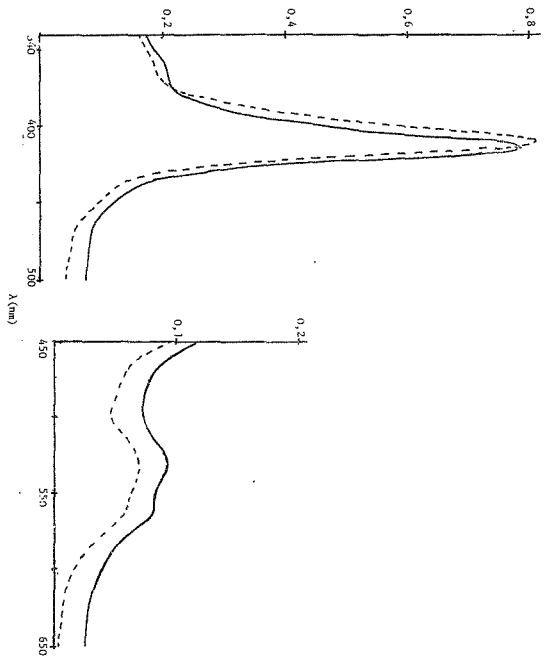

Figure 5.6 Spectra of 7,9 μM monomeric bis-histidine hemin (---) and cytochrome b_5 (——) at pH 8,5 and pH 7 respectively (former solution contains 0,2M histidine); 25°C

Figure 5.6 shows the spectra of cytochrome b_5 and the monomeric bis-histidine hemin (see later). (Note that the protein solution is slightly turbid.) They are similar which supports the assignment as the bis-histidine complex with coordination occurring through the imidazole (as does the negligible effect of glycine and acetate on the spectrum). There are subtle differences in the position and intensity of the Soret intensity which must reflect the effect of the protein. (Table 5.1 summarises the λmax and ε(λmax) for the systems.

Table 5.1 : The λmax and ε(λmax) for the imidazole and analogous complexes with hemin (the 412 nm species)

Ligand/Protein	λmax [a] (ε(λmax))[b]	Reference
imidazole	412(112);530(11);556(9)[c]	16
N-ethyl imidazole	411(121);538(12);560(10)[c]	44a
histidine	411(110);532(10);557(8)	this study
histamine	409(113);530(20);560(9)	this study
pilocarpate	411(111);534(10,1);560(8,5)	this study
cytochrome b_5	413(108);532(13,4);560(11,8)	this study
imidazole methemoglobin	412(105);535(14,7);562(12,5)	87

[a] in nm [b] in x 10^3 M^{-1} cm^{-1} [c] read off spectra

All show similar λmax and extinction coefficients as would be expected for complexes where the iron is coordinated to the same group.

Hence all these bases show a similar pattern in alkaline

solution, viz:

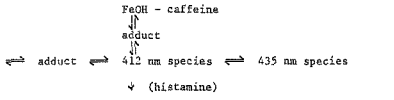

All equilibria were set up rapidly except those between the 412 nm and 435 nm species and the aggregation with the histamine species.

No evidence was found for any significant concentrations of the mono-imidazole complexes.

It is useful to divide these equilibria into major (which involve changes in the coordination sphere) and minor ones (which may involve hydrogen bonding, donor-acceptor or hydrophobic interactions).

The D ⇌ adduct and adduct ⇌ 412 nm species will now be studied more quantitatively with histidine, histamine and pilocarpate as ligands. These were chosen in order to see the effects of the side chains on the equilibria. (Note - the instability of the histamine complex makes the quantitative results unreliable.)

5.2.2 Quantitative determinations of the binding constants

5.2.2.1 Low ligand concentrations

The D ⇌ adduct equilibrium was studied at 590 nm, which is the isosbestic point for the next equilibrium.

The results are given in full in the tables in appendix 4A and summarized in table 5.2. The data fitted a D ⇌ D' equilibrium but not a D ⇌ M equilibrium. Figure 5.7 shows typical

plots of $\log \frac{A-A_o}{A_\infty - A}$ versus $\log$ [ligand], which are linear as is required if a D $\rightleftharpoons$ D' equilibrium holds (appendix 1).

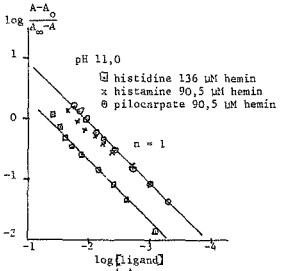

Figure 5.7 Plots of $\log \frac{A-A_o}{A_\infty - A}$ versus $\log$ [ligand] at pH 11 for histidine, histamine and pilocarpate at low [ligand].

In addition the slope gives the number of ligands bound per dimer. In all cases the slope was one, i.e. the equilibrium was

$$D + L \rightleftharpoons D \cdots L \qquad (K_1)$$

Table 5.2 : Summary of the titrations of hemin with low [L]

25^oC; $\mu = 0,5$.

Ligand	pH	$[hemin]_T$/M	slope[a]	log K_1[b]
histidine	8,50	68×10^{-6}	1,05	2,0±0,2
	8,50	136×10^{-6}	1,03	2,1±0,2
	10,00	136×10^{-6}	0,95	1,9±0,2
	11,00	136×10^{-6}	1,06	1,8±0,1
		Av:	1,02	1,9±0,2

Ligand	pH	$[hemin]_T$/M	slope[a]	log K_1[b]
histamine	8,50	$90,5x10^{-6}$	0,91	2,6±0,1
	10,00	$90,5x10^{-6}$	1,16	2,7±0,1
	11,00	$90,5x10^{-6}$	0,86	2,4±0,1
		Av:	0,98	2,6±0,2
pilocarpate	8,50	$90,5x10^{-6}$	1,04	2,23±0,03
	10,00	$90,5x10^{-6}$	0,94	1,8±0,1
	11,00	$90,5x10^{-6}$	1,03	1,9±0,1
		Av:	1,00	2,0±0,2

[a] slope of plot of $\log \frac{A-A_o}{A_\infty-A}$ vs $\log [L]$ (see appendix 1 for derivation

[b] K_1 refers to the equation $D + L \rightleftharpoons D\cdots L$ (units of M^{-1})

Within experimental error there is no effect of pH which indicates no loss of OH^- or uptake of H^+. Hence the K_1 equilibrium can be written:

$$(FeOH)_2 + L \rightleftharpoons (FeOH)_2\cdots L \qquad (K_1)$$

5.2.2.2 High ligand concentrations

The titration at high ligand concentrations was carried out close to the isosbestic point of the first equilibrium, and was done at 413 nm, 409 nm and 410 nm for histidine, histamine and pilocarpate respectively.

In order to obtain the bis-ligand complex, one hydroxide per iron must be lost and hence the equilibrium K_2 would be expected.

$$(FeOH)_2\cdots L + 3L \rightleftharpoons 2FeL_2 + 2OH^- \qquad (K_2)$$

The presence of this equilibrium can be tested in two ways,

viz. by varying the ligand concentration and by varying the hemin concentration. The derivations in appendix 1, show that a plot of log $\frac{[ML_2]^2}{[D\cdots L]}$ versus log [L] should be linear with a slope of three if this equilibrium holds. This is in fact so, with the exception of histamine which is unstable. (Table 5.3 ; figure 5.8; Tables in appendix 4Bi).

Table 5.3 : Summary of the ligand titration results with hemin at high ligand concentrations; 25°C; μ = 0,5

Ligand	pH	slope[a]	log K_2[b]
histidine	9,0	3,1 ; 3,1	-11,2 ; -11,2 (±0,1)
histamine	9,0	2,3	-12,1 (±0,3)
pilocarpate	9,3	$2,9_5$	- 8,4 (±0,3)
pilocarpate	10,2	3,0	- 8,31 (±0,03)

[a] of plot of log $\frac{[ML_2]^2}{[D\cdots L]}$ versus log [L]

[b] K_2 refers to the equilibrium $(FeOH)_2\cdots L + 3L \rightleftharpoons 2FeL_2 + 2OH^-$

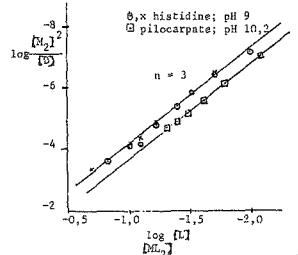

Figure 8 Plots of Log $\frac{[ML_2]}{[D]}$ versus log [ligand] at high [ligand] for histidine and pilocarpate

If the hemin concentration is varied, then if the proposed equilibrium holds, a plot of log $[Fe]_{TOT}\,\alpha$ versus log $[Fe]_{TOT}(1-\alpha)$ (where α is the degree of transformation) should be linear with a slope of 0,5 (appendix 1). This is true for all systems except histamine which is known to be unstable (see table 5.4; figure 5.9 ; tables in appendix 4Bii).

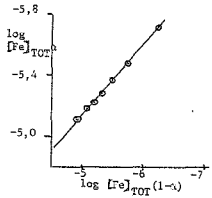

Figure 5.9 Plot of log $[Fe]_{TOT}\,\alpha$ versus log $[Fe]_{TOT}(1-\alpha)$ at high [ligand] for histidine

Table 5.4 : *Summary* of the dilution plot results with hemin at high ligand concentrations; 25°C; μ = 0,5

pH	[ligand]/M	slope[a]	log K_2[b]
a) histidine			
8,5	0,05	0,4	-11,8
9,0	0,05	0,5	-11,1
10,0	0,1	0,5;0,5	$-9,4;-9,4_5$
11,0	0,05	0,5	-8,8
11,5	0,20	0,5	-8,6
12,0	0,20	$0,5_5$	-8,2
b) histamine			
8,5	0,05	$0,2_3$	-12,7
9,0	0,05	0,3	-12,2
10,0	0,10	$0,3;0,2_5$	-9,7;-9,7
11,0	0,10	0,5	-8,1
c) pilocarpate			
8,5	0,005	0,4;0,4;0,4	-9,5;-9,5;-9,7
9,0	0,005	0,5	-9,0
10,0	0,025	0,5	-8,4
11,0	0,05	$0,5;0,5;0,4_5$	-7,4;-7,5;-7,3

[a] of plot of log $[Fe]_{TOT}\alpha$ versus log $[Fe]_{TOT}(1-\alpha)$

[b] refers to the equilibrium $(FeOH)_2\cdots L + 3L \rightleftharpoons 2FeL_2 + 2OH^-$

Log K_2 is not independent of pH which means that something is happening to the ligands. However, if corrections are made for the ionisation of the $-NH_2$ and -OH groups (free and

coordinated respectively), the binding constant becomes pH independent (see table 5.5) (derivations in appendix 5).

Table 5.5 : Correction of the binding constants for the pKas of the ligands

	pH	log K_1	log K_2	log K_1K_2	log K_3 [a]
histidine[b]	8,5	2,0	-11,8	-9,9	-6,4
	9,0	-	-11,2	-9,2	-7,2
	10,0	1,9	- 9,4	-7,5	-7,2
	11,0	1,8	- 8,8	$-6,8_5$	-6,8
	11,5	-	- 8,6	-6,9	-6,7
	12,0	-	- 8,2	-6,3	-6,3
					Average:-6,6±0,6
histamine[c]	8,5	2,6	-12,7	-10,3	-5,2
	9,0	-	-12,2	$-9,5_5$	-6,2
	10,0	2,7	- 9,7	-7,1	-6,3
	11,0	2,4	- 8,1	-5,5	-5,4
					Average:-5,5±0,8
pilocarpate[d]	8,5	2,2	- 9,6	-7,6	-7,6
	9,0	-	- 9,0	-7,0	-7,1
	10,0	1,8	- 8,4	-6,4	-7,0
	11,0	1,9	- 7,4	-5,4	-7,5
					Average:-7,2±0,4

[a] K_3 refers to the equilibrium $(FeOH)_2 + 4RX \rightleftharpoons 2Fe(RX)_2 + 2OH^-$ where X = NH_2 for histidine, histamine; X = OH for pilocarpate

[b] pKa of $-NH_3^+$ (free) used was 9,33 [c] pKa of $-NH_3^+$ (free) used was 9,76 [d] pKa of -OH (coordinated) used was 10.[119]

Hence, the conjugate base in all systems is stabilized by the residual positive charge on the iron(III).

A slight difference in the spectrum above and below the pKa of the coordinated pilocarpate was found. Below the pKa at pH 8,5 the bands were found at 411 nm (111 mM^{-1} cm^{-1}); 534 nm (10,1 mM^{-1} cm^{-1}) and 560 nm (8,5 mM^{-1} cm^{-1}) while above the pKa at pH 12 the bands were at 413 nm (113 mM^{-1} cm^{-1}); 531 nm (10,7 mM^{-1} cm^{-1}) and 559 nm (9,0 mM^{-1} cm^{-1}). The latter are more similar to cytochrome b_5 than the former (table 5.1). Hence neighbouring group interactions in the cytochrome b_5 could account for the difference of the bis-histidine complex spectrum from that of the protein.

The differences in the binding constants are fairly small (and amount to a maximum difference of 1,3 kJ $mole^{-1}$) and are probably due to varying hydrogen bonding and coulombic effects.

Comparisons of the binding constants in other aqueous or mixed aqueous solvents can be made if the binding constant is broken into two parts, i.e. monomerization followed by ligand binding.

$$(FeOH)_2 \rightleftharpoons 2FeOH \qquad K_D^{-1}$$

$$FeOH + 2L \rightleftharpoons FeL_2 + OH^- \qquad K_L$$

Hence $K_1K_2 = (K_D^{-1})(K_L)^2$

K_L is $\geq$ 1,2; 1,8 and 0,9 M^{-1} for histidine, histamine and pilocarpate. These compare well with the values of K_L found in 44% aqueous ethanol (1 M^{-1}) [47] and in micellar detergents (10^{-2} to 10^{1} M^{-1}). [48,49]

5.3 Discussion

The quantitative study of the equilibrium between dimeric hemin and histidine, histamine and pilocarpate in alkaline solution has shown that the main product (412 nm) is the monomeric bis-ligand hemin.

The pH dependence of the equilibrium constants further indicates that the pKa of the $-NH_2$ of histidine and histamine is reduced from about 9,5 to less than 8 on coordination while the pKa of -OH of pilocarpate is reduced from about 15 to 10, on coordination. This can be ascribed to the stabilization of the conjugate base by the residual positive charge on the iron.

We have confirmed that imidazole forms the usual 412 nm species which converts to an unusual 435 nm form. This equilibrium has been shown to be shifted to the right by increasing hemin concentration but to the left by increasing the imidazole concentration, but low concentrations of detergent suppressed it which may be a way of studying the normal bis-imidazole hemin in aqueous solution. This equilibrium was also observed with N-methyl imidazole and was affected in the same way. However, it was not observed with 2-methyl imidazole, histidine, histamine and pilocarpate suggesting that steric hinderance prevents its formation. We conclude that the 435 nm, species is probably dimeric but has less than four imidazoles per dimer.

Adduct formation of the ligand with the dimer has been observed in the systems tested. Quantitative studies of this equilibrium (from the alkaline hemin dimer) with histidine, histamine and pilocarpate showed a pH-independent addition of one ligand to the dimer. Because hydroxide was not lost, it was concluded that the ligand was not coordinated but is forming a

hydrogen bonded or donor-acceptor adduct.

The reaction between the monomeric hemin-caffeine and low concentrations of imidazole or histidine shows the formation of additional complex(es) before the normal 412 nm species. These intermediates show spectra similar to that of the dimeric hemin-caffeine. There appears to be no significant amount of the mono-imidazole complex. Hence one of the roles of the protein in peroxidase, for example, is to stabilize the mono-imidazole form, as $K_1 < K_2$ in aqueous solution as well as in organic solvents.[42,43]

The spectra of the bis-histidine and other bis-ligand complexes (with analogues) are very similar to that of cytochrome b_5. The differences may be explained by neighbouring group interactions as shown by the slight spectral changes above and below the pKa of -OH on coordinated pilocarpate.

CHAPTER 6 - STUDY OF THE REDUCTION OF B_{12a} BY DITHIOTHREITOL

6.1 Introduction

B_{12a} is a useful model for hemoproteins in which one imidazole is coordinated. Hence the monomeric hemins and B_{12a} will be studied in parallel. B_{12a} reduction is discussed here while that of the monomeric hemins is discussed in Chapter 7 (as more is known about B_{12a}).[9] An understanding of reduction is necessary to understand the rate of O_2 uptake (Chapters 8, 9).

Thiols have been used as the reducing agents because they are mild and because they are implicated in the mechanism of cytochrome P 450.[8] It is well known that thiols readily coordinate to B_{12a} and that the rate of reduction to Co(II) increases with pH, but no Co(I) has ever been observed.[9] A quantitative study[64] on the reaction of B_{12a} with cysteine has largely focused on coordination, but it was noted that reduction required another cysteine in addition to the one coordinated, and was only observed above pH 7,2.

Dithiothreitol (Figure 6.1) can reduce B_{12a}[107] but no

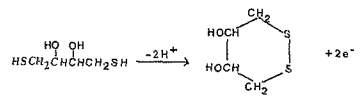

Figure 6.1 Dithiothreitol

quantitative studies have been carried out with this thiol or apparently with any other dithiol. Dithiols are of interest as it is known that some proteins contain two thiol groups close to each other which appear to act in concert,[65] one of the functions of these groups being to transfer electrons.

It was shown that the reduction of FeTPP by thiols in toluene results in the quantitative formation of the disulphide.[58] This was also shown to be the case in the oxidation of thiols by O_2 catalysed by aquocyanocobinamide in aqueous solution [71] and hence will be assumed to be the same here.

The aims of this chapter are to study the kinetics of reduction of B_{12a} by dithiothreitol quantitatively and to propose a mechanism. By comparison with the results of Nome and Fendler on cysteine,[64] the effect of the neighbouring thiol group will be examined.

In considering the mechanism, it must be borne in mind that it may be inner or outer sphere and that the homolytic fission of the Co-S bond may be assisted by another thiol group to give the two-centre three-electron bond species (figure 6.1) or may be unassisted to give the thiol radical.

6.2 Results

6.2.1 Qualitative changes

In preliminary experiments, the spectral changes which occur on adding dithiothreitol to B_{12a} under N_2, were investigated between pH 1 and 12. In all cases Co(II) corrinoid was obtained. Below pH 3 the product bands were at 315 nm; 400 nm (shoulder); and 470 nm which are the bands of the base off Co(II) corrinoid (315 nm; ~405 nm; 470 nm) [9] (i.e. the benzimidazole group becomes

protonated (pKa 2,9) [101] and dissociates from the cobalt). Above pH3, the product bands were at 312 nm; 405 nm and 474 nm which are the base on Co(II) corrinoid bands (312,5 nm; 405 nm and 473 nm).[9]

The intermediate spectra differ in acid (pH ⩽ 6) and alkaline (pH ⩾ 7) solution.

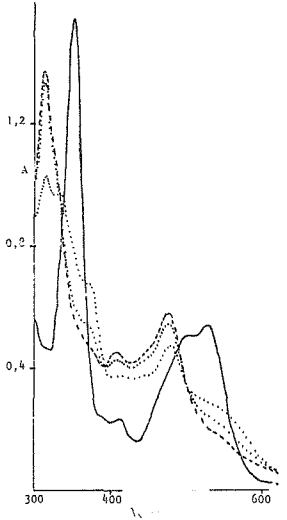

Figure 6.2 Spectral changes occ... ...g on addition dithiothreitol to B_{12a} at pH 4,0 under N_2; $6{,}5\times10^{-5}$M B_{12a};1×10^{-3}M dtt; 25°C;μ=0,1
—— B_{12a}; ····30s and 3,5 minutes after mixing; --- final product (after 40 minutes)

Figure 6.2 shows typical changes occurring in acid solution, which do not show isosbestic points except in the latter part of the reaction at 332 nm; 392 nm; 498 nm. (Initial bands were found at 350 nm; 410 nm; 500 nm; and 526 nm and are those of the aquocobalamin (351 nm; 411 nm; 500 nm and 527 nm.)[102] Intermediate bands are evident at 370 nm; 532 nm and 552 nm which correspond to those of the thiolatocobalamin (370 nm; 532 nm; 552 nm).[64]

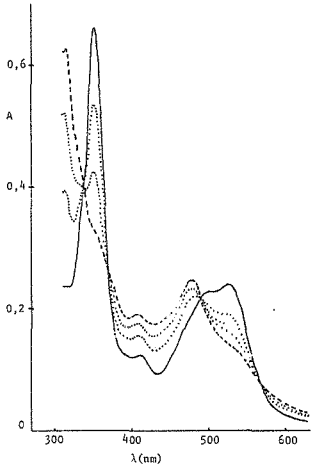

Figure 6.3 Spectral changes occurring on adding dithiothreitol to B_{12a} at pH8,0 under N_2; 3×10^{-5}M B_{12a}; 2×10^{-4}M dtt; 25°C; μ=0,1
—— B_{12a}; ····3,5 and 10 minutes respectively after mixing;
----- final product (after 40 minutes)

Figure 6.3 shows typical changes occurring in alkaline solution where isosbestic points are found at 337 nm; 372 nm; 490 nm and 568 nm throughout. No thiolatocobalamin bands are evident. The initial bands at 357 nm; 420 nm; 514 nm and 536 nm at pH > 8 correspond to those of the hydroxocobalamin (358 nm; 421 nm; 516 nm and 537 nm).[102]

6.2.2 Quantitative kinetic studies

The kinetic studies were carried out using UV-visible spectrophotometry. The absorbance changes at 474 nm (a B_{12r} band) were followed as a function of time, under pseudo first order conditions in B_{12r}, under anaerobic conditions. All the runs gave pseudo first order kinetics.

Most of the runs gave monophasic kinetics over four half lives and in these cases k_{obs} was determined from a plot of $\ln(A_\infty - A)$ vs t (where A_∞ = absorbance at infinite time, A = absorbance time t, t = time) (k_{obs} = -slope). At pH 4 and 5 the runs were biphasic while at higher dithiothreitol concentrations at pH 6,0 they were triphasic (lower dithiothreitol concentrations at pH 6,0 gave biphasic kinetics). By curve stripping,[103] the observed rate constants can be evaluated for the different phases.

There was an induction period, the length of which was dependent on the oxygen concentration. This was minimised by flushing the solutions with N_2 and maintaining the reacting system under N_2 and was reduced to < 20% of the reaction time.

The standard deviations within a run were within 2% while the deviation between different runs was within 6% when there was minimal or constant trace metal contamination.

The dependence of the rate on pH and on the dithiothreitol concentration was determined in these studies.

The qualitative studies indicate a difference in spectral changes in acid and alkaline solution.

In acid, the B_{12a}-thiolate was formed rapidly followed by a relatively slow conversion to B_{12r}.

In alkaline solution, there were isosbestic points between the initial and final species which implies the absence of any significant amount of intermediate. The reduction could be outer sphere but if it is inner sphere, as at low pH, the coordination of thiolate must be slow and the reduction fast.

Hence to understand this system, both regions must be studied. However, the region below pH 3 is not of much interest. The spectra indicate that in this region, the base off B_{12r} was the product and because of the strong trans effect of RS^- [9], the B_{12a}-thiolate may also be base off. The purpose of studying the kinetics of B_{12a} was to simplify the system because of the presence of only one coordination site and at pH < 3 this may no longer be the case.

6.2.2.1 pH profile

Table 6.1 and figure 6.4 show the variation of k_{obs} with pH.

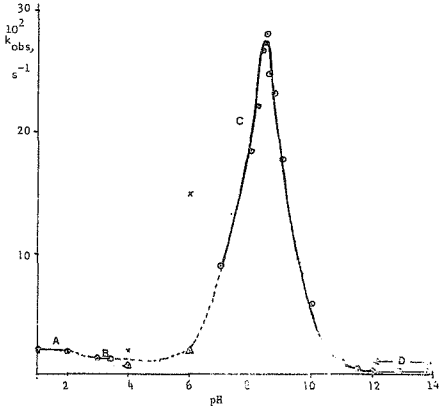

Figure 6.4 Effect of pH on k_{obs} for the reduction of B_{12a} by dithiothreitol; $6{,}5\times10^{-5}$M B_{12a}; 1×10^{-3}M dtt; 25°C;μ=0,1 (under N_2); ⊖ k_{obs}; × k_{obs_1} ; Δ k_{obs_2}

Table 6.1 : The effect of pH on the rate of reduction of B_{12a} by dithiothreitol, $[B_{12a}] = 6,5 \times 10^{-5}$M; [dtt] = 1×10^{-2}M; 25°C; μ = 0,1

pH	$10^2 k_{obs}, s^{-1}$ [a]	(R) [c]	Region
1,10	1,93	(0,9986)	A
1,10	2,17	(0,9988)	
2,00	1,93	(0,9987)	
3,04	1,35	(0,9984)	B
3,33	1,38	(0,9939)	
4,00	1,96 ; 0,68	(0,939) [b]	
6,00	14,9 ; 1,89	(0,999) [b]	
7,00	9,10	(0,9992)	C
7,00	8,72	(0,9995)	
8,00	18,32	(0,9994)	
8,25	22,08	(0,9982)	
8,40	26,66	(0,9990)	
8,50	27,20	(0,9968)	
8,50	28,12	(0,9980)	
8,60	24,74	(0,9964)	
8,75	23,15	(0,9933)	
9,00	17,65	(0,9999)	
10,00	5,79	(0,9988)	
10,52	2,01	(0,9933)	
11,00	1,03	(0,9990)	
11,50	0,35	(0,9984)	
12,00	0,11	(0,9987)	D
12,88	0,11	(0,9986)	
13,74	0,11	(0,9990)	

[a] obtained from -slope of semilog plot

[b] obtained from curve stripping of semilog plot [103]

[c] R is the correlation coefficient

As the kinetics are complex between pH 4 and 6, the kinetic study in acid will be focused on the pH 3 region where the kinetics are monophasic (region B). The other region of interest is between pH 7 and pH 12 (region C). At pH $\geq$ 12, k_{obs} becomes pH independent (region D).

6.2.2.2 pH 3 region (region B)

A comparison of the k_{obs} at pH 3,04 and pH 3,33 (Table 6.1) indicates that in this region, k_{obs} is independent of pH, i.e. independent of both H^+ and OH^- concentrations. Table 6.2 shows that k_{obs} is also independent of the thiol concentration.

Table 6.2 : The effect of the dithiothreitol concentration on the rate of reduction of B_{12a} by dithiothreitol at pH 3,20; 6,5 x 10^{-5}M B_{12a}; μ = 0,1; 25°C.

10^3[dithiothreitol] M	10^2 k_{obs}, s^{-1}	R
1,0	1,47	0,9989
2,5	1,42	0,9990
5,0	1,42	0,9993
10,0	1,00	0,9996

Even at 1x10^{-4}M $CuSO_4$ and 1x10^{-3}M EDTA the rate was unaffected (k_{obs} was 1,35x10^{-2} s^{-1} and 1,39x10^{-2} s^{-1} respectively) unlike the effect of the same concentrations in the alkaline region (see later).

The k_{obs} for the reduction of B_{12a} by mercaptoethanol at pH 5 was found to be 3x10^{-5} s^{-1} with 0,38M mercaptoethanol. The thiolatocobalamin was observed within 20s (bands at 370 nm; 533 nm

and 553 nm), indicating a slow reduction, but relatively fast coordination.

6.2.2.3 pH 7 - 12 region (region C)

a) Effect of pH

The pH profile of the rate of reduction of B_{12a} by dtt in this region is bell-shaped implying two opposing pH effects, for example between the conjugate base of one reagent and the conjugate acid of the other. Both B_{12a} and dtt ionise in this pH region with pKas 7,6 [9] and 9,12; 10,15 [66] respectively. Hence the two possibilities are $Co\text{-}H_2O + RS^-$ or $Co\text{-}OH + RSH$. As RS^- is more effective than RSH as a reducing agent and $Co\text{-}CH_2$ more effective than Co-CH as an oxidising agent, the first alternative will be focused on.

k_{obs} can be corrected for both the fraction of aquocobalamin and thiolate present at each pH. Figure 6.5 shows the plot of k_{obs} corrected for the fraction of aquocobalamin present (k_{corr}) as a function of pH. The midpoint of the curve lies at pH 10,1.

Correcting for the presence of thiolate present at each pH is more tricky because of the two thiol groups. It was found, however, that dividing by either the fraction of $^-S\text{-}R\text{-}SH$ or $^-S\text{-}R\text{-}S^-$ present did not give a constant value at all pHs in this region, but that dividing by (the fraction of $^-S\text{-}R\text{-}SH$ + the fraction of $^-S\text{-}R\text{-}S^-$) did. The implication of this is that B_{12a} does not discriminate between $^-S\text{-}R\text{-}SH$ and $^-S\text{-}R\text{-}S^-$ in the rate determining step. The k_{obs} corrected for both the fraction of aquocobalamin present and the fraction of thiolate (both types) is shown in table 6.3.

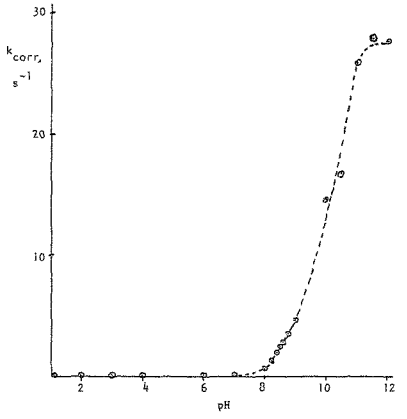

Figure 6.5 Variation of k_{corr} (i.e. k_{obs} corrected assuming only aquocobalamin reacts) with pH (Conditions as in figure 5.3)

Table 6.3 : Correction of k_{obs} for the fraction of aquocobalamin and then for the fraction of thiolate

pH	$10^2 k_{obs}, s^{-1}$	k_{corr}, s^{-1} [a]	k'_{corr}, s^{-1} [b]
7,00	8,91	0,112	14,85
8,00	18,32	0,643	9,05
8,25	22,08	1,21	10,0
8,40	26,66	1,95	12,0
8,50	27,66	2,47	12,5
8,60	24,74	2,72	11,5
8,75	23,15	3,51	11,4
9,00	17,65	4,65	10,3
10,00	5,79	14,48	15,6
10,52	2,01	16,75	17,0
11,00	1,03	25,8	25,8
11,50	0,35	27,8	27,8
12,00	0,11	27,5	27,5

a $k_{corr} = \frac{k_{obs}}{[H^+]/[(H^+)+K_a]}$ where $K_a = 10^{-7,6}$ [9] and refers to the dissociation of a proton from aquo-cobalamin

b $k'_{corr} = \frac{k_{corr}}{f_{RSH-RS^-} + f_{RS^--RS^-}}$ where $f_{RSH-RS^-} = \frac{1}{1 + \frac{[H^+]}{K_1} + \frac{K_2}{[H^+]}}$

$$f_{RS^--RS^-} = f_{RSH-RS^-} \frac{K_2}{[H^+]}$$

(K_1 and K_2 are the first and second acid dissociation constants for the thiols on dithiothreitol, $pK_1 = 9,12$; $pK_2 = 10,15$ [66])

b) Effect of the dithiothreitol concentration on k_{obs}

The effect of the dithiothreitol concentration on k_{obs} is shown in table 6.4

Table 6.4 : The effect of dithiothreitol concentration on the rate of reduction of B_{12a} by dithiothreitol at pH 8,6 in the presence of EDTA; $6,5 \times 10^{-5}$M B_{12a}; 2×10^{-3}M EDTA; $\mu = 0,1$; 25°C

10^2[dithiothreitol], M	k_{obs}, s^{-1}	R
0,1	0,0169	0,9991
1,0	0,102	0,9996
2,5	0,305	0,9996
5,0	0,519	0,9995
7,0	0,708	0,9994
10,0	1,08	0,9993

The plot of k_{obs} against dtt concentration is shown in figure 6.6. It is linear with slope = 10,5 M^{-1} s^{-1} (Sd = 0,3).

The slope is a second order rate constant and can be corrected for the fraction of aquocobalamin and both types of thiolate.

k_{corr} (slope corrected for the fraction of aquocobalamin)
= 115 M^{-1} s^{-1}

k'_{corr} (k_{corr} corrected for fraction of RS^- = RSH + RS^- - RS^-)
= 489 M^{-1} s^{-1}

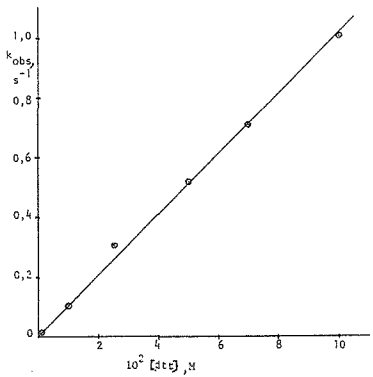

Figure 6.6 Dependence of the rate of reduction of B_{12a} by dithiothreitol on the dithiothreitol concentration at pH 8,6 (in the presence of 2×10^{-3} M EDTA); $6{,}5 \times 10^{-5}$ M B_{12a} ; 25°C ; μ = 0,1 (under N_2)

The linear dependence of k_{obs} on the dtt concentration is consistent with both an inner and outer sphere mechanism. However, k'_{corr} falls within the range of second order rate constants 10^4 reported for the coordination of various ligands (200 - 2000 M^{-1} s^{-1}) even when halved because two thiol groups are present and this lends support to an inner sphere mechanism.

c) Effect of $CuSO_4$ and EDTA on the rate

Table 6.5 shows the effect of $CuSO_4$ and EDTA on the rate of reduction at pH 8,5. It can be seen that $CuSO_4$ increases the rate by approximately a factor of two while EDTA decreases it by about the same amount. Both show a limiting effect.

Table 6.5 : Effect of $CuSO_4$ and EDTA on the rate of reduction of B_{12a} by dithiothreitol at pH 8,50; $5x10^{-3}$M dtt; $6,5x10^{-5}$M B_{12a}; 25°C ; μ = 0,1 (under N_2)

10^4[$CuSO_4$], M	k_{obs}, s^{-1}	10^4[EDTA], M	k_{obs}, s^{-1}
0	0,13	0	0,13
1,0	0,17	2	0,088
4,0	0,20	4	0,063
10,0	0,21	6	0,064

At pH 9, $6x10^{-4}$M cysteamine reduced B_{12a} (k_{obs} $1x10^{-3}$ s^{-1}), even in the presence of $5x10^{-4}$M EDTA (k_{obs} $9x10^{-4}$ s^{-1}) in conflict with Cavallini's results.[105] As found above Cu(II) increased the rate (k_{obs} in the presence of $5x10^{-4}$M $CuSO_4$ was $2x10^{-3}$ s^{-1}). Similar results were found with cysteine, mercaptoethanol and penicillamine. These results show that trace metals such as Cu^{2+} do increase the rate, but are not essential as EDTA did not totally inhibit the reaction. Hence there are intrinsic reactions between B_{12a} and thiols.

6.3 Discussion

The kinetics of the reduction of B_{12a} by dithiochreitol differ in acidic and basic solutions.

In acidic solutions, spectral studies show a rapid formation of Co^{III}-thiolate, followed by a relatively slow formation of Co^{II}. This implies that the rate of coordination is greater than the rate of reduction and that the reaction is most likely inner-sphere.

In alkaline solutions, no Co^{III}-thiolate intermediate is evident which means either that the rate of coordination is slower than the rate of reduction or else the reaction is outer sphere.

In the acid region, the focus will be on the pH 3 region (region B). Above this pH, the kinetics become complex, while below this pH, more than one coordination site may be available (the base off B_{12r} is formed and the base off Co^{III}-thiolate may be involved because of the strong trans effect of thiolate) (region A).

In the alkaline region, the focus will be on pHs between 7 and 12 (region C). At pH > 12 (region D), the rate becomes independent of pH.

pH 3 region (region B)

At pH 3 spectral studies show that the rate determining step is the reduction of Co^{III}-dtt to Co^{II} as thiolatocobalamin was formed rapidly but converted to Co(II) slowly. The rapid rate of coordination of dtt requires that B_{12a} react with the undissociated thiol rather than the thiolate whose concentration is very small at pH 3 (binding of thiolate would require the rate constant for binding to be $\geq 2 \times 10^5$ which is one hundred fold larger than other

reported values for coordination to aquocobalamin).[104] The binding of thiol is probably followed by a rapid proton loss to give the Co^{III}-thiolate. Supporting this is the apparent pH independence of the B_{12a}-cysteine spectrum.[64]

The quantitative studies showed that the rate was first order in B_{12a}, zero order in dtt and independent of pH, and k_{obs} = $(1,35 \pm 0,1) \times 10^{-2}$ s^{-1}. Because of the rapid coordination of dtt, the rate law can be written as:

$$\text{rate} = k_{obs}\,[Co^{III}\text{-dtt}]$$

The rate of reduction of B_{12a} by mercaptoethanol is considerably slower (at pH 5 k_{obs} was 3×10^{-5} s^{-1} with 0,38M mercaptoethanol). This implies that the second thiol group (presumably undissociated) must be responsible for increasing the rate of reduction. Supporting this is the report by Nome and Fendler[64] that a second thiol group is involved in the reduction of B_{12a} by cysteine and also evidence for RS ⟶ SR radicals which stabilize the radical.[67,68] (For the equilibrium $RS^{\cdot} + RS^{-} \rightleftharpoons RS^{-}\!\!-\!\!SR$ $k_f = 3\times10^{9}$ M^{-1} s^{-1} $k_r = 8\times10^{5}$ s^{-1} for cysteine.)

Possible mechanisms are:

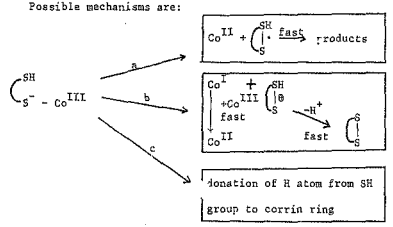

Mechanism c is unlikely because of the strong donor effect of RS^- on the Co and hence a high electron density on the ring.

In mechanisms a and b the further reactions are fast [106] (k for reaction of two thiol radicals is $1,7 \times 10^9\ M^{-1}\ s^{-1}$; [65] proton transfers are usually rapid) and hence the kinetics cannot distinguish between them. However, as the protonated disulphide is not known, mechanism a is the preferred one. (Some of the complications in the pH 5 - 6 region could be due to the pKa (5,5) [68] of the dtt radical.

pH 7 - 12 region (region C)

In this pH region, spectral studies showed no intermediate in the reduction of B_{12a} by dithiothreitol. This could either be due to an outer sphere mechanism or else an inner sphere mechanism where coordination is slow while reduction is fast.

The pH profile is bell shaped and this can be explained by the major reaction being between aquocobalamin and thiolate, with aquocobalamin not distinguishing between ^-S-RSH and $^-S^--RS^-$. (The reaction could be inner or outer sphere.)

The rate is first order in B_{12a} and thiol and this is consistent with either rate determining coordination in an inner sphere mechanism or an outer sphere mechanism. When the second order rate constant obtained is corrected for the fraction of aquocobalamin and thiolate a value of $489\ M^{-1}\ s^{-1}$ is obtained. This value is within the range of rate constants for coordination ($200 - 2000\ M^{-1}\ s^{-1}$) previously reported. [104] This is support for the inner sphere mechanism but does not rule out the outer sphere mechanism. However, the inner sphere mechanism is preferred because this is the mechanism operating in acid.

The rate of reduction at high pH is considerably faster than at low pH. This implies that a second thiolate group, rather than a second thiol group, results in a lower activation energy in the reduction step. In the alkaline region at pH's where the ^{-}S —RS^{-} concentration is low, coordination of dtt could well be followed by a rapid proton loss from the second thiol group, resulting in a rapid reduction step. The radical intermediate  is kinetically more stable than  (the bimolecular decay rate constants are $1,7 \times 10^{8}\ M^{-1}\ s^{-1}$ and $1,7 \times 10^{9}\ M^{-1}\ s^{-1}$ respectively [68]) and this stability could result in a lower activation energy for the formation reaction of the former.

The effect of Cu^{2+} in this pH region and not in the pH 3 region could well be a consequence of relatively slow coordination in this pH region, which enables the Cu - dtt complex to reduce the B_{12a} by an outer sphere mechanism. In the pH 3 region, the high electron density on the corrin ring in the Co(III)-thiolate complex would inhibit an outer-sphere reduction.

pH 12 - 14 region (region D)

The rate was pH independent in this region and no thiolatocobalamin was observed. This indicates that direct reaction between hydroxocobalamin and thiolate (most likely ) either by outer sphere electron transfer or via coordination, as at other pHs. However, there is insufficient evidence to decide.

It can be concluded that the main redox reaction involves coordination of thiolate to Co(III). The reduction is not simply

$$RS^{-}\text{—Co(III)} \longrightarrow RS^{\cdot} + \text{Co(II)}$$

but must be assisted by a second RSH, or better RS^- to give $RS\overset{\delta-}{-}\overset{\delta+}{S}HR$ or $R\overset{\delta+}{S}\overset{\delta-}{S}R$.

This emphasises the importance of having two neighbouring -SH groups (as found in the thioredoxins).[65]

Catalysis by copper(II) was also found when the rate of coordination was slow compared to reduction.

CHAPTER 7 - REDUCTION OF THE HEMIN-CAFFEINE ADDUCT AND THE BIS-HISTIDINE HEMIN COMPLEX BY THIOLS

7.1 Introduction

As hemin is the actual prosthetic group of hemoproteins, it would obviously be of interest to study its reduction under conditions where it is monomeric. In chapter 3, it was shown that the caffeine adduct of hemin in alkaline solution (hemin-caffeine) is monomeric as long as the hemin concentration does not exceed $1,5 \times 10^{-5}$M. In chapter 5, it was shown that the complex with histidine at high histidine concentrations was the monomeric bis-histidine hemin (referred to here as hemin-histidine). The reduction of both these complexes will be discussed.

Most studies of the reactions between iron porphyrins and thiols have focused on model studies of oxidised cytochrome P-450, where cysteine coordination in the resting and substrate-bound oxidised forms can account for its observed spectral properties.[59-61] The other ligand in the resting state could be H_2O or histidine, with recent model studies supporting the former.[59] In addition to these model studies, a study of the reduction of FeTPP by thiols in toluene has been reported.[58]

As was mentioned in chapter 6, reduction could occur via an inner or outer sphere mechanism and if the former, could go via the mono and/or bis thiolate complexes and may or may not be assisted by the second thiol functional group in the molecule. In addition, dithiothreitol has a number of hydrogen bonding sites and could hydrogen bond to the propionate side chains of the porphyrin and to the ligand, histidine. Hence dithiothreitol can act as a ligand, as a reducing agent and can hydrogen bond.

It has been shown in our laboratory[108] that the reduction of the bis-histidine hemin complex by cyclic voltametry requires the simultaneous uptake of a proton between pH 8 and 10. It was shown in chapter 5, that on coordination of histidine to hemin, the pKa of the $-NH_3^+$ groups drops from 9,3 to less than 8 because of the stabilization of the conjugate base by the residual positive charge on the Fe(III). No residual charge is present on the Fe(II) and hence the pKa should be close to its normal value. Therefore on reduction between pH 8 and 10, a proton must be taken up by the $-NH_2$. This should also be the case if the bis-histidine complex is reduced by thiols and this will be investigated.

Hence the aims of this study are to elucidate the mechanism of reduction both by quantitative kinetic measurements and from the spectral changes. In addition the effect of different thiols and the presence of copper(II) on the rate of reduction will be examined qualitatively, the former to establish the effectiveness of dithiols as opposed to monothiols, and the latter to see whether copper(II) is necessary for the reduction of hemin, as it is involved in the mechanism of reaction of cytochrome c oxidase.

7.2 Results

7.2.1 Hemin-caffeine

Only qualitative experiments were carried out with hemin-caffeine, as preliminary experiments showed that the kinetics of reduction by dithiothreitol were generally biphasic. Curiously the pseudo first order rate constants increase with hemin concentration, suggesting reduction via a dimeric species whose rate of formation is fast.

The addition of thiols such as dithiothreitol (dtt), mercapto-

ethanol and cysteine to hemin-caffeine, resulted in a final species with bands at 396 nm (shoulder), 414 nm, 428 nm (shoulder), 536 nm and 571 nm, which corresponds well to those reported for heme-caffeine (416 nm, 434 nm (shoulder), 537 nm, 569 nm).[12] No bands due to heme c (412 nm, 542 nm, 560 nm) were evident.[109] (Heme c could be formed by addition of the thiol across the vinyl groups on the porphyrin ring.) Isosbestic points were found at 412 nm, 456 nm, 523 nm, 586 nm, 670 nm, but the original hemin-caffeine spectrum did not pass through the last three which indicates the presence of an intermediate. Because of the shoulders of the Fe(III)OH caffeine and the Fe(II) caffeine at 360 nm and 440 nm respectively, the intermediate could not be identified but presumably is the monothiolate hydroxo complex (see later).

It was found that different thiols reduced hemin-caffeine at different rates. At pH 10,0; in the presence of 0,1M caffeine at 25°C, the approximate half lives for the reduction of $1x10^{-5}$M hemin by $4x10^{-4}$M thiol (under N_2) were 17s (dithiothreitol); $1x10^{3}$s (mercaptoethanol); $7x10^{3}$s(cysteine). It can be seen quite clearly that the dithiol, dithiothreitol, reduced hemin-caffeine markedly faster than either of the monothiols. This was also found to be the case for the reduction of B_{12a} (chapter 6) where it was attributed to a second thiol group which is nearby in the dithiols, assisting the homolytic fission of the Co-S bond, resulting in a fairly stable RS——SR radical.

The addition of $CuSO_4$ and EDTA had no effect on the rate of reduction by dithiothreitol, cysteine and mercaptoethanol under the conditions outlined above (i.e. rate varied by < 5%). However, no reduction of hemin-caffeine by $1,2x10^{-3}$M penicillamine

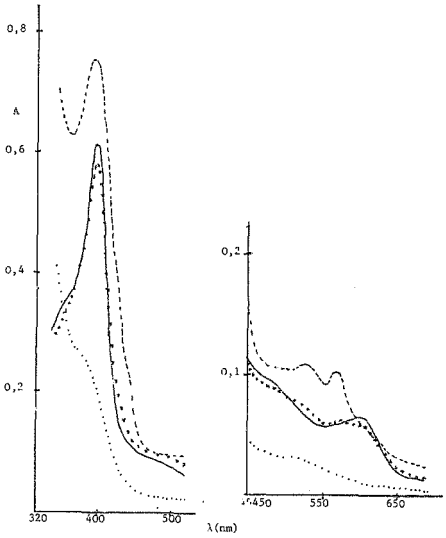

Figure 7.1 : Spectral changes on adding penicillamine to hemin-caffeine in the presence and absence of $CuSO_4$. All solutions in pH9 buffer at 25°C; μ=0,1;(caffeine)=0,05M; —— no penicillamine; (hemin)=7,6x10^{-6}M; xxxx plus 5x10^{-3}M penicillamine 5 hours after addition to hemin-caffeine (no $CuSO_4$ added); ---- 5x10^{-3}M penicillamine + 1x10^{-4}M $CuSO_4$ between 15s and 3 min after the addition of $CuSO_4$; .... 1x10^{-4}M $CuSO_4$ added to 1x10^{-3}M penicillamine between 15s and 3 min after mixing (no hemin)

$((CH_3)_2C(SH)CH(NH_2)CO_2H)$ was observed up to an hour after mixing in the absence of Cu(II). When $1x10^{-4}$M $CuSO_4$ was added, the half time was less than two minutes for the formation of the $\alpha\beta$ bands of heme-caffeine (537 nm, 569 nm) (see figure 7.1) Unfortunately the Cu-penicillamine complex (reportedly $[Cu(1)_8Cu(II)_6L_{12}C\ell]^{5-}$)[110] absorbs in the UV-visible at ~320 nm, 380 nm (shoulder) and 510 nm. These bands are evident in the presence and absence of hemin-caffeine when Cu(II) is present. This Cu-penicillamine complex could be reducing hemin-caffeine by an outer mechanism, an inner mechanism being unlikely because of steric hindrance.

The bands of heme-caffeine decrease with time, and this could be due to either aggregation and/or decomposition but has not been studied further.

7.2.2 Hemin-histidine

7.2.2.1 Qualitative studies

On adding $1x10^{-2}$M thiol (dithiothreitol, cysteine and mercapto-ethanol to $\sim10^{-5}$M hemin at pH 10, a final spectrum with bands at 421 nm, 526 nm and 556 nm (see figures 7.2a, b) was found. Table 7.1 shows the band positions of the bis-histidine, bis-histamine and bis-pilocarpate complexes reduced by a few grains of dithionite at pH 8,5 (0,2M ligand; $7,3 \times 10^{-6}$ M hemin). (Reduction is complete within 5s. Reoxidation by O_2 is rapid (complete within 1 minute on shaking in air).) The bands of reduced cytochrome b_5 are also included as are those of the monothiomate and bis-thiolate complexes.

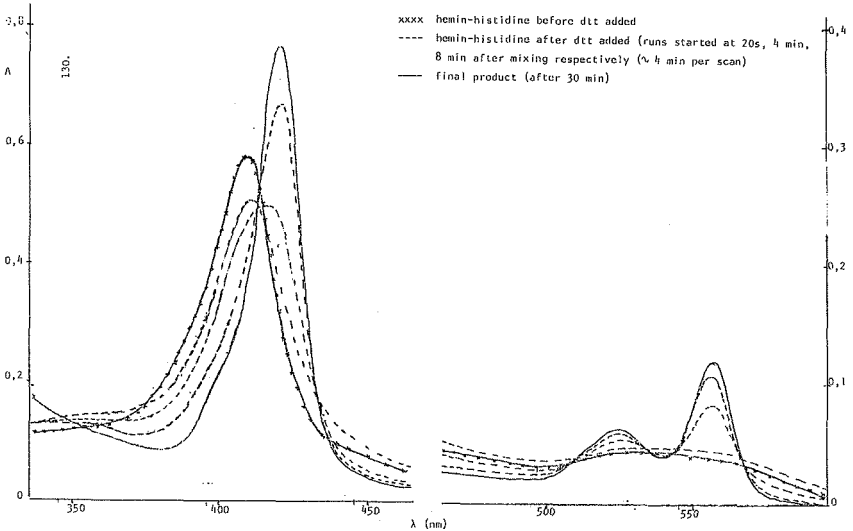

Figure 7.2a: Spectral changes observed on adding low concentrations of dithiothreitol to hemin-histidine at 2°C; [hemin] = 5×10^{-6} M; [histidine] = 0,4 M; [dtt] = 4×10^{-4} M; pH 10; μ = 0,5

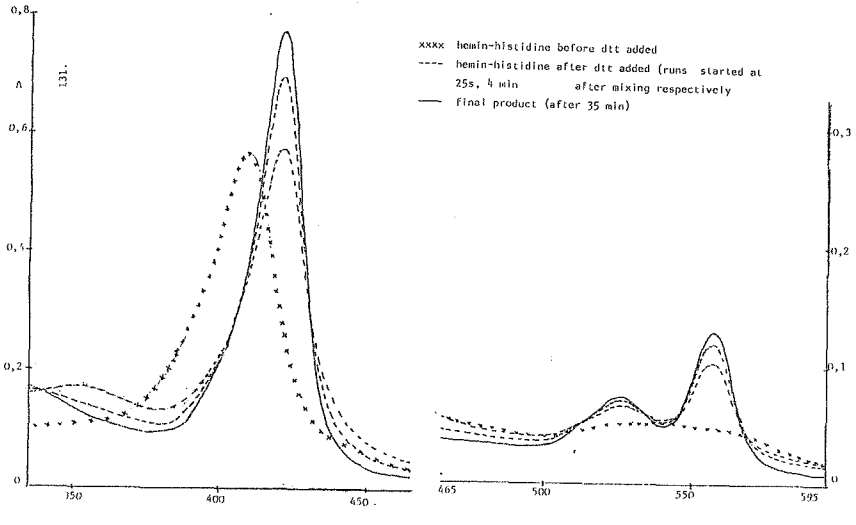

Figure 7.2b: Spectral changes observed on adding high concentrations of dithiothreitol to hemin-histidine at 2°C; [hemin] = 5×10^{-6}M; [histidine] = 0,32M; pH 10,0; μ = 0,5; [dtt] = 0,1M.

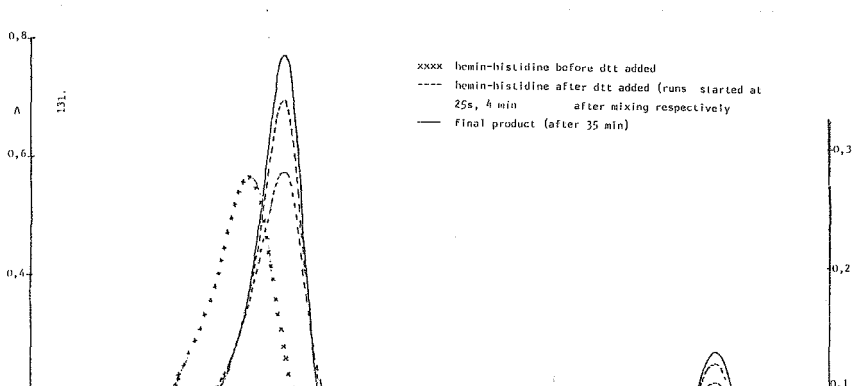

Figure 7.2b: Spectral changes observed on adding high concentrations of dithiothreitol to hemin-histidine at 2°C; [hemin] = 5×10^{-6}M; [histidine] = 0,32M; pH 10,0; μ = 0,5; [dtt] = 0,1M.

Table 7.1 : Band positions of species relevant to the reduction of hemin-histidine by thiols

System	/nm	Ref.
bis-histidine hemin reduced by *thiols*; ~$1x10^{-5}$M *hemin*; 0,4M histidine; pH 10	421;526;556	this study
bis-histidine hemin reduced by dithionite; $7,3x10^{-6}$M hemin; 0,2M histidine; pH 8,5	421;525;556	this study
bis-histamine hemin reduced by dithionite; $7,3x10^{-6}$M hemin; 0,2M histamine; pH 8,5	421;526;556	this study
bis-pilocarpate hemin reduced by dithionite; $7,3x10^{-6}$M hemin; 0,2M pilocarpate; pH 8,5	422;529;556	this study
reduced cytochrome b_5 pH 7,4; reduced by dithionite	422,5;525;556	80
reduced cytochrome b_5 pH 7; reduced by dithionite	423;527;556	this study
imidazole-thiol-hemin in CH_2Cl_2	~360;428;538;568	59
ethanol-thiol-hemin in CH_2Cl_2 + CH_3CH_2OH	~360(sh);415;530;561	59
resting P-450_{LM_2} in aqueous solution	360(sh);418;538;568	8
bis-thiol hemin in CH_2Cl_2	377;475;565	59
P-450_{LM_2} plus 1-octanethiol in aqueous solution	377;467;550	59

It will be clearly seen that the reduced bis-histidine, bis-histamine and bis-pilocarpate hemin complexes all have very similar bands to those of reduced cytochrome b_5 which indicates that they are $Fe(II)L_2$. It makes no difference to the final spectrum whether hemin-histidine is reduced by thiols or dithionite. Certainly the final bands are not those of the oxidised hemin with thiol coordinated. It must be noted that at high hemin concentrations ($1x10^{-3}M$) in histidine (reduced by dithionite) the 526 nm and 556 nm bands are only found by themselves in saturated histidine (~0,6M) and as the histidine concentration is decreased they decrease in intensity while new bands at 558 nm and 580 nm appear. They also decrease with time (~8% per min at 0,06M; 4% at 0,6M) at a particular histidine concentration while the bands at 558 nm and 580 nm increase showing that the Fe(II) bis-histidine complex is unstable. At 0,06M histidine only these new bands are evident. These bands correspond well to that reported by Shack and Clark[10] for the heme dimer (560 - 580 nm). Hence $Fe(II)L_2$ tends to aggregate.

In the spectrum of hemin-histidine reduced by dithiothreitol, cysteine, ethanethiol andmercaptoethanol, there were no bands due to heme c bis-histidine (which would be at 414 nm, 520 nm and 549 nm).[109]

Figures 7.2a and b show the spectral changes observed on adding dithiothreitol to hemin-histidine at $2^{o}C$ at pH 10,0 at low ($4x10^{-4}M$) and high (0,1M) dithiothreitol concentrations. Isosbestic points were found both at low dithiothreitol concentrations (at 402 nm, 433 nm, 509 nm, 534 nm, 544 nm and 566 nm) and at high dithiothreitol concentrations (at 402 nm, 430 nm, 509 nm,

535 nm, 544 nm and 566 nm) which were the same within experimental error. The initial spectrum (i.e. before the addition of dithiothreitol did not pass through these isosbestic points, which indicates the presence of a rapidly formed intermediate. There were no major bands of coordinated thiolate species (see table 7.1) but these could well be masked by those of the reduced species. However, shoulders at 360 nm and 440 nm are present and as these are found in the monothiolate complexes (with imidazole or ethanol coordinated) but not the initial or final species, these are possible intermediates (in this case with histidine or H_2O/OH^- coordinated). There is no spectral evidence for the bis-thiolate complex. Similar shoulders at 360 nm as well as isosbestic points between the intermediate and final product but not the starting species were found at room temperature with $4x10^{-5}$M dithiothreitol (at higher concentrations, the reaction was too fast to follow with the spectrophotometer at 25°C); and $4x10^{-4}$M mercaptoethanol, cysteine and ethanethiol. Only a small amount of the 360 nm band was found with cysteine, indicating a shift in the equilibrium towards the starting species.

As found with hemin-caffeine, the Fe(II) bands decreased with time and could be due to aggregation and/or decomposition, but has not been studied further. In light of the studies at high hemin concentrations, is is probably aggregation. Care has been taken in the quantitative studies to ensure that this subsequent reaction is negligible during the reduction reaction. Dithiothreitol was chosen because the reduction was much faster than the subsequent reaction. The overlap with the subsequent reaction ruled out quantitative studies with the monothiols.

Different thiols reduced hemin-histidine at different rates. The reduction of $1x10^{-5}$M hemin in the presence of 0,4M histidine at pH 10; 25°C under N_2 by $4x10^{-4}$M thiol occurred with the following half lives: 18s (dithiothreitol); $1x10^{4}$s (mercaptoethanol); $2,4x10^{3}$ (cysteine). These rates are similar to those found with hemin-caffeine and also show the greater efficiency of the dithiol compared to the monothiol.

The addition of $CuSO_4$ and EDTA had no effect on the rates of reduction at pH 10 by thiols, including penicillamine. (Rate varied by < 5% in the presence of $1x10^{-4}$M $CuSO_4$ or $1x10^{-3}$M EDTA.)

7.2.2.2 Quantitative studies with dithiothreitol as the reducing agent

The kinetics were followed by stopped-flow UV-visible spectrophotometry. The absorbance changes were monitored at 556 nm which is a peak position of Fe(II) bis-histidine protoporphyrin where the absorbance changes are fairly large and are mainly due to the conversion from the monothiolate complex to the product (see figures 7.2a and b). All runs had an induction period, the length of which depended on the oxygen. This was minimised to < 10% of the reaction time by thorough flushing of the solutions with N_2 before mixing and maintaining them under N_2 during the reaction.

Conditions were such that the runs were pseudo first order in hemin and in fact plots of $\ln(A_\infty - A_t)$ versus time were linear over at least four half lives. All results will be reported as k_{obs} which is (-slope) of the above plot. Repeat runs gave results within 8% of each other (the reported values are the average of three repeat runs) while the standard deviations within a run were within 1% and the correlation coefficients $\geq 0,999$.

The dependence of the rate on the hemin, thiol and histidine concentrations as well as the pH was determined quantitatively.

k_{obs} at $5{,}6\times10^{-6}$M and 3×10^{-5}M hemin with 2×10^{-4}M dtt, in the presence of 0,4M histidine at pH 10,0 was $2{,}13\times10^{-2}$ s^{-1} and $2{,}15\times10^{-2}$ s^{-1} respectively. Hence as required by pseudo first order kinetics, k_{obs} is independent of the hemin concentration.

The dependence of k_{obs} on the dithiothreitol concentration was studied over a 500-fold concentration range because of the complex dependence found, as shown in figure 7.3 and table 1 (appendix 6).

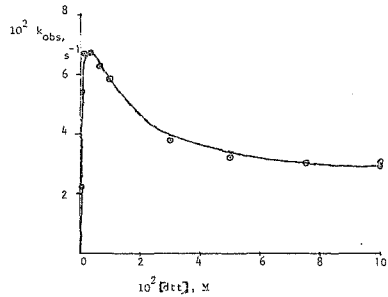

Figure 7.3 Effect of the dithiothreitol concentration on the reduction of hemin-histidine by dithiothreitol; 3×10^{-5}M hemin; 0,4M histidine; pH 10,0; μ = 0,5; 25°C. Line is theoretical curve calculated from proposed rate law and calculated parameters.

The histidine concentration dependence was studied at high and low dithiothreitol concentrations. The effect on the rate could only be studied over a two-fold concentration range. The histidine concentration had to be $\geq$ 0,2M to ensure over 98% formation of the monomeric hemin-bis-histidine complex. This was necessary to avoid complications from reactions of other species (see chapter 5). The solubility of histidine prevented the use of concentrations greater than 0,4M at 25°C. Thus, the study was restricted to concentrations of histidine between 0,2 and 0,4M.

Figure 7.4a shows the effect on k_{obs} of the histidine concentration at low dithiothreitol concentration. It can be seen that k_{obs} is inversely proportional to the histidine concentration. The zero intercept indicates that no reaction occurs at infinite histidine concentration, which rules out an outer sphere reduction of the bis-histidine as a possible mechanism.

Figure 7.4b shows the effect on k_{obs} of the histidine concentration at high dithiothreitol concentration. It is quite clearly independent of the histidine concentration. (Data at both high and low dithiothreitol concentrations are given in tables 2a and b, appendix 6.)

The effect of pH at low dithiothreitol concentrations, where the kinetics are simpler (see later) was determined. Table 3 (appendix 6) gives the experimental data as well as these values corrected for the fraction of bis-histidine present initially. (As the pH increases, OH^- competes with histidine as a ligand to Fe(III)).

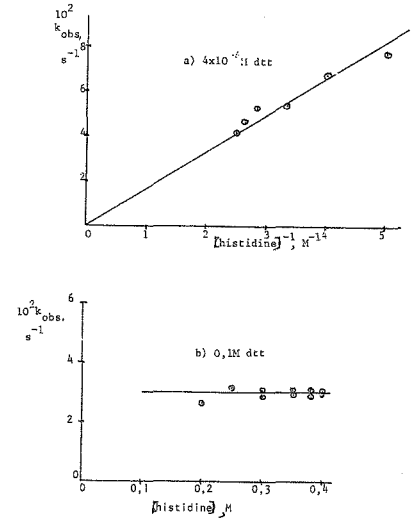

Figure 7.4 Effect of the histidine concentration on the reduction of hemin-histidine by dithiothreitol; $3x10^{-5}$M hemin; pH 10,0 ; μ = 0,5; 25°C (under N_2)

Figure 7.5 shows the effect of pH on these corrected values.

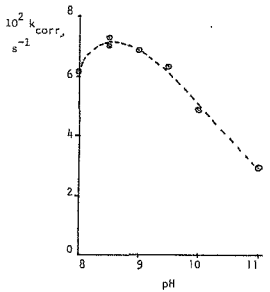

Figure 7.5 Correction of k_{obs} for the fraction of hemin-histidine present initially; $3x10^{-5}$M hemin; 0,4M histidine; $4x10^{-4}$M dtt; 25°C; μ = 0,5

The maximum in the pH profile occurred at pH 8,5 and the inflection in the downward limb occurred at pH 10. A bell shaped pH profile is indicative of two opposing pH effects, and was found with B_{12a} where aquocobalamin reacted with the thiolate (chapter 6). In this system, however, the decrease from pH 8,5 to 8 could be a consequence of some aggregation of the starting species.

7.3 Discussion

Both spectral and kinetic results must be considered in deciding on the mechanism. Broad possibilities are inner or outer sphere reduction. Outer sphere reduction of the bis-histidine hemin can be ruled out because no reduction occurs at infinite histidine

concentration (figure 7.4a). Outer sphere reduction of *thiolate* complexes is not likely, as their greater electron density compared to that of the bis-histidine complex would make reduction more difficult. Hence reduction must occur via an inner sphere mechanism. The bis-thiolate complex has been reported [59] but can be ruled out as a significant intermediate in this system as none of the expected bands (see table 7.1) were observed. The inhibition *by dithiothreitol* at high dithiothreitol concentrations, however, requires a species containing two thiolates which reduces more slowly than the species containing one thiolate. If the second thiolate is hydrogen bonded, this would explain the kinetics and would be in accord with the observed spectral changes (hydrogen bonding would not be expected to affect the UV-visible spectrum significantly).

In the inner sphere mechanism, either coordination or reduction can be rate limiting. However, rapid formation of the intermediate followed by relatively slow reduction was observed (see figures 7.2a and b). Hence reduction is rate limiting, which is consistent with the mathematical analysis (see appendix 7). Since good first order kinetics were found even where a mixture of species must be present, a rapid equilibration of the Fe(III) species must occur, together with slow reduction steps.

In deriving a rate law the following assumptions were made:

1) The reverse reactions of the reduction steps are negligible because of the low concentrations of radicals expected (the second order rate constant for the dithiothreitol radical is $1.7 \times 10^8\ M^{-1}\ s^{-1}$).

2) The ligand binding and dissociation reactions of the Fe(II)

complexes are rapid and hence do not appear in the rate law, as they occur after the rate determining step(s) (the first order rate constants for ligand dissociation from Fe(II) porphyrins are of the order of 10^2 s^{-1}). [111]

A mechanism which can account for the observed kinetics and spectra is given in equations (7 - 1) - (7 - 4) (ignoring the pKas of the dithiothreitol), where dtt' is the oxidised radical form.

$$Fe(III)(his)_2 + dtt \underset{k_{-1}}{\overset{k_1}{\rightleftharpoons}} Fe(III)(his)(dtt) + his \qquad (7\text{-}1)$$

$$Fe(III)(his)(dtt) \xrightarrow{k_2} Fe(II)(his) + dtt \xrightarrow{fast} products \qquad (7\text{-}2)$$

$$Fe(III)(his)(dtt) + dtt \underset{k_{-3}}{\overset{k_3}{\rightleftharpoons}} Fe(III)(his)(dtt)\cdots(dtt) \qquad (7\text{-}3)$$

$$Fe(III)(his)(dtt)\cdots(dtt) \xrightarrow{k_4} Fe(II)(his)\cdots dtt + dtt' \xrightarrow{fast} prod. \qquad (7\text{-}4)$$

(The reduction of the hydrogen bonded adduct is not likely to go via an outer sphere mechanism because of the high electron density.)

A rate law was derived (see appendix 7) which predicts three phases. [112] As all the kinetic runs were monophasic, two of these must be rapid and these are the thiol binding steps because the rapid formation of an intermediate is seen. The monophasic rate law can be shown to be:

Rate = k_{obs} [hemin-histidine] where

$$k_{obs} = \frac{x[dtt] + y[dtt]^2}{z + v[dtt] + w[dtt]^2}$$

and $x = k_1k_2(k_{-3} + k_4)$

$y = k_1k_3k_4$

$z = (k_2 + k_{-1}(his))(k_{-3} + k_4)$

$v = k_3k_4 + k_1(k_2 + k_4 + k_{-3})$

$w = k_1k_3$ (see appendix 7)

Values for x, y, z, v, w were found using a simplex optimization routine. Figure 7.6 shows the theoretical curve where x = 43,9; y = 1346; z = 0,282; v = 432; w = 57020. The theoretical values lay within 5% of all the experimental points.

Values of the microscopic rate constants can be calculated if approximations are made.

If the ligand dissociation steps are rapid compared to the reduction steps then $(k_2 + k_{-1}[his]) \approx k_{-1}[his]$; $(k_{-3} + k_4) \approx k_{-3}$; $[k_3k_4 + k_1(k_2 + k_4 + k_{-3})] \approx k_1k_{-3}$ and the values of k_2 ($= \frac{x}{v}$); k_4 ($= \frac{y}{w}$); $K_1 = \frac{k_1}{k_{-1}}$ ($= \frac{v}{z}$ [his]) and $K_3 = \frac{k_3}{k_{-3}}$ ($= \frac{w}{v}$) were 0,102 s^{-1}; 2,36 x 10^{-2} s^{-1}; 613 and 132 M^{-1} respectively. (If ligand dissociation is slow compared with reduction, the dependence of the rate on the histidine concentration at low thiol concentrations cannot be accounted for.)

These values are reasonable. The binding constant for the second thiol, K_3 (132 M^{-1}), is comparable with those found for the histidine (and analogues) adduct with the alkaline hemin dimer (chapter 5) (79 - 400 M^{-1}) and is consistent with a weak interaction such as hydrogen bonding (there is certainly no shortage of suitable sites!).

The dependence on the histidine concentration can also be accounted for with this rate law. At low dithiothreitol concentrations, the $[dtt]^2$ terms are unimportant and hence

$$k_{obs} \approx \frac{x[dtt]}{z+s[dtt]} \approx \frac{k_1k_2k_{-3}[dtt]}{k_{-1}[his]k_{-3}+k_1k_{-3}[dtt]}$$

$$\therefore \frac{1}{k_{obs}} \approx \frac{k_{-1}}{k_1k_2[dtt]}[his] + \frac{1}{k_2}$$

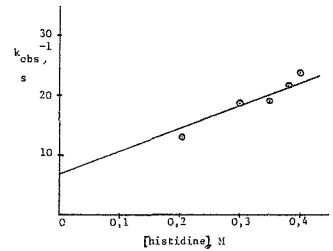

Figure 7.6 Plot of $\frac{1}{k_{obs}}$ versus histidine concentration 3×10^{-5}M hemin; 4×10^{-4}M dtt; pH 10,0; μ = 0,4; 25°C (under N_2)

The plot of $\frac{1}{k_{obs}}$ versus [his] is in fact linear with slope = 37,5 M s and intercept = 7 s^{-1} (figure 7.6). This results in $\frac{k_1}{k_{-1}} = K_1 = 467$ and $k_2 = 0,14\ s^{-1}$ which is in fair agreement with the values found above (612 and 0,10 s^{-1} respectively). This inverse dependence of the rate on the histidine concentration shows that the intermediate is in fact the thiolate-histidine hemin complex as the thiolate-aquohydroxo hemin complex would not give this result.

At high dithiothreitol concentrations, the z term becomes negligible and hence

$$k_{obs} \approx \frac{k_1 k_2 k_{-3}[dtt] + k_1 k_3 k_4 [dtt]^2}{k_1 k_{-3}[dtt] + k_1 k_3 [dtt]^2}$$

k_{obs} is independent of the histidine concentration which is what was observed. (The results are not good enough to rule out the loss of histidine in reaction (7 - 3) but the similarity of the isosbestic points at high and low dtt concentrations make this possibility very unlikely.)

Hence the proposed rate law can account for the spectral changes and for the observed dependences on the dithiothreitol concentration and the histidine concentration as well as of course the hemin concentration.

The effect of pH on the rate is too complex to analyse what with two parallel reduction steps and pKas of thiol and histidine ($-NH_3^+$) probably being significant, as well as having limited data. We merely note that the apparent pKa of 10 in the downward limb could be associated with the pKa of dithiothreitol or possibly an uptake of a proton on reduction as found by cyclic voltametry.[108]

7.4 Conclusions

Hemin-histidine like B_{12a} is reduced by thiols via an inner sphere mechanism. Reduction was found to be rate limiting. The simple monothiolate complex reduced with $k = 0,1\ s^{-1}$, compared with that of B_{12a} in alkaline solution $k>0,3\ s^{-1}$ (coordination was rate limiting at alkaline pHs). Hence the rate of reduction of B_{12a} is faster than that of hemin-histidine.

Presumably the faster reduction by the dithiol compared to the monothiols, reflects the homolytic fission of Fe-S being assisted by a second thiol group (which is close at hand in the dithiol) as found for the B_{12a} reduction by cysteine.[64] This suggests a method of preventing the reduction of Fe(III) in the resting P-450 form, by the coordinated cysteine, i.e. by the

protein preventing a second thiol approaching the active site and in doing so, only permitting the apparently unfavourable formation of the $RS^{\bullet}$ to occur, which cannot diffuse away being part of the protein and hence can recombine with Fe(II).

Fe(II) bis-histidine has a very similar spectrum to that of reduced cytochrome b_5 and therefore is a good model as far as the electronic structure is concerned. Curiously the reduction of the bis-histidine complex requires proton uptake, [108] which follows from the change in pKa of the $-NH_3^+$ of the coordinated histidine, while the reduction of cytochrome b_5 requires Na^+/K^+ uptake. But whether a proton or cation is required on reduction of a hemoprotein depends on the pKas of the neighbouring groups in the active site. [108]

A clearcut example of catalysis by copper(II) in the reduction of FeOH-caffeine by penicillamine was found. Some catalysis by Cu(II) was found in the reduction of B_{12a} but the effect in the former case is more dramatic because no reduction occurs in the absence of Cu(II).

CHAPTER 8 - THE CATALYSIS OF THE AUTOXIDATION OF THIOLS BY COBALT CORRINOIDS

8. Introduction

It is well known that cobalt corrinoids such as B_{12a} are good catalysts for the autoxidation of thiols.[9] The only quantitative kinetic studies are those of Peel who used mainly aquocyanocobinamide (factor B)[71] but unfortunately the presence of CN^-, which will poison some of the cobalt, complicates the interpretation of the results.

The aims of this study are to establish a general mechanism for the autoxidation of thiols catalysed by cobalt corrinoids through a quantitative study of B_{12a} (as it has effectively only one potential coordination site) and a monothiol. Cysteine was chosen because the reduction of B_{12a} by cysteine has been studied.[64] With less detailed study the effect of changing from a mono to a dithiol (viz. dithiothreitol) on the rate will be investigated. (The reduction of B_{12a} by dithiothreitol was discussed in chapter 6.) The effect of replacing the axial benzimidazole by H_2O will be examined by studying the diaquocobinamide catalysed autoxidations of cysteine as well as those of mercaptoethanol and ethanethiol. It is also of interest to see to what extent cobalt corrinoids might serve as models for the reactions of hemoproteins with O_2 and to what extent one can model the high turnover number and suppression of H_2O_2 formation characteristic of cytochrome c oxidase.[113]

The stoichiometry has been shown by Peel to be

$$2RSH + \tfrac{1}{2}O_2 \longrightarrow RSSR + H_2O$$

and will be assumed here.

8.2 Results

8.2.1 B_{12a} plus cysteine

Figure 8.1 shows a typical plot for the rate of O_2 uptake catalysed by B_{12a} in the presence of cysteine in an O_2 saturated solution.

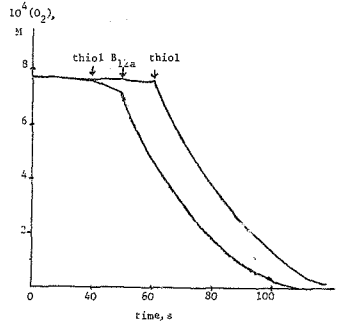

Figure 8.1 A typical experimental plot for O_2 uptake in the presence of B_{12a} and cysteine in O_2 saturated buffers; pH 10; $2x10^{-2}$M cysteine; $2,5x10^{-5}$M B_{12a}; 25°C.

It shows the uncatalysed as well as the catalysed autoxidation of cysteine. The lag period due to mixing is < 3 seconds, and hence no build up can be seen within this period. There is clearly no effect of the order of addition on either the initial rate or the course of the reaction. In general, the initial rates will be reported.

By contrast, the plots of the disquocobinamide cat- sed

reactions are autocatalytic (figure 8.2).

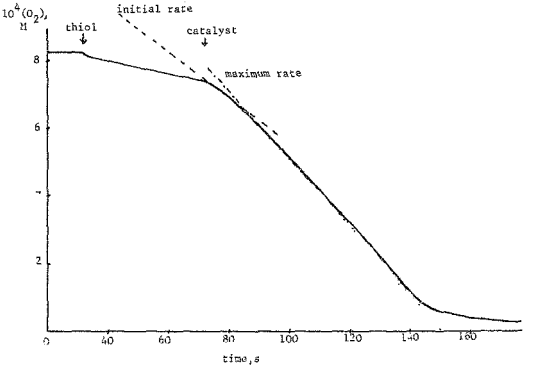

Figure 8.2 A typical experimental plot for O_2 uptake by thiols catalysed by diaquocobinamide; pH 9.5; $2x10^{-3}$M mercaptoethanol; $1x10^{-7}$M disquocobinamide; O_2 saturated buffer; 25°C

Figure 8.3 shows the pH profile in O_2 saturated buffers, without EDTA, both with and without B_{12a} (data in table 1, appendix 8). The catalysed reaction has a maximum rate at pH 10 and hence further studies will concentrate on pH 10. The uncatalysed rate reaches a plateau in the alkaline region, probably because of complete formation of the thiolate.

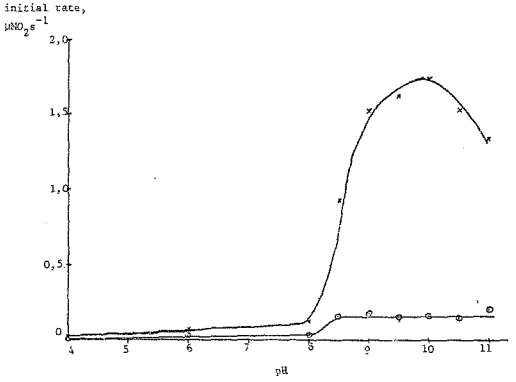

Figure 8.3 The pH profile for the autoxidation of cysteine catalysed by B_{12a}; $2x10^{-2}$M cysteine; $1x10^{-5}$M B_{12a}; O_2 saturated buffers; 25°C

Table 8.1 shows the different rates (and order in oxygen) in air and O_2 saturated buffers as well as the effects of superoxide dismutase, Cu(II), EDTA on the rate.

Table 8.1 : Effects of conditions on the rate of O_2 uptake by B_{12a} *plus cysteine*; *pH* 10,0; $2x10^{-2}$M cysteine; $2,2x10^{-5}$M B_{12a}; 25°C; μ = 0,1

Added reagent	Initial rate/μMO_2 s^{-1}	
	Air saturated buffer	O_2 saturated buffer
none	2,32 [a] ($n \approx 0$ initially)	3,95 [a] ($n \approx 0,5$)
$2x10^{-6}$M superoxide dismutase	2,27 [a] ($n \approx 0$)	2,45 [a] ($n \approx 0$)
$1x10^{-3}$M EDTA	-	1,84
$2x10^{-3}$M EDTA	1,15 [a] ($n \approx 0$)	1,66
$2x10^{-5}$M $CuSO_4$	-	3,51

[a] slope of a plot of log rate versus log(O_2)

It can be seen that there is an additional reaction in O_2 saturated buffers which is suppressed by superoxide dismutase and thus involves superoxide. Hence air saturated and not O_2 saturated buffers will be used. EDTA suppresses the reaction by about 50%, as was the case in the reduction of B_{12a} by cysteine under N_2 (chapter 6). Hence $2x10^{-3}$M EDTA will be used to suppress reactions catalysed by trace metals. Little effect of Cu(II) was found at the concentration used. The half order dependence in O_2 found in O_2 saturated buffers is similar to that reported earlier for the rate of O_2 uptake by Cu(II) plus ascorbate [114] as well as Fe(III) plus cysteine [73] but it is not part of the intrinsic reaction in this case as it was suppressed by superoxide dismutase.

Figure 8.4 (and table 2, appendix 8) shows the effect of the B_{12a} concentration on the rate and the rate is quite clearly first order in B_{12a} with only a small amount of uncatalysed rate (given by the intercept).

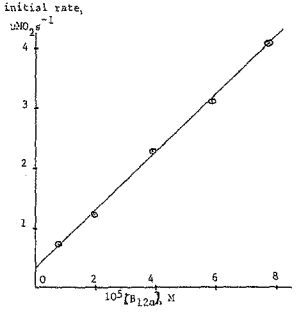

Figure 8.4 The rate dependence on the B_{12a} concentration for the autoxidation of cysteine catalysed by B_{12a} in air saturated solutions containing 2×10^{-3} M EDTA; 5×10^{-3} M cysteine; pH 10; $\mu = 0,1$; 25°C.

Figure 8.5 (and table 3, appendix 8) shows the effect of the cysteine on both the rate of O_2 uptake as well as reduction.

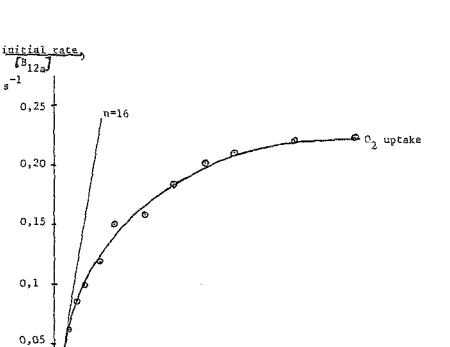

Figure 8.5 The rate dependence on the cysteine concentration for both the autoxidation of cysteine catalysed by B_{12a} (in air saturated solutions) as well as for the reduction of B_{12a} by cysteine (under N_2) in solutions containing 2×10^{-3} M EDTA; $1{,}94 \times 10^{-5}$ M B_{12a}; pH 10; $\mu \approx 0{,}1$; 25°C.

The slope for the reduction is 0,38 M^{-1} s^{-1} compared with the tangent at low cysteine concentrations to the O_2 uptake curve which has a slope of 15,8 M^{-1} s^{-1} giving a ratio of 42 between the rate of O_2 uptake and reduction. The turnover number (i.e. equivalents ℓ^{-1}/(M B_{12a} x s)) is $\geq 0{,}9$ at limiting thiol

concentrations.

Nome and Pandlers results [64] indicate that at pH 10, coordination is rate limiting but reduction involves RS^- + (RS - Co(III)). Even if the stoichiometry of the reaction is ignored, the rate of O_2 uptake is faster than the rate of reduction (if the stoichiometry is taken into account the asymtotic rate of O_2 uptake increases by a factor of four). Quite clearly, a different dependence on thiol concentration is found for O_2 [illegible] duction which is rather surprising.

[illegible]ctra of the steady state at high and low cysteine concentrations were run 15 seconds after mixing. The spectrum in the Soret region could be taken within a minute while the complete spectrum took ~2 minutes. At low thiol concentrations, the uptake of O_2 under the same conditions was complete within 2,5 minutes while at high thiol concentrations it was complete within 1,5 minutes. In both cases, the Soret band was at 357 nm while at low thiol concentrations, the α,β bands were at 420 nm, 516 nm and 536 nm. These correspond to the bands of the hydroxocobalamin (358 nm, 421 nm, 516 nm, 537 nm).[102] As hydroxocobalamin builds up, it must precede the rate determining step which must involve Co-OH or Co-OH_2 (pKa 7,6).[9] There were no detectable bands due to Co(II) (312 nm, 405 nm, 473 nm)[9] or thiolatocobalamin (371 nm, 425 nm, 534 nm, 554 nm).[102] However, as the O_2 is depleted Co(II) is formed (bands at 312 nm, 470 nm), but with no sign of the thiolatocobalamin bands which is consistent with either coordination being slower than reduction, or an outer sphere mechanism.

All experiments in air are zero order in O_2 at least initially.

At high cysteine concentrations (>$8x10^{-2}$M) at $2x10^{-5}$M B_{12a}, there was a slight lag period which was, however, within the mixing time of 3 seconds. This was not observed at lower thiol concentrations where a smaller volume of thiol was added. The independence of the rate on O_2 agrees with the spectra which indicate that the rate determining step is one of the reduction steps.

The effect of catalase was investigated at high and low cysteine concentrations in an air saturated pH 10,0 buffer containing $2x10^{-3}$M EDTA ($1,9x10^{-5}$M B_{12a}). At low cysteine concentrations ($5x10^{-3}$M), the rate decreased from 1,22μMO_2 s^{-1} to 0,78 μMO_2 s^{-1} (duplicate experiments run) (i.e. a 36% decrease in rate) on addition of 5700 units of catalase. At 0,1M cysteine however, the rate was unaffected by catalase (4,45 μMO_2 s^{-1} without catalase; 4,47 μMO_2 s^{-1} with catalase).

In neither case was the order in O_2 affected. It appears that the amount of H_2O_2 detected decreases with thiol concentration. Qualitatively the activity of catalase was not affected by the presence of 0,1M cysteine, up to ten minutes.

8.2.2 B_{12a} plus dithiothreitol

Figure 8.6 (id table 4, appendix 8) shows the pH profile for rate of O_2 uptake in air saturated buffers.

It shows a maximum like that observed for the B_{12a}-cysteine system in O_2 saturated buffers as well as for the reduction of B_{12a} by dithiothreitol under N_2. However, the maximum occurs at pH 9,2 unlike the B_{12a}-cysteine system (pH 10) and the reduction system (pH 8,5). Other experiments were carried out at pH 10.

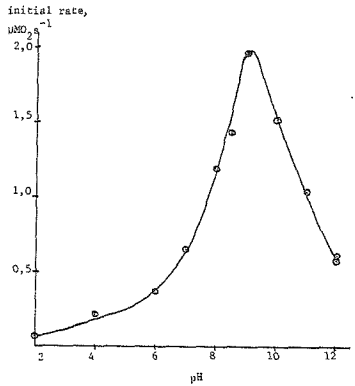

Figure 8.6 The pH profile for the autoxidation of dithiothreitol catalysed by B_{12a} in air saturated buffers; $1{,}94 \times 10^{-5}$M B_{12a}; 1×10^{-3}M dithiothreitol; μ = 0,1; 25°C.

Figure 8.7 (and table 5 in appendix 8) shows the effect of the dithiothreitol concentration on the rate. The same saturating effect which was observed with cysteine is evident here but has not been taken far enough to level off, because the rates are too great. The rate of reduction by dithiothreitol has been included and as found for B_{12a} plus cysteine, is slower than the rate of O_2 uptake. It has a slope of 5,2 M^{-1} s^{-1} compared with that of the tangent to the origin of O_2 uptake curve which is

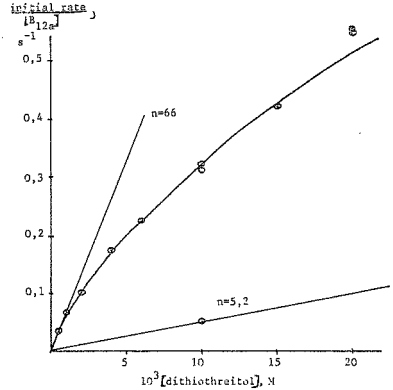

Figure 8.7 The rate dependence on the dithiothreitol (dtt) concentration for both the autoxidation of dtt catalysed by B_{12a} (in air saturated solutions) as well as for the reduction of B_{12a} by dtt (under N_2); $1,94 \times 10^{-5}$ M.B_{12a}; pH 10; μ = 0,1; 25°C.

66 M^{-1} s^{-1} i.e. a 12 fold difference, which is less than that found for the B_{12a}-cysteine system (a 42 fold difference) whic' is largely a consequence of the difference in the reduction rates (14 fold) rather than O_2 uptake results (4 fold) in the two systems (ignoring the fact that dtt has two thiol groups).

The turnover number is > 2,2 equivalents/(M B_{12a} x s) which is larger than that for B_{12a} plus cysteine (≳ 0,9 equivalents/(M B_{12a} x s)).

Figures 8.8a and b (and tables 6 a and b in appendix 8) show that at both high and low dithiothreitol concentrations, the rate is first order in B_{12a}.

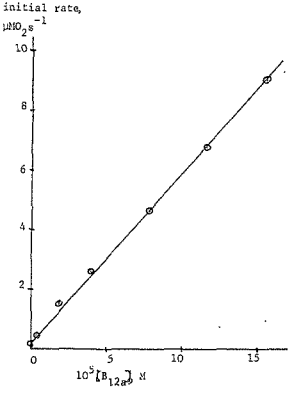

Figure 8.8a The rate dependence on the B_{12a} concentration for the autoxidation of dtt catalysed by B_{12a} in air saturated solutions at a low dtt concentration ($1x10^{-3}$M) at pH 10,0; μ = 0,1; 25°C.

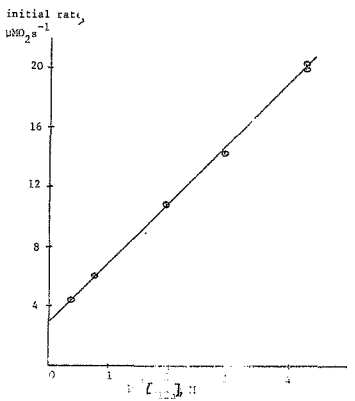

Figure 8.8b The rate dependence on the B_{12a} concentration for the autoxidation of dtt catalysed by B_{12a} in air saturated solutions at a high dtt concentration ($2x10^{-2}$M) at pH 10,0; u = 0,1; 25°C.

As the dithiothreitol concentration increases, the order in O_2 changes from 0,5 to zero. Conditions affecting the rate and order at low thiol concentrations were superoxide dismutase and catalase. At 1 mM dithiothreitol ($1,94x10^{-5}$M B_{12a}; pH 10; air saturated) $2x10^{-6}$M superoxide dismutase reduced the rate from 1,52 $\mu MO_2 s^{-1}$ to 0,87 $\mu MO_2 s^{-1}$ (a 42% decrease) and changed the order from 0,5 to zero while 5700 units of catalase reduced it to

0,60 $\mu MO_2 s^{-1}$ (a 60% decrease) also changing the order to zero. In addition $3x10^{-4}$M $CuSO_4$ increased the rate to 3,37 $\mu MO_2 s^{-1}$ (i.e. doubling the rate) but did not affect the order. At $2x10^{-2}$M dithiothreitol ($3,9x10^{-6}$M B_{12a}) $2x10^{-6}$M superoxide dismutase and 5700 units of catalase decreased the rate by less than 3% in both cases without changing the order. The effect of EDTA was not studied.

The steady state species at both high and low dithiothreitol concentrations is the hydroxocobalamin as shown by bands at 357 nm, 420 nm, 516 nm and 536 nm (literature 358 nm, 421 nm, 516 nm, 537 nm).[102] Hence the rate determining step involves reduction as found with B_{12a} plus cysteine.

8.2.3 Diaquocobinamide plus monothiols

Qualitative experiments indicated that thiols reduced the diaquocobinamide much faster than B_{12a} at pH 9,5 at least. Hence at least one step in the reaction has been speeded up. Figure 8.2 shows a typical autocatalytic plot characteristic of diaquocobinamide plus thiols. The maximum rate is always 1,5 - 2,5 times greater than the initial slope (see tables 8 and 9 in appendix 8). Only the initial slopes will be used unless otherwise noted.

Figure 8.9 and table 7 in appendix 8 show the variation in rate with pH in the presence of ethanethiol, mercaptoethanol and cysteine. Ethanethiol reacts about ten times faster than cysteine. We cannot be sure that part of the effect is not due to impurities such as H_2S but the results are still of interest in establishing an upper limit to oxidase activity of cobalt corrinoids. All three of the thiols show a maximum at pH 10 (as did B_{12a} plus

cysteine) in spite of the different pKas of the thiol group (ethanethiol 10,6; mercaptoethanol 9,4; cysteine 8,5).[65]

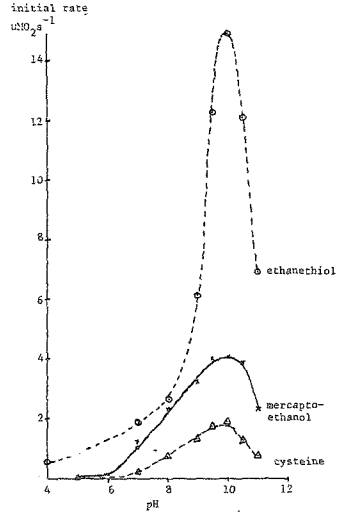

Figure 8.9 The pH profile for the autoxidation of ethanethiol, mercaptoethanol and cysteine catalysed by diaquocobinamide ($1x10^{-7}$M); $2x10^{-2}$M thiol; O_2 saturated buffers; 25°C.

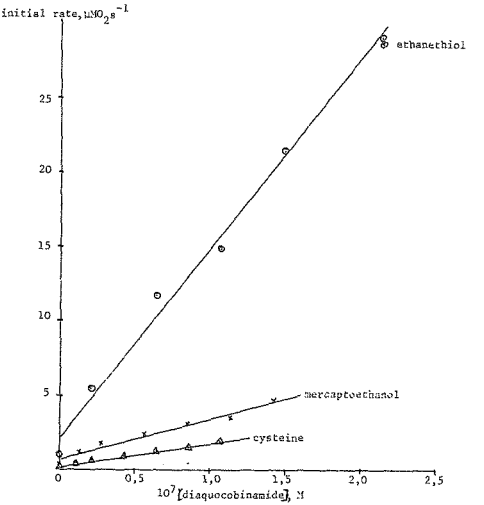

Figure 8.10 The rate dependence on the diaquocobinamide concentration for the autoxidation of ethanethiol, mercaptoethanol and cysteine at pH 10; pH 9,5 and pH 10 respectively, catalysed by diaquocobinamide; $2x10^{-2}$M thiol; O_2 saturated buffers; 25°C

Figure 8.10 and table 8 in appendix 8 show that the reactions are all first order in diaquocobinamide and that there is some uncatalysed reaction.

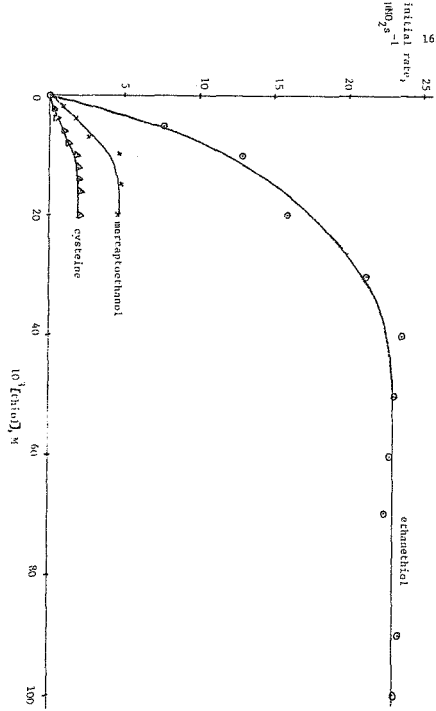

Figure 8.11 The rate dependence on the thiol concentration for the autoxidation of ethanethiol (pH 10), mercaptoethanol (pH 9,5) and cysteine (pH 10) catalysed by diaquocobinamide ($1x10^{-7}$M) in O_2 saturated solutions at 25°C.

Figure 8.11 and table 9 in appendix 8 shows the effect of the thiol concentration on the rate. All show a saturating effect.

Table 8.2 shows the effect of EDTA, $CuSO_4$ and catalase on the rate of O_2 uptake in the presence of mercaptoethanol.

Table 8.2 : The effect of EDTA, $CuSO_4$ and catalase on the rate of O_2 uptake in the presence of mercaptoethanol (2×10^{-2}M) and 1×10^{-7}M diaquocobinamide at 25°C; pH 9,5

Added reagent	Initial rate / $\mu MO_2 s^{-1}$	Maximum rate / $\mu MO_2 s^{-1}$
none	4,00	15,7
1×10^{-2}M EDTA	4,32	15,2
1×10^{-2}M EDTA	4,00	15,7
1×10^{-5}M $CuSO_4$	8,32	13,7
1×10^{-4}M $CuSO_4$	7,80	10,5
1×10^{-3}M $CuSO_4$	7,40	8,6
~100 units catalase	4,00	4,6

There was no effect of EDTA indicating a genuine reaction. Any catalysis by Cu(II) was small compared to that of diaquocobinamide. In the presence of catalase, the rate was zero order in O_2 *at least initially*. This is the only evidence for the independence of the rate on O_2 concentration. Hence it is probable that reduction is still the slow step, as found for the B_{12a} systems. No spectra were run of the steady state, as the diaquocobinamide concentrations used for the O_2 uptake studies were too low.

8.3 Discussion

All reactions studied share several features in common such as the

sharp pH maximum at ~pH 10 as well as the saturation effect of the thiol, which suggest a common basic mechanism. The pH profile appears similar to that observed for reduction but the two are probably only indirectly related (see below).

Absolute values of catalytic activity observed vary over the range ≥ 0,9 equivalents $\ell^{-1}/(M\ Co \times s)$ for B_{12a} plus cysteine to 920 for diaquocobinamide plus ethanethiol.

All reactions are accompanied by additional reactions as revealed by the effects of superoxide dismutase, EDTA and autocatalysis.

8.3.1 B_{12a}

Experiments at pH 10 (maximum in the pH profile) show that the main features to be explained are:

1. The rate of O_2 uptake initially increases with cysteine and dithiothreitol concentrations, then becomes independent (figure 8.5 and figure 8.7).
2. Free H_2O_2 is produced at low but not at high cysteine concentrations.
3. The rate depends linearly on the cobalt concentration, and in the absence of accompanying reactions, is independent (at least initially) of the O_2 concentration, while spectra show the presence of hydroxocobalamin during the steady state. Hence the rate determining step involves the reduction of Co(III).
4. The observed rate of O_2 uptake is, however, greater than the observed rate of reduction of Co(III) under N_2. Even ignoring the stoichiometric requirement for four thiols to reduce O_2,

the asymptotes in figures 8,5 and 8,7 indicate that the rates of O_2 uptake are still 42 and 12 times greater than the rates of reduction for cysteine and dithiothreitol respectively.

We therefore suggest the following mechanism: It is known that Co(II) reversibly forms an adduct with O_2 which has only been detected at low temperatures [19] (reaction 8 - 1)

$$Co(II) + O_2 \rightleftharpoons Co(II)O_2 \qquad (8-1)$$

The autoxidation of Co(II) is greatly accelerated by reducing agents such as quinols, thiols, $Fe(II)(CN)_6$ through reactions such as reaction (8 - 2). [70]

$$Co(II)O_2 + RSH \longrightarrow Co(III)O_2H^- + RS^{\cdot} \qquad (8-2)$$

Furthermore, thiyl radicals are known to react rapidly [65] according to reaction (8 - 3) (for cysteine, kf is $3,1x10^9\ M^{-1}\ s^{-1}$; kr $8x10^5\ s^{-1}$) while the hydroperoxide complex can dissociate according to reaction (8 - 4) to give free H_2O_2, which (together with any subsequent $HO^{\cdot}$) can be further reduced by Co(II), RSH, $\dot{RS}\dot{S}R$.

$$RS^{\cdot} + RS^- \rightleftharpoons \dot{RS}\dot{S}R \qquad (8-3)$$

$$Co(III)O_2H^- + H_2O \longrightarrow Co(III) + H_2O_2 \qquad (8-4)$$

Hence the anion radical $\dot{RS}\dot{S}R$ can be formed in the immediate vicinity of the cobalt. This is expected to be a much more powerful reducing agent than RS^- and by analogy with the electron transfer reactions observed in Cu containing electron transfer proteins with $\dot{RS}\dot{S}R$ on the protein, [115] will probably reduce $Co(III)OH^-$ or more likely $Co(III)OH_2$ according to reaction (8 - 5) by an outer sphere mechanism.

$$\dot{RS}\dot{S}R + Co(III)OH_2 \longrightarrow RSSR + Co(II) + H_2O \qquad (8-5)$$

It can also undergo rapid disproportionation according to reaction

(8 - 6)[65] and could presumably reduce other compounds such as $Co(II)O_2$, H_2O_2, OH.

$$2R\dot{S}\dot{S}R \longrightarrow RSSR + 2RS^- \qquad (8 - 6)$$

The reaction (8 - 7)[63] does not occur, at least in air saturated as distinct from O_2 saturated buffers as shown by the lack of effect of superoxide dismutase.

$$R\dot{S}\dot{S}R + O_2 \longrightarrow RSSR + O_2^- \qquad (8 - 7)$$

This scheme immediately explains the main experimental observations:

1. The main reductant of Co(III) is not RS^- but more powerful, faster $R\dot{S}\dot{S}R$.
2. As the cysteine concentration increases so will the steady state concentrations of all the abovementioned intermediates so we may expect:
   (a) an increased rate of removal of $R\dot{S}\dot{S}R$ by reactions other than (8 - 5), hence a fall-off in the effect of the thiol concentration is expected, as observed.
   (b) an increased rate of reduction of $Co(III)O_2H^-$ (and presumably also free H_2O_2) by RSH and $R\dot{S}\dot{S}R$, leading to the suppression of the formation of free H_2O_2, as observed.

We therefore suggest that the observ 1 rate of O_2 uptake can be considered to represent the sum of:

A. the abovementioned reactions in which are shown in figure 8.12.

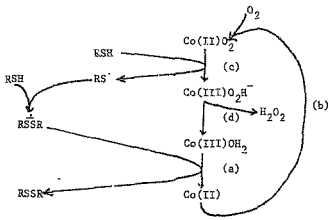

Figure 8.12 Scheme of reactions occurring in the autoxidation of cysteine catalysed by B_{12a}

B. the further reactions of H_2O_2 together with smaller contributions from

C. the reduction of Co(III) by cysteine (RSH) itself

D. the uncatalysed reaction of O_2 with RSH

All four groups of reactions will undoubtedly interact because of the existence of common intermediates such as H_2O_2 and RS̈SR. In particular, reaction (c) is required not only to start reaction (A) but also, since one can never expect all of the RS̈SR formed to be used in reducing Co(III), it is needed to keep reaction (A) going, i.e. there is bound to be an intimate relationship between reactions (A) and (C) even though the bulk of the "current" is carried by (A). This could explain why both the overall oxidase activity and the rate of reduction show similar sharp pH maxima around pH 10.

These remarks apply to the B_{12a}-dithiothreitol system as well. However, the RS̈SR is a cyclic monomer formed by the interaction

between the two -SH groups in the dithiol. The greater difference in the rates of reduction of B_{12a} by dithiothreitol (~14) compared with the rates of O_2 uptake (~4) is support for the importance of the $R\bar{S}\bar{S}R$ in the latter, in carrying the reaction, as this would blur the distinction between mono and dithiols.

8.3.2. Diaquocobinamide

The much more limited data again show a saturation effect with all three thiols (see figure 8.11), a first order dependence on diaquocobinamide (see figure 8.10) and at least with high mercaptoethanol concentrations, the initial rate is independent of the O_2 concentration and does not produce H_2O_2.

It is reasonable to assume the same basic mechanism as for B_{12a} plus cysteine but in this case the much higher turnover number (920 equivalents ℓ^{-1}/(MCox5)) for ethanethiol for example can be correlated with the much higher rate of reduction of diaquocobinamide compared with B_{12a}, even by monothiols. This turnover number is greater than that for electron transfer between cytochromes a and a_3 (750 equivalents ℓ^{-1}/(M catalyst x s)) and between cytochromes c and a (450 equivalents ℓ^{-1}/(M catalyst x s)).[113]

8.4 Conclusions

All the above evidence is consistent with a radical mechanism which involves the cycle of steps (a) - (d) of figure 8.12 (which in turn contains two different types of reduction of Co(III) to Co(II) and of Co(II)O_2 to Co(III)O_2H^-) and with radical anions ($R\bar{S}\bar{S}R$) playing a key role.

In the case of B_{12a} and low cysteine concentrations, the reaction produces H_2O_2 but this formation of H_2O_2 as "seen" by catalase can be suppressed by increasing the cysteine concentration,

presumably merely by increasing the rate of reduction of coordinated $Co\text{-}O_2H^-$ (and also perhaps free H_2O_2), without any dramatic increase in the turnover number.

The turnover number can be dramatically increased by increasing the rate of reduction of Co(III) to Co(II) by changing from a cobalamin to a cobinamide. The following maximum turnover numbers were found:

B_{12a} + cysteine : 0,9 equivalents ℓ^{-1}/(M catalyst x s)

B_{12a} + dithiothreitol : > 2,2 equivalents ℓ^{-1}/(M catalyst x s)

diaquocobinamide + cysteine: 78 equivalents ℓ^{-1}/(M catalyst x s) (initial rate)

diaquocobinamide + ethanethiol : 920 equivalents ℓ^{-1}/(M catalyst x s) (initial rate)

The rate could possibly be increased still further by increasing the rate of supply of reducing equivalents to both Co(III) and $Co(II)O_2$, for example, by very efficient outer sphere electron transfer but the rate of O_2 uptake in the diaquocobinamide plus ethanethiol system is already greater than that of both electron transfer between cytochromes c and a (450) as well as between cytochromes a and a_3 (750).[113]

These results provide interesting parallels to the hemoproteins. It has been shown that the O_2 adduct of hemoglobin which is not an active catalyst, reacts with reagents such as quinols[116] and phenylhydrazines[117] to give Fe(III) and H_2O_2 by steps analogous to (c) and (d), i.e. this can probably be considered to be the basic mechanism common to iron porphyrins which cannot form dimers (as for example when bound in a protein) and cobalt corrinoids which have a coordination site available for coordinating O_2 to the M(II).

Terminal oxidases such as cytochrome c oxidase also contain iron porphyrins but differ from hemoglobin in their high catalytic activity (maximum rate of electron transfer from cytochrome a to a_3 is 750 equivalents ℓ^{-1}/(mole ℓ^{-1} catalyst x seconds) and in not forming free H_2O_2.[13] Although the mechanism of reduction of O_2 by cytochrome a_3 is not known, it is generally agreed that the initial step involves coordination of O_2 to Fe(II) cytochrome a_3 and it is reasonable at least to start, by assuming the occurrence of the basic steps (b), (c), (d). Our results with cobalt corrinoids show that both the high turnover number and the suppression of the formation of H_2O_2 can be achieved by manipulation of this basic mechanism. It is probable, however, that the $Fe(III)O_2H^-$ complex is converted to the "ferryl" $(FeO)^{3+}$ complex, analogous to compound I of catalase and peroxidase before further reduction.

CHAPTER 9 - THE CATALYSIS OF THE AUTOXIDATION OF DITHIOTHREITOL BY THE MONOMERIC BIS-HISTIDINE HEMIN COMPLEX

9.1 Introduction

This chapter will extend the study of the catalysis of the autoxidation of thiols by looking at the catalysis by the bis-histidine hemin complex in an attempt to elucidate the mechanism. Catalysis will involve, at least initially, reduction of the complex by dithiothreitol, the kinetics of which were discussed in Chapter 7.

9.2 Results

The effect of the dithiothreitol, O_2, hemin and histidine concentrations on the rate of O_2 uptake were investigated. As the pH studies were not informative in the reduction studies, they have not been done here.

Figure 9.1 and table 1 in appendix 9 show the effect of the rate on the dithiothreitol concentration.

This profile is similar to that found for the reduction of bis-histidine hemin by dithiothreitol (figure 7.3). The parameters used to fit the latter, do not fit the former, but there are parallels. To ensure readily measurable rates, the reduction studies were carried out at a hemin concentration five times greater than that used in the O_2 uptake studies. The maximum rate occurs at $2,4 \times 10^{-3}$M in dithiothreitol in the reduction and at 5×10^{-4}M in the O_2 uptake studies, i.e. a factor of five different. In addition there is approximately a two fold difference in both systems between the maximum and limiting rate. However, the initial rates of O_2 uptake/concentration of bis-histidine hemin are all larger (3 - 6 times larger) than k_{obs}

found for the reduction, as found for the B_{12a}-cysteine system.

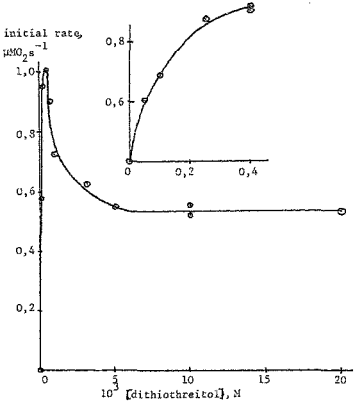

Figure 9.1 The rate dependence on the dtt concentration for its autoxidation catalysed by bis-histidine hemin, 6×10^{-6}M hemin; 0,4M histidine; pH 10,0; μ = 0,5; 25°C

Because of the complex dependence of the dithiothreitol concentrations, other effects were studied both at high and low dithiothreitol concentration.

9.2.1 Low dithiothreitol concentrations

At low dithiothreitol concentrations, the O_2 and dithiothreitol

concentrations were very similar. Hence the dependence of the rate on the O_2 concentration could not be determined.

Figure 9.2 and table 2a in appendix 9 show that at $3x10^{-4}$M dithiothreitol at pH 10 the rate is first order in hemin.

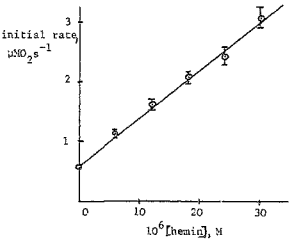

Figure 9.2 The rate dependence on the hemin concentration for the autoxidation of dtt catalysed by bis-histidine hemin at a low thiol concentration ($3x10^{-4}$M); 0,4M histidine; pH 10,0; μ = 0,5; 25°C.

Figure 9.3 and table 3 in appendix 9 show that the rate is independent of the histidine concentration as is the uncatalysed rate.

In 0,4M histidine at pH 10 using 26,3 µM hemin and $3x10^{-4}$M dithiothreitol, 5000 units of catalase reduced the rate from 2,70 $\mu MO_2\ s^{-1}$ to 1,77 $\mu MO_2\ s^{-1}$, i.e. a 34% decrease in rate.

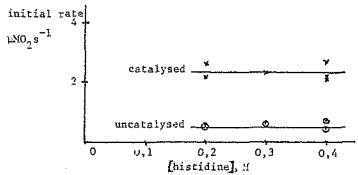

Figure 9.3 The rate dependence on the histidine concentration for the autoxidation of dtt catalysed by bis-histidine hemin at a low thiol concentration ($3x10^{-4}$M; $2,6x10^{-5}$M hemin; pH 10,0; μ = 0,5; 25°C.

The uncatalysed rate is only 21% that catalysed, which suggests that at least some of the hydrogen is being generated by the catalysed reaction. Unfortunately the range of concentrations of hemin which can be studied is limited by the dimerization of bis-histidine hemin (chapter 5) as well as the range of rates which can be studied by this technique.

The spectrum of $1x10^{-5}$M hemin in the presence of 0,4M histidine and $3x10^{-4}$M dithiothreitol in air saturated pH 10,0 buffer in the steady state (~1 minute after mixing) showed shoulders at 360 nm and 440 nm characteristic of those of monothiolate hemin (see chapter 7) in addition to a band at 412 nm, characteristic of the bis-histidine hemin. In addition, reoxidation of the Fe(II) bis-histidine complex was complete within 5 s. Hence reduction is the slow step and coordination of RS^- is fast.

However, at $3x10^{-4}$M dithiothreitol, k_{obs} ($= \frac{\text{rate}}{\text{hemin concentration}}$) was 2 times greater for the O_2 uptake (0,08 s^{-1}) (from slope of

figure 9.2) compared with reduction ($3,4x10^{-2}$ s^{-1}) which requires that the reduction is carried out by a faster and presumably more powerful reducing agent, as was the case with the cobalt corrinoid catalysed reactions, but the difference is not as marked.

9.2.2 High dithiothreitol concentrations

Three regions are evident at high dithiothreitol concentrations (figure 9.4). At low hemin concentrations, the rate is half order in oxygen (from a plot of log rate vs log (O_2)).

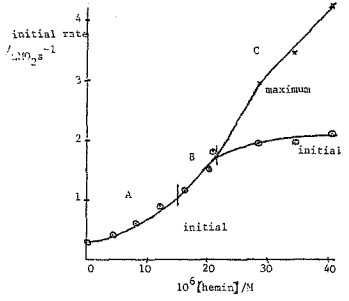

Figure 9.4 The rate dependence on the hemin concentration for the autoxidation of dtt catalysed by bis-histidine hemin at a high thiol concentration ($5x10^{-3}$M); 0,4M histidine; pH 10,0; μ = 0,5; 25°C.

As the hemin concentration is increased, a zero order in O_2 dependence is found initially. The proportion of the reaction that

is zero order increases with hemin concentration. At high hemin concentrations, the reaction is autocatalytic initially, becoming zero order.

At the hemin concentrations where the rate is half order in oxygen, the rate of the uncatalysed reaction (which is half order in oxygen) is significant, and the half order dependence probably does not reflect the true situation in the hemin catalysed reaction. It is possible that the zero order dependence on the O_2 concentration does reflect the hemin catalysed reaction but too little data is at hand to be certain.

Figure 9.5 shows that the rate is second order in hemin suggesting the involvement of a dimer (data in table 2b, appendix 9).

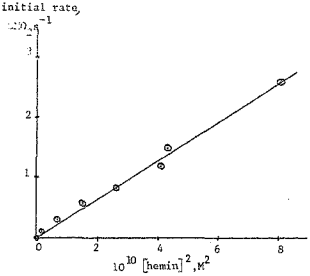

Figure 9.5 Plot of initial rate of O_2 uptake (corrected for the uncatalysed reaction) versus [hemin]^2 at a high thiol concentration (5×10^{-3}M) (conditions as in figure 9.4).

Because of the complexity of the kinetics under these conditions, no further studies were done.

9.3 Discussion

At low dithiothreitol concentrations rate $\propto [Fe]^1 [O_2]^? [RSH]^{?1} [his]^0$. The spectrum of the steady state shows the presence of the monothiolate hemin (bands at 360 nm and 440 nm) and reoxidation is rapid, indicating that reduction is the slow step while the coordination of RS^- is fast. (In contrast coordination of RS^- to B_{12a} is slow.) The greater rate of O_2 uptake compared with reduction (2 fold difference) suggests that a strong reducing agent such as $R\dot{S}\dot{S}R$ is largely responsible for reduction, as proposed for the B_{12a}-cysteine system. If it reduces hemin by an outer sphere mechanism as it must do with B_{12a}, to overcome the slow coordination step, the independence of the rate on the histidine concentration, suggests that $R\dot{S}\dot{S}R$ does not discriminate between the bis-histidine and monothiolate complexes. The maximum turnover number (corrected for the uncatalysed rate) is 0,3 equivalents ℓ^{-1}/(M hemin x s) seven fold smaller than with B_{12a} and dithiothreitol.

At high dithiothreitol concentrations

$$\text{rate} \propto [Fe]^2 \quad [O_2]^{?0} \quad [RSH]^0$$

This change in rate law may suggest either a change in the rate determining step or a change in mechanism but as it was complex and a strong interaction between the catalysed and uncatalysed reaction appeared probable, no further studies were made. However, the complexity as well as the change in the rate law shows the variety of reactions which can occur and correlates with the range of reactions found between O_2 and hemoproteins.

CHAPTER 10 - SUMMARY AND CONCLUSIONS

In chapter 3, hemin was studied in aqueous alkaline solution. Five distinct types of complex were found. These were monomers, dimers, and polymers with spectra falling into two types - A (typical high spin) and B (μ-oxo type) but the latter type was even given by monomeric species. These species were related by equilibria which were independent of pH but which depended on the hemin concentration and the ionic strength. The dimerization constant for the usual dimeric hemin (μ = 0,1) was found to be $\geq 10^9\ M^{-1}$. In addition, the formation of the monomeric hemin-caffeine adduct was confirmed and the complex found to contain one OH^- ligand. It was also shown that some detergent molecules at least, can form adducts with dimeric alkaline hemin, well below the critical micellar concentration ($K \sim 10^5\ M^{-1}$ per mole detergent bound). The large dimerization constant, the stabilization of the monomeric species by caffeine, micellar detergents [13-15] and organic solvents [24] as well as adduct formation with single detergent molecules re-emphasizes the known fact that one of the roles of the protein is to stabilize the monomer[2] and that it can do this by hydrophobic and/or donor-acceptor interactions.[118]

Chapter 4 dealt with the study of hemin in aqueous acid, where hemin rapidly aggregates. However, unstable monomeric and dimeric forms of the aquo-complex at pH 1 were formed by rapid dilution from pH 8 and the equilibrium between them was studied (the dimerization constant was $1,1 \times 10^5\ M^{-1}$). Comparison of the spectrum of the monomer with that of hemin in acidic aqueous ethanol, indicates that it is probably a six coordinate, high spin bis-aquo complex with the Soret maximum at 397 nm and an extinction

coefficient (at 397 nm) of 120 ± 3 mM^{-1} cm^{-1}. Since the same spectrum was also observed in very dilute solutions at low ionic strength on rapid dilution to pH 7,[97] the pKa for the coordinated H_2O is > 8 compared with that of 6,5 in 44% aqueous ethanol [46] (organic solvents would be expected to stabilize FeOH rather than $FeOH_2$ because of its lower charge (ignoring the side chains)).

In chapter 5, the coordination of imidazole and its analogues to hemin was studied. In addition to the expected equilibria leading to the formation of the bis-ligand complex, additional equilibria involving adduct formation and aggregation were found. However, no significant formation of any monomeric mono-ligand complex was evident, even when the starting complex was the caffeine adduct of hemin in alkaline solution. This was also the case in organic solvents.[42] This is consistant with the binding constant for the third ligand (K_3) being less than that for the second (K_2) which has been ascribed to the change from high spin to low spin iron(III) on coordinating the second ligand.[43] Hence a second role of the protein in hemoproteins such as peroxidase, which have one histidine coordinated to an Fe(III), is to stabilize the monohistidine complex.

Quantitative determinations of the equilibria involved as a function of pH showed that

1) dimeric alkaline hemin reacts with histidine, histamine and pilocarpate to first give an adduct (possibility hydrogen bonded) containing one base per dimer and then to give the monomeric bis-ligand complexes.

2) on coordination, the pKa of the pendant -OH of pilocarpate is reduced from 15 to 10 (and a difference in the spectrum

noted above and below pH 10), and that of the pendant $-NH_2$ of histidine and histamine from ~9,5 to < 8, which was ascribed to the stabilization of the conjugate base and/or the destabilization of the conjugate acid by the residual positive charge on the iron.

This latter finding provides a mechanism for proton or cation uptake on reduction observed with some hemoproteins,[2] reduction of course eliminating the residual positive charge and allowing the pKas of the neighbouring amino acid residues to revert to their normal values. For example, prior to reduction, the pendant $-NH_2$ group of histidine should be deprotonated in the pH range 8 - 10, but on reduction at these pHs should become protonated thus picking up a proton. This was in fact found on reducing bis-histidine by cyclic voltametry in this pH range.[108]

In chapter 6, the study of the rate of reduction of B_{12a} to B_{12r} by dithiothreitol over the pH range 1 - 13, revealed an interesting interplay between the rates of coordination of the thiolate to the Co(III) and reduction to Co(II). Significant differences were found in the acid region between the rate of reduction by the dithiols, dithiothreitol and the monothiols cysteine[64] and mercaptoethanol. It was concluded that over the pH range 3 - 12, coordination always precedes reduction and that the mechanism probably involves a one electron reduction of the cobalt by the coordinated thiol, assisted by the second thiol (which is faster if dissociated (i.e. RS^-) than if protonated (i.e. RSH)), to give the cyclic disulphide radical anion  or its conjugate acid (pKa 5,5) as the immediate product. No redox potentials are known for the one electron oxidation of thiols but

it would appear that the $RS^-/R\bar{S}\bar{S}R$ couple is a better reducing agent than $RS^-/RS^{\cdot}$. The absence of a second neighbouring cysteine in cytochrome P-450 may explain why the Fe(III) is not reduced by the coordinated cysteine, as occurs in protein free hemin.

In chapter 7, the reduction of the monomeric bis-histidine complex of hemin by dithiothreitol was shown to proceed via the rapid formation of an intermediate, identified by spectra and analysis of the rate data as the histidine thiolate complex, which then underwent a first order reaction to give Fe(II), i.e. the mechanism was inner sphere analogous to that of B_{12a}, and no detectable outer sphere electron transfer was found. In addition, inhibition by dithiothreitol at high concentrations was consistent with a second dithiothreitol forming an adduct (possibly hydrogen bonded) but not coordinating (as UV-visible bands expected for the bis-thiolate complex were not evident)[59] to give a species which reduced more slowly than the histidine-thiolate complex. The much slower reaction with cysteine and mercaptoethanol suggests, by analogy with B_{12a}, that a second thiol group is required.

In chapter 8, the detailed study at pH 10 of the oxidation of cysteine by O_2 catalysed by B_{12a}, revealed that the rate determining step in the catalytic cycle was the reduction of Co(III) but that this was forty-two times greater than the rate of reduction by cysteine! It was shown that all the results could be explained by a scheme involving a rapid reaction of the transient $Co(II)O_2$ with the thiol (RSH) to give $Co(III)O_2H^-$ (and hence H_2O_2 which was detected by catalase) and the radical $RS^{\cdot}$ which reacts rapidly with a second thiol to give the disulphide radical anion ($R\bar{S}\bar{S}R$) which is the main reductant of Co(III). It was also shown that the

formation of free H_2O_2 could be suppressed by increasing the thiol concentration. The catalysed oxidation of dithiothreitol showed very similar features but was not markedly faster. The cobinamides (which lack the benzimidazole ligand of B_{12a}) have a much greater catalytic activity, reacting about 920 equivalents ℓ^-/(M catalyst x s) which is faster than cytochrome c oxidase due to the faster reduction rate of Co(III).[113] Hence Co corrinoids are able to model both the suppression of H_2O_2 formation and the high turnover number, though in cytochrome a_3, $Fe(III)O_2H^-$ may convert to $[FeO]^{3+}$. Evidence was also found for Cu(II) catalysis which is of interest as cytochrome c oxidase contains copper.

In chapter 9, the oxidation of dithiothreitol catalysed by bis-histidine hemin was studied. The kinetics were complex which is of interest in light of the variety of reactions between hemoproteins and O_2. The rate dependence on the thiol concentration showed similar features to that found for the reduction, yet once again was faster. As at low thiol concentrations, spectra in the steady state showed the presence of the monothiolate, reduction must be rate determining and hence by analogy to B_{12a} involves reduction by RSSR. Bis-histidine hemin is not as good a catalyst as diaquocobinamide or even B_{12a}, which once again shows the influence of the protein in cytochrome oxidase in increasing the rate.

In this thesis, some of the structures, ligand binding, redox and catalytic reactions of hemin, and to a lesser extent cobalt corrinoids, in aqueous solution have been investigated and some pointers to the role of the protein in modulating these reactions have been given.

APPENDIX 1 : DERIVATION OF EQUATIONS FOR THE EQUILIBRIUM STUDIES (CHAPTERS 3, 4, 5)

Equations [10] required to analyse the data for the binding of ligands and the loss of protons (pKa) are derived in this appendix in parts (a) and (b) respectively. In each part, equations will be derived for monomer-monomer, dimer-dimer and monomer-dimer interconversions.

The following abbreviations have been used here: M for the hemin monomer; D for the hemin dimer; L for the ligand or a species interacting with the porphyrin ring; n for the number of "ligands" bound; $(Fe)_{TOT}$ for the hemin concentration in terms of the concentration of the iron porphyrin units; A for absorbance with A_o and A_∞ referring to the absorbance of the initial and final species respectively.

a) *Ligand binding equations*

Equations required to treat the data if the ligand concentration, the hemin concentration or the pH is varied will be derived.

1) Derivation of equations for binding n ligands to a monomer

$$M + nL \rightleftharpoons ML_n \qquad (I)$$

$$\therefore K = \frac{(ML_n)}{(M)(L)^n}$$

$$\therefore \log K = \log \frac{(ML_n)}{(M)} - n \log (L) \qquad (1)$$

i) Varying (L) ($(Fe)_{TOT}$ constant)

now $A = \varepsilon_M(M) + \varepsilon_{MLn}(ML_n)$

and $(Fe)_{TOT} = (M) + (ML_n)$

$\therefore (ML_n) = \varepsilon_M(M)_{TOT} - (M)$

$\therefore A = \varepsilon_M(M) + \varepsilon ML_n((Fe)_{TOT} - (M))$

$$= (M)\ (\varepsilon_M - \varepsilon_{ML_n}) + \varepsilon ML_n\ (Fe)_{TOT}$$

$$\therefore\ (M) = \frac{A - \varepsilon ML_n (Fe)_{TOT}}{\varepsilon M - \varepsilon ML_n}$$

now $A_o = \varepsilon_M (Fe)_{TOT} \Longrightarrow \varepsilon_M = \frac{A_o}{(Fe)_{TOT}}$

$$A_\infty = \varepsilon_{ML_n} (Fe)_{TOT} \Longrightarrow \varepsilon_{ML_n} = \frac{A_\infty}{(Fe)_{TOT}}$$

$$\therefore\ (M) = \frac{A - A_\infty}{A_o - A_\infty} \times (Fe)_{TOT}$$

$$\therefore\ (ML_n) = \frac{A_o - A}{A_o - A_\infty} \times (Fe)_{TOT}$$

$$\therefore\ \log K = \log \frac{A_o - A}{A - A_\infty} - n \log (L) \qquad (2)$$

$$\therefore\ \log \frac{A - A_o}{A_\infty - A} = \log K + n \log (L) \qquad (3)$$

$\therefore$ plot of $\log \frac{A - A_o}{A_\infty - A}$ vs $\log (L)$ should be linear with slope = n and intercept = log K

if OH^- released (reaction II)

$$M + nL \rightleftharpoons ML_n + d\ OH^- \qquad (II)$$

then equation (3) becomes

$$\log \frac{A - A_o}{A_\infty - A} = \log K' + d(14 - pH) + n \log (L) \qquad (4)$$

ii) Varying $(Fe)_{TOT}$ ((L) constant)

let α be the fraction of metalloporphyrin combined with ligand

i.e. $\alpha = \frac{(MLn)}{(Fe)_{TOT}}$ $\qquad [(Fe)_{TOT} = (M) + (ML_n)]$

$(ML_n) = \alpha\ (Fe)_{TOT}$

$(M) = (1 - \alpha)(Fe)_{TOT}$

$$\log K = \log \frac{\alpha(Fe)_{TOT}}{(1-\alpha)(Fe)_{TOT}} - n \log (L)$$

$$\therefore \log \alpha (Fe)_{TOT} = \log K + n \log(L) + \log(1-\alpha) (Fe)_{TOT}$$

$\therefore$ A plot of $\log \alpha(Fe)_{TOT}$ versus $\log(1-\alpha) (Fe)_{TOT}$ (5) should be linear with slope = 1 and intercept = $\log K + n \log(L)$

In general, for dilution experiments where (L) is constant the slope of $\log \alpha(Fe)_{TOT}$ versus $\log (1-\alpha)(Fe)_{TOT}$ = $\frac{\text{no. FeP units in prod}}{\text{no. FeP units in react}}$ if reaction (II) applies then equation (5) becomes

$$\log \alpha(Fe)_{TOT} = \log K' + d(14-pH) + n \log(L) + \log(1-\alpha)(Fe)_{TOT} \quad (6)$$

2) Derivation of equations for binding n ligands to a dimer

$$D + nL \rightleftharpoons DL_n \qquad (III)$$

$$\log K = \log \frac{(DL_n)}{(D)(L)^n}$$

$$\therefore \log K = \log \frac{(DL_n)}{(D)} = n \log(L)$$

i) Varying (L) ($(Fe)_{TOT}$ constant)

$$A = \varepsilon_D(D) + \varepsilon_{DLn}(DL_n)$$

$$(Fe)_{TOT} = 2(D) + 2(DL_n)$$

$$\therefore A = (D)(\varepsilon_D - \varepsilon_{DLn}) + \varepsilon_{DLn} \frac{(Fe)_{TOT}}{2}$$

$$\therefore (D) = \frac{A - \varepsilon_{DLn} \frac{(Fe)_{TOT}}{2}}{\varepsilon_D - \varepsilon_{DLn}}$$

$$A_o = \varepsilon_D \frac{(Fe)_{TOT}}{2} \Longrightarrow \varepsilon_D = \frac{2A_o}{(Fe)_{TOT}}$$

$$A_\infty = \varepsilon_{DLn} \frac{(Fe)_{TOT}}{2} \Longrightarrow \varepsilon_{DLn} = \frac{2A_\infty}{(Fe)_{TOT}}$$

$$\therefore \quad (D) = \frac{A - A_\infty}{A_o - A_\infty} \times \frac{(Fe)_{TOT}}{2}$$

$$\therefore \quad (DLn) = \frac{A_o - A}{A_o - A_\infty} \times \frac{(Fe)_{TOT}}{2}$$

$$\therefore \quad \log K = \log \frac{A_o - A}{A - A_\infty} - n \log (L) \qquad (7)$$

$$\therefore \quad \log \frac{A - A_o}{A_\infty - A} = \log K + n \log (L) \qquad (8)$$

i.e. plot of $\log \frac{A - A_o}{A_\infty - A}$ vs log (L) should be linear with

slope = n

intercept = log K

If OH^- is involved in the reaction (i.e. reaction (IV) applies)

$$D + nL \rightleftharpoons DLn + d\ OH^- \qquad (IV)$$

then equation (8) becomes

$$\log \frac{A - A_o}{A_\infty - A} = \log K' + d(14-pH) + n \log (L) \qquad (9)$$

ii) Varying $(Fe)_{TOT}$ $\left((L) \text{ constant}\right)$

let $\alpha = \frac{2(DLn)}{(Fe)_{TOT}}$

$$\therefore \quad (DLn) = \alpha \frac{(Fe)_{TOT}}{2}$$

$$(D) = (1-\alpha) \frac{(Fe)_{TOT}}{2}$$

$$\log K = \frac{\log \frac{1}{2} \alpha (Fe)_{TOT}}{\log \frac{1}{2} (1-\alpha) (Fe)_{TOT}} - n \log (L)$$

$$\therefore \quad \log K = \log \frac{\alpha (Fe)_{TOT}}{(1-\alpha)(Fe)_{TOT}} - n \log (L)$$

$$\therefore \quad \log \alpha (Fe)_{TOT} = \log K + n \log (L) + \log (1-\alpha)(Fe)_{TOT} \qquad (10)$$

A plot of log α $(Fe)_{TOT}$ vs log $(1-\alpha)$ $(Fe)_{TOT}$ will therefore be linear with slope = 1 and

intercept = log K + n log(L)

If d moles of OH^- released then equation (10) becomes

$$\log\alpha(Fe)_{TOT} = (\log K' + d(14-pH) + n \log(L) + \log(1-\alpha)(Fe)_{TOT} \quad (14)$$

3) Derivation of equations for binding of n ligands and splitting a dimer to give a monomer

$$D + 2nL \rightleftharpoons 2ML_n \quad (V)$$

$$K = \frac{(ML_n)^2}{(D)(L)^n}$$

$$\therefore \log K = \log \frac{(ML_n)^2}{(D)} - 2n \log (L) \quad (15)$$

i) Varying (L) $(Fe)_{TOT}$ constant

now $A = \varepsilon_D (D) + \varepsilon_{MLn} (MLn)$

and $(Fe)_{TOT} = 2(D) + (MLn)$

$$\therefore (ML_n) = (Fe)_{TOT} - 2(D)$$

$$\therefore A = \varepsilon_D(D) + \varepsilon_{MLn} \left[(Fe)_{TOT} - 2(D)\right]$$

$$\therefore A = (D)(\varepsilon_D - 2\varepsilon_{MLn}) + \varepsilon_{MLn} (Fe)_{TOT}$$

$$\therefore (D) = \frac{A - \varepsilon_{MLn}(Fe)_{TOT}}{\varepsilon_D - 2\varepsilon_{MLn}} \qquad (ML_n) = \frac{(\varepsilon D/2)(Fe)_{TOT} - A}{(\frac{\varepsilon D}{2} - \varepsilon MLn)(Fe)_{TOT}} \times (Fe)_{TOT}$$

now $A_\infty = \varepsilon_{MLn} \left[(Fe)_{TOT}\right] \Longrightarrow \varepsilon_{MLn} = \frac{A_\infty}{(Fe)_{TOT}}$

and $A_o = \varepsilon_D \frac{(Fe)_{TOT}}{2} \Longrightarrow \varepsilon_D = \frac{2A_o}{(Fe)_{TOT}}$

$$\therefore (D) = \frac{A - A_\infty}{A_o - A_\infty} \times \frac{(Fe)_{TOT}}{2}$$

$$\therefore (MLn) = \frac{A_o - A}{A_o - A_\infty} \times \frac{(Fe)_{TOT}}{1}$$

$$\therefore \log K = \log\left(\frac{A_o-A}{A-A_\infty} \times \frac{(Fe)_{TOT}}{2}\right)^2 \times \frac{A_o-A_\infty}{A-A_\infty} \times \frac{2}{(Fe)_{TOT}} - 2n \log(L)$$

$$= \log \frac{(A_o-A)^2}{A-A_\infty} \times \frac{2(Fe)_{TOT}}{A_o-A_\infty} - 2n \log(L) \qquad (16)$$

$$\therefore \log \frac{(A_o-A)^2}{A-A_\infty} \times \frac{2(Fe)_{TOT}}{A_o-A_\infty} = \log K + 2n \log (L)$$

$$\therefore \log \frac{(A-A_o)^2}{A_\infty-A} \times \frac{2(Fe)_{TOT}}{A_\infty-A_o} = \log K + 2n \log (L) \qquad (17)$$

$\therefore$ a plot of $\log \frac{(A-A_o)^2}{A_\infty-A} \times \frac{2(Fe)_{TOT}}{A_\infty-A_o}$ versus $\log (L)$

should be linear with slope = $2n$ and

intercept = $\log K$.

Also $\log \frac{(A-A_o)^2}{A_\infty-A} = \log K - \log \frac{2(Fe)_{TOT}}{A_\infty-A_o} + n \log (L)$ (18)

$\therefore$ a plot of $\log \frac{(A-A_o)^2}{A_\infty-A}$ vs $\log (L)$ should be linear with

slope = $2n$ and

intercept = $\log K - \log \frac{2(Fe)_{TOT}}{A_\infty-A_o}$

ii) Varying (hemin) ((L) constant)

if α is the fraction of metalloporphyrin $[(Fe)_{TOT}]$ combined with ligand

i.e. $\alpha = \frac{(MLn)}{(Fe)_{TOT}} = \frac{\left(\varepsilon_{D/2}\right)(Fe)_{TOT} - A}{(\varepsilon_{D/2} - \varepsilon_{MLn})(Fe)_{TOT}}$ (19)

and $(Fe)_{TOT} = (MLn) + 2(D)$

then $(MLn) = \alpha(Fe)_{TOT}$

and $2(D) = (Fe)_{TOT} - \alpha (Fe)_{TOT}$

$\therefore (D) = (1-\alpha) \frac{(Fe)_{TOT}}{2}$

$$\therefore \log K = \log \frac{(\alpha(Fe)_{TOT})^2}{(1-\alpha)(Fe)_{TOT}/2} - 2n \log (L)$$

$$= 2 \log \alpha(Fe)_{TOT} - \log \tfrac{1}{2}(1-\alpha)(Fe)_{TOT} - 2n \log (L)$$

$$= 2 \log \alpha(Fe)_{TOT} - \log (1-\alpha)(Fe)_{TOT} - \log \tfrac{1}{2} - 2n \log (L) \quad (20)$$

$$\therefore 2 \log \alpha(Fe)_{TOT} = \log K + 2n \log(L) + \log \tfrac{1}{2} + \log(1-\alpha)(Fe)_{TOT}$$

$$\therefore \log \alpha(Fe)_{TOT} = \tfrac{1}{2}(\log K + 2n \log(L) + \log \tfrac{1}{2}) + \tfrac{1}{2} \log(1-\alpha)(Fe)_{TOT} \quad (21)$$

$\therefore$ a plot of $\log \alpha(Fe)_{TOT}$ against $\log (1-\alpha)(Fe)_{TOT}$

should give slope $= \tfrac{1}{2}$ and

intercept $= \tfrac{1}{2} (\log K + 2n \log (L) + \log \tfrac{1}{2})$

iii) Effect of pH

if the reaction involves the release of OH^- (i.e. reaction (VI)

$$D + 2nL \rightleftharpoons ML_n + d\ OH^- \quad (VI)$$

then $\log K' = \log \frac{(ML_n)^2}{(D)} - 2n \log (L) - d(14-pH)$

and equation (17) then becomes

$$\log \frac{(A-A_o)^2}{(A_\infty - A)} \times \frac{2(Fe)_{TOT}}{A_\infty - A_o} = \log K' + 2n \log(L) + d(14-pH) \quad (22)$$

and equation (20) becomes

$$\log \alpha(Fe)_{TOT} = \tfrac{1}{2}(\log K' + 2n \log(L) + \log \tfrac{1}{2} + d(14-pH)) + \tfrac{1}{2}(\log(1-\alpha)(Fe)_{TOT} \quad (23)$$

b) Derivation of pKa equations

1) Proton loss involving monomeric species only

$$M \rightleftharpoons M' + nH^+ \quad (IV)$$

$$K_a = \frac{(M')(H^+)^n}{(M)} \Longrightarrow \log K_a = \log \frac{(M')}{(M)} + n \log (H^+)$$

$$\Longrightarrow pKa = -\log \frac{(M')}{(M)} + n\ pH$$

$$\Longrightarrow \log \frac{(M')}{(M)} = n\ pH - pKa.$$

Now $A = \varepsilon_M(M) + \varepsilon_{M'}(M)$

$(Fe)_{TOT} = (M) + (M') \Longrightarrow (M') = (Fe)_{TOT} - (M)$

$\therefore A = \varepsilon_M (M) + \varepsilon_{M'} [(Fe)_{TOT} - (M)]$

$\therefore A = (M)(\varepsilon_M - \varepsilon_{M'}) + \varepsilon_{M'} (Fe)_{TOT}$

$$\therefore (M) = \frac{A - \varepsilon_{M'}(Fe)_{TOT}}{\varepsilon_M - \varepsilon_{M'}}$$

initially $(M) = (Fe)_{TOT}$

$$\therefore A_o = \varepsilon_M (Fe)_{TOT} \Longrightarrow \varepsilon_M = \frac{A_o}{(Fe)_{TOT}}$$

finally $(M') = (Fe)_{TOT}$

$$\therefore A_\infty = \varepsilon_{M'} (Fe)_{TOT} \Longrightarrow \varepsilon_{M'} = \frac{A_\infty}{(Fe)_{TOT}}$$

$$\therefore (M) = \frac{A - A_\infty}{A_o - A_\infty} \times (Fe)_{TOT}$$

$$(M') = (Fe)_{TOT} - (M)$$

$$= (Fe)_{TOT} \left(1 - \frac{A - A_\infty}{A_o - A_\infty}\right)$$

$$= (Fe)_{TOT} \frac{A_o - A}{A_o - A_\infty}$$

$$\therefore \frac{(M')}{(M)} = \frac{A_o - A}{A - A_\infty} = \frac{A - A_o}{A_\infty - A}$$

$$\therefore \log \frac{A - A_o}{A_\infty - A} = n\ pH - pKa$$

and $pKa = -\log \frac{A - A_o}{A_\infty - A} + n\ pH$

A plot of log $\frac{A - A_o}{A_\infty - A}$ versus pH should be linear with slope = n and intercept = -pKa.

2. Proton loss involving dimeric species only

$$D \rightleftharpoons D + nH^+ \qquad (V)$$

$$K = \frac{(D')}{(D)(H^+)^n} \Longrightarrow \log \frac{(D')}{(D)} = n\,pH - pKa$$

$$A = \varepsilon_D (D) + \varepsilon_{D'} (D')$$

$$(Fe)_{TOT} = 2 \times (D) + 2(D')$$

$$\therefore (D') = \frac{(Fe)_{TOT} - 2(D)}{2}$$

$$\therefore A = \varepsilon_D (D) + \varepsilon_{D'} \left(\frac{(Fe)_{TOT}}{2} - (D) \right)$$

$$= (D)(\varepsilon_D - \varepsilon_{D'}) + \varepsilon_{D'} \frac{(Fe)_{TOT}}{2}$$

$$\therefore (D) = \frac{A - \varepsilon_{D'} \frac{(Fe)_{TOT}}{2}}{\varepsilon_D - \varepsilon_{D'}}$$

initially $(D) = \frac{1}{2} (Fe)_{TOT}$

$$\therefore A_o = \varepsilon_D \frac{(Fe)_{TOT}}{2} \Longrightarrow \varepsilon_D = \frac{2A_o}{(Fe)_{TOT}}$$

finally $(D') = \frac{1}{2} (Fe)_{TOT}$

$$\therefore A_\infty = \varepsilon_{D'} \frac{(Fe)_{TOT}}{2} \Longrightarrow \varepsilon_{D'} = \frac{2A_\infty}{(Fe)_{TOT}}$$

$$\therefore (D) = \frac{A - A_\infty}{A_o - A_\infty} \times \frac{(Fe)_{TOT}}{2}$$

$$(D') = \frac{(Fe)_{TOT}}{2} - (D) = \frac{A_o - A}{A_o - A_\infty} \times \frac{(Fe)_{TOT}}{2}$$

$$\therefore \frac{(D')}{(D)} = \frac{A_o - A}{A - A_\infty} = \frac{A - A_o}{A_\infty - A}$$

$\therefore$ log $\dfrac{A - A_o}{A_\infty - A}$ = n pH - pKa

$\therefore$ plot of log $\dfrac{A - A_o}{A_\infty - A}$ vs pH should be linear with slope = n and intercept = -pKa.

3) Proton loss involving dimerisation

$$2M \rightleftharpoons D + nH^+ \qquad \text{(VI)}$$

$K_a = \dfrac{(D)(H^+)^n}{(M)^2} \Longrightarrow \log \dfrac{(M)^2}{(D)} = -n\ pH + pKa$

$A = \varepsilon_M (M) + \varepsilon_D (D)$

$(Fe)_{TOT} = (M) + 2(D) \Longrightarrow (M) = (Fe)_{TOT} - 2(D)$

$\therefore A = \varepsilon_M [(Fe)_{TOT} - 2(D)] + \varepsilon_D (D)$

$= (D)(\varepsilon_D - 2\varepsilon_M) + \varepsilon_M (Fe)_{TOT}$

$\therefore (D) = \dfrac{A - \varepsilon_M (Fe)_{TOT}}{\varepsilon_D - 2\varepsilon_M}$

initially $(Fe)_{TOT} = (M)$ initial

$\therefore A_o = \varepsilon_M (Fe)_{TOT} \Longrightarrow \varepsilon_M = \dfrac{A_o}{(Fe)_{TOT}}$

initially $(D) = (Fe)_{TOT}$

$\therefore A_\infty = \varepsilon_D (Fe)_{TOT}/2 \Longrightarrow \varepsilon_D = \dfrac{2A_\infty}{(Fe)_{TOT}}$

$\therefore (D) = \dfrac{A - A_o}{A_o - A_\infty} \times \dfrac{(Fe)_{TOT}}{2}$

$(M) = (Fe)_{TOT} - 2(D) = \dfrac{A - A_\infty}{A_o - A_\infty} \times (Fe)_{TOT}$

$\therefore \dfrac{(M)^2}{(D)} = \dfrac{(A - A_\infty)^2}{(A_o - A_\infty)^2} \times (Fe)_{TOT}^2 \times \dfrac{A_o - A_\infty}{A - A_o} \times \dfrac{2}{(Fe)_{TOT}}$

$$= \frac{(A - A_\infty)^2}{A_o - A} \times \frac{(Fe)_{TOT}}{A_o - A_\infty} = \frac{(A_\infty - A)^2}{(A - A_o)} \times \frac{2(Fe)_{TOT}}{A_\infty - A_o}$$

$$\therefore \log \frac{(A_\infty - A)^2}{(A - A_o)} \times \frac{2(Fe)_{TOT}}{(A_\infty - A_o)} = -n\,pH + pKa$$

$$\therefore \log \frac{(A_\infty - A)^2}{(A - A_o)} = -n\,pH + pKa - \log \frac{2(Fe)_{TOT}}{A_\infty - A_o}$$

a) $\therefore$ A plot of $\log \frac{(A_\infty - A)^2}{(A - A_o)}$ vs pH should be linear with slope = n and intercept = $+pKa - \log \frac{2(Fe)_{TOT}}{A_\infty - A_o}$

$\Longrightarrow$ $pKa = + \log \frac{2(Fe)_{TOT}}{A_\infty - A_o}$ + intercept.

The pKa can be calculated at each point using

$$pKa = \log \frac{(A_\infty - A_o)^2}{(A - A_o)} + n\,pH + \log \frac{2(Fe)_{TOT}}{A_\infty - A_o}$$

b) If the pH is kept constant but $(Fe)_{TOT}$ varied then

$$\log \frac{(A_\infty - A)^2}{(A-A_o)(A_\infty - A_o)} = -\log (Fe)_{TOT} + npH - pKa - \log 2$$

$\therefore$ plot of $\frac{(A_\infty - A)^2}{(A-A_o)(A_\infty - A_o)}$ versus $\log (Fe)_{TOT}$ should be linear with slope = -1 and intercept = npH - pKa - log 2.

$\therefore$ pKa = npH - intercept - log 2 (n determined in a)

$$pKa = \log \frac{(A_\infty - A)^2}{A - A_o} \times \frac{1}{A_\infty - A_o} + npH + \log (Fe)_{TOT} + \log 2$$

Note - both reactions (IV) and (V) have no $(Fe)_{TOT}$ term in the final expression and hence $\log \frac{(D')}{(D)}$ and $\log \frac{(M')}{(M)}$ should be invariant with $(Fe)_{TOT}$.

APPENDIX 2 : TABLES OF DATA FOR THE STUDY OF HEMIN IN ALKALINE SOLUTION (ALL EXPERIMENTS DONE IN SOLUTIONS WITH μ = 0,1 at 25°C)

Equations used in analysis of data were:

$$\log K = \log \frac{(A_o - A)^2}{A - A_\infty} \times \frac{2(Fe)_{TOT}}{A_o - A_\infty} - 2n \log (L) \qquad (1)$$

$$\alpha = \frac{\varepsilon_{D/2}\,(Fe)_{TOT} - A}{(\varepsilon_{D/2} - \varepsilon_{MLn})\,(Fe)_{TOT}} \qquad (2)$$

$$\log K = 2 \log \alpha\,(Fe)_{TOT} - \log(1-\alpha)(Fe)_{TOT} - \log \tfrac{1}{2} - 2n\log(L) \qquad (3)$$

Table 1a : Titration of hemin by caffeine at pH 8,50;
$10,1 \times 10^{-6}$M hemin

10^3(caffeine) TOTAL, M	A_{400}	log(caffeine) free	log $\frac{(A-A_o)^2}{A_\infty-A} \times \frac{2(Fe)_{TOT}}{A_\infty-A_o}$	log K[a] (M^{-1})
0,10	0,344	-4,00	-7,29	0,71
0,30	0,363	-3,52	-6,32	0,72
0,50	0,379	-3,30	-5,90	0,70
0,79	0,402	-3,10	-5,42	0,78
1,09	0,420	-2,96	-5,21	0,71
1,57	0,444	-2,81	-4,90	0,72
2,34	0,472	-2,63	-4,55	0,71
3,29	0,494	-2,48	-4,24	0,72
4,76	0,517	-2,32	-3,80	0,84

A_o = 0,334 A_∞ = 0,538 Av: 0,74 ± 0,1

[a] calc. using equation (1) with n = 2 *intercept = 0,85(Sd=0,09)
slope = 2,04(Sd=0,03)

Table 1b : Titration of hemin by caffeine at pH 12,00;
$10,2 \times 10^{-6}$M hemin

10^3(caffeine) TOTAL, M	A_{400}	log(caffeine) free	log $\frac{(A-A_o)^2}{A_\infty-A} \times \frac{2(Fe)_{TOT}}{A_\infty-A_o}$	log K[a] (M^{-1})
0,10	0,466	-4,00	-7,18	0,82
0,20	0,481	-3,70	-6,55	0,85
0,30	0,492	-3,53	-6,26	0,80
0,40	0,505	-3,40	-6,00	0,80
0,60	0,527	-3,22	-5,66	0,78
0,89	0,553	-3,05	-5,34	0,76
1,19	0,576	-2,93	-5,10	0,76
1,67	0,601	-2,78	-4,86	0,70

A_o = 0,451 A_∞ = 0,723 Av: 0,79 ± 0,09

[a] calc. using equation (1) with n = 2 *intercept=0,46(Sd=0,07)
slope=1,90 (Sd=0,02)

* Plot of log $\frac{(A-A_o)^2}{A_\infty-A} \times \frac{2(Fe)_{TOT}}{A_\infty-A_o}$ vs log(caffeine)free

Table 2 : Dilution experiments with hemin-caffeine

a) pH 8,50; $1,68 \times 10^{-3}$ M caffeine

$10^6 (Fe)_{TOT}$, M	A_{400}	α	$\log(Fe)_{TOT}\ \alpha$	$\log(Fe)_{TOT}(1-\alpha)$	$\log_M K$ [a]
(2,12	0,147	0,745	-5,80	-6,27	0,52)
4,23	0,287	0,701	-5,53	-5,90	0,69
6,35	0,419	0,647	-5,39	-5,65	0,72
8,45	0,545	0,603	-5,29	-5,47	0,74
10,55	0,665	0,560	-5,22	-5,33	0,74
15,80	0,964	0,500	-5,10	-5,10	0,75
21,03	1,242	0,443	-5,03	-4,93	0,72

Av: 0,73 ± 0,04

Plot of $\log(Fe)_{TOT}\ \alpha$ versus $\log(Fe)_{TOT}(1-\alpha)$

intercept = -2,19 (Sd = 0,13)
slope = 0,57 (Sd = 0,02

[a] Calculated using equation (3) (n = 2)

b) pH 10,0; $1,68 \times 10^{-3}$ M caffeine

$10^6 (Fe)_{TOT}$, M	A_{400}	α	$\log(Fe)_{TOT}\ \alpha$	$\log(Fe)_{TOT}(1-\alpha)$	$\log K_M^{-1}$ [a]
(3,79	0,258	0,708	-5,57	-5,96	0,67)
5,68	0,384	0,694	-5,40	-5,76	0,81
7,57	0,502	0,656	-5,30	-5,58	0,83
9,47	0,614	0,613	-5,24	-5,44	0,81
11,36	0,721	0,573	-5,19	-5,31	0,78
15,14	0,922	0,497	-5,12	-5,12	0,73
18,93	1,136	0,471	-5,05	-5,00	0,75
22,72	1,333	0,431	-5,01	-4,89	0,72

Av: 0,78 ± 0,05

Plot of $\log(Fe)_{TOT}$ versus $\log(Fe)_{TOT}(1-\alpha)$

intercept = -2,58 (Sd = 0,16)
slope = 0,49 (Sd = 0,03)

[a] Calculated using equation (3) (n = 2)

c) 20 mM NaOH; $2,34 \times 10^{-3}$M caffeine

$10^6(Fe)_{TOT}$, M	A_{400}	α	$\log(Fe)_{TOT}\,\alpha$	$\log(Fe)_{TOT}^{(1-\alpha)}$	$\log K^a$ (M^{-1})
3,90	0,281	0,825	-5,49	-6,17	0,75
7,79	0,535	0,726	-5,25	-5,67	0,73
11,69	0,788	0,688	-5,09	-5,44	0,82
19,48	1,237	0,574	-4,95	-5,08	0,74

Av: 0,76 ± 0,06

Plot of $\log(Fe)_{TOT}\,\alpha$ versus $\log(Fe)_{TOT}^{(1-\alpha)}$

intercept = -2,37 (Sd = 0,18)

slope = 0,51 (Sd = 0,03)

[a] Calculated using equation (3) (see 2)

Calculations in Table 2a, b, c carried out using

$$\frac{\varepsilon_D}{2} = 4,4 \times 10^4\ M^{-1}$$

$$\varepsilon_{MLn} = 7,8 \times 10^4\ M^{-1}$$

and equations (2) and (3) (where n = 2)

Table 3a) : Titration of hemin by cetyl trimethyl ammonium bromide

i) 0,1M NaOH; $9,72 \times 10^{-6}$M hemin

$(detergent)_{TOT}$, µM	A_{384}	log(detergent) free [a]	$\log \frac{A-A_o}{A_\infty - A}$	log K [a]
0,3	0,552	-6,98	-1,69	12,27
0,9	0,550	-6,29	-1,38	11,20
1,8	0,545	-6,04	-1,00	11,08
3,6	0,535	-5,76	-0,62	10,90
6,0	0,524	-5,52	-0,36	10,68
9,0	0,510	-5,33	-0,10	10,56
12,0	0,495	-5,21	0,17	10,59
15,0	0,484	-5,09	0,38	10,56
18,0	0,476	-4,99	0,57	10,55
24,0	0,466	-4,81	0,90	10,54
30,0	0,461	-4,68	1,19	10,56

Av: 10,56 ± 0,03

[a] n = 2 using equation (1)

A_o = 0,554 A_∞ = 0,435 n = 2 (det) 0,9 → 30,0
slope = 1,94 (Sd = 0,04)
intercept = 10,26 (Sd = 0,18)

ii) pH 8,50 (borax); $9,64 \times 10^{-6}$M hemin

(detergent), µM	A_{450}	log(detergent) free [a]	$\log \frac{A-A_o}{A_\infty - A}$	log K [a,b]
0,6	0,087	-6,72	-1,35	12,09
1,5	0,093	-6,32	-0,92	11,72
3,0	0,105	-6,13	-0,51	11,75
6,0	0,114	-5,55	-0,31	10,79
12,0	0,139	-5,20	0,17	10,57
18,0	0,152	-4,96	0,44	10,36
24,0	0,165	-4,81	0,83	10,45
30,0	0,174	-4,68	1,48	10,84

a n=2 b calculated using equation (1) Av: 10,64 ± 0,3

A_o = 0,083 A_∞ = 0,177 n=2 (det) 6,0 → 30,0
* slope = 1,87 (Sd = 0,34)
intercept = 9,97 (Sd = 1,73)

* Plot of $\log \frac{A-A_o}{A_\infty - A}$ versus log (detergent) free

iii) 0,1M NaOH; $1,5 \times 10^{-5}$M CTMAB; 25°C

$10^6(Fe)_{TOT}$, M	A_{450}	α	$\log(Fe)_{TOT}\,\alpha$	$\log(Fe)_{TOT}(1-\alpha)$	log K [a] (M^{-1})
4,44	0,075	0,78	-5,46	-6,00	10,42
6,66	0,109	0,73	-5,31	-5,74	10,42
8,88	0,148	0,76	-5,17	-5,66	10,66
13,29	0,221	0,75	-5,00	-5,48	11,08

Av: 10,7 ± 0,3

[a] using equation (3)

Table 3b : Titration of hemin with triton X-100;

$10,0 \times 10^{-6}$M hemin; 0,1M NaOH

(detergent) µM	A_{384}	log (detergent) free [a]	$\log \frac{A-A_o}{A_\infty-A}$	log K [a,b]	
2,67	0,563	-5,92 (-5,71)	-0,769	11,07	(4,94)
6,67	0,558	-5,37 (-5,26)	-0,509	10,23	(4,75)
11,96	0,553	-5,06 (-4,99)	-0,313	9,81	(4,68)
19,90	0,546	-4,81 (-4,75)	-0,079	9,54	(4,67)
31,75	0,538	-4,59 (-4,54)	0,176	9,36	(4,72)
51,33	0,527	-4,36 (-4,32)	0,602	9,32	(4,92)
70,33	0,520	-4,21 (-4,18)	1,106	9,53	(5,29)
			Av:	9,45 ± 0,13	(4,76) ± 0,18

[a] n = 2 (n = 1) [b] Calculated using equation (1)

A_o = 0,571 A_∞ = 0,516

* n = 1 (det) 2,67 → 31,75 | n = 2 (det) 19,90 → 70,33

slope = (0,79) (Sd = 0,07) | 1,93 (Sd = 0,30)

intercept = (3,71) (Sd = 0,38) | 9,11 (Sd = 1,35)

* Plot of $\log \frac{A-A_o}{A_\infty-A}$ versus log (detergent) free

Table 3c : Titration of hemin with sodium lauryl sulphate;

0,1M NaOH; $11,1 \times 10^{-6}$ M hemin

(detergent), µM	A_{384}	log(detergent free)[a]	$\log \frac{A-A_o}{A_\infty-A}$	log K [a,b]
3	0,629	-5,69	-0,68	5,01
6	0,623	-5,41	-0,21	5,20
9	0,621	-5,19	-0,09	5,10
12	0,619	-5,04	0,03	5,07
15	0,616	-4,94	0,21	5,15
18	0,613	-4,85	0,42	5,27
21	0,610	-4,79	0,50	5,29
23,9	0,610	-4,71	0,68	5,39
29,9	0,609	-4,60	0,80	5,40
41,8	0,609	-4,43	0,80	5,23
53,7	0,607	-4,31	1,13	5,44
65,5	0,606	-4,22	1,45	5,67

Av: (5,25) ± 0,2

[a] n = 1 [b] Calculated using equation (1)

$A_o = 0,634$ $A_\infty = 0,605$

n = 1 (det) 3 → 53,7

slope = 1,27 (Sd = 0,07)

intercept = 6,58 (Sd = 0,34)

APPENDIX 3 : TABLES OF DATA FOR THE STUDY OF HEMIN IN AQUEOUS ACID (CHAPTER 4)

Table 1 : Variation in absorbance at the Soret maximum (397 m) at pH 1,1; 25°C; μ = 0,1

10^6(hemin), M	A_{397}	α [a]	$\log(Fe)_{TOT}\,\alpha$	$\log(Fe)_{TOT}(1-\alpha)$	log K [b]
0,71	0,085				
1,10	0,136				
1,19	0,141				
1,27	0,148				
2,07	0,252				
2,45	0,270	0,767	-5,73	-6,24	-4,92
2,50	0,269	0,705	-5,75	-6,13	-5,07
4,31	0,449	0,623	-5,57	-5,79	-5,05
6,52	0,659	0,549	-5,45	-5,53	-5,07
7,84	0,776	0,500	-5,41	-5,41	-5,11
9,83	0,960	0,468	-5,34	-5,28	-5,10
14,36	1,135				
18,03	1,343				
21,80	1,677				

Average: -5,05 ± 0,13

[a] $\varepsilon_{D/2} \approx 78 \times 10^3\ M^{-1}\ cm^{-1}$

$\varepsilon_M \approx 120 \times 10^3\ M^{-1}\ cm^{-1}$

(from assymtotes of Beers law plot)

[b] K refers to the reaction $D \rightleftharpoons 2M$

Table 2 : Variation in the absorbance of the Soret as a function of pH for hemin with and without caffeine; 25°C; μ=0,1

pH	Absorbance	
	-caffeine (397 nm) ($2,15 \times 10^{-6}$ M hemin)	+ caffeine (402 nm) ($3,09 \times 10^{-6}$ M hemin; 0,05M
1,0	0,514	0,915
1,5	0,514	0,915
2,0	0,514	0,909
2,2	0,510	0,905
2,4	0,480	-
2,5	-	0,865
2,6	0,467	-
2,8	0,443	0,832
3,0	0,427	0,805
3,2	0,404	-
3,4	-	0,770
3,8	0,381	0,725
4,0	0,380	0,713
4,5	0,380	0,698
5,0	0,380	0,698
5,2	-	0,673
5,4	-	0,650
5,6	0,382	0,616
5,8	-	0,593
6,0	0,335	0,564
6,2	0,313	-
6,4	0,300	0,540
6,6	0,288	-
6,8	0,264	-
7,0	0,245	0,530
7,8 (phosphate)	0,222	0,522
7,8 (carbonate)	0,216	0,511
9,0 (carbonate)	0,215	0,511
11,0 (carbonate)	0,218	0,510

APPENDIX 4 : TABLES OF DATA FOR THE TITRATION OF HEMIN WITH HISTIDINE, HISTAMINE AND PILOCARPATE

All titrations done at 25°C with μ = 0,5 ($NaNO_3$)

A. Titrations at low ligand concentrations

1. Histidine

a) pH 8,50; (hemin) = 68×10^{-6} M

$10^3(L)_T$, M	$\log(L)^b$ (M)	A_{590}	$\log \frac{A-A_o}{A_\infty - A}$	$\log K_1$ [a] (M^{-1})
0,80	-3,10	0,277	-0,98	2,12
1,59	-2,80	0,277	-0,98	1,82
2,38	-2,62	0,278	-0,78	1,84
3,95	-2,40	0,280	-0,51	1,89
7,05	-2,15	0,282	-0,30	1,85
10,11	-2,00	0,284	-0,12	1,88
13,11	-1,88	0,285	-0,04	1,84
18,99	-1,72	0,288	0,21	1,93
24,70	-1,61	0,291	0,51	2,12
35,60	-1,45	0,292	0,63	2,08

Av: 2,0 ± 0,2

A_o = 0,275 A_∞ = 0,296

Plot of $\log \frac{A - A_o}{A_\infty - A}$ vs log(his)

slope = 1,05 (Sd = 0,08)

intercept = 2,04 (Sd = 0,17)

b) pH 8,50; (hemin) = 136×10^{-6} M

$10^3(L)_T$, M	log(L) (M) [b]	A_{590}	$\log \frac{A-A_o}{A_\infty - A}$	$\log K_1$ [a] (M^{-1})
0,79	-3,10	0,547	-0,90	2,20
2,37	-2,63	0,550	-0,62	2,01
3,94	-2,40	0,551	-0,54	1,86
7,03	-2,15	0,557	-0,20	1,95
13,08	-1,88	0,563	0,10	1,98
18,94	-1,72	0,567	0,30	2,02
24,63	-1,61	0,571	0,54	2,15
30,15	-1,52	0,573	0,70	2,22

Av: 2,1 ± 0,2

A_o = 0,543 A_∞ = 0,579

Plot of $\log \frac{A - A_o}{A_\infty - A}$ vs log(his):

slope = 1,03 (Sd = 0,09)

intercept = 2,10 (Sd = 0,21)

c) pH 10,0 ; (hemin) = $1,36 \times 10^{-6}$ M

$10^{...}$ M	log(L) [b](M)	A_{590}	$\log \frac{A-A_o}{A_\infty - A}$	$\log K_1$ [a](M^{-1})
0,79	-3,10	0,580	-1,20	1,90
2,..	-2,63	0,582	-0,67	1,96
3,94	-2,40	0,583	-0,51	1,89
7,03	-2,15	0,585	-0,26	1,89
13,08	-1,88	0,587	-0,05	1,83
18,94	-1,72	0,589	0,15	1,87
24,63	-1,61	0,590	0,26	1,87

Av: 1,9 ± 0,1

A_o = 0,579 A_∞ = 0,596

Plot of $\log \frac{A - A_o}{A_\infty - A}$ vs log(his)

slope = 0,95 (Sd = 0,03)

intercept = 1,78 (Sd = 0,06)

d) pH 11,0 ; (hemin) = 136×10^{-6} M

$10^3(L)_T$, M	log (L) (M) [b]	A_{590}	$\log \frac{A-A_o}{A_\infty - A}$	$\log K_1$ (M^{-1}) [a]
0,79	-3,10	0,578	-1,34	1,76
2,37	-2,63	0,580	-0,82	1,81
3,94	-2,40	0,582	-0,56	1,84
7,03	-2,15	0,584	-0,36	1,79
13,08	-1,88	0,587	-0,11	1,77
18,94	-1,72	0,589	0,04	1,76
24,63	-1,61	0,591	0,19	1,80
30,15	-1,52	0,593	0,36	1,88
40,71	-1,39	0,595	0,56	1,95

Av: 1,8 ± 0,1

A_o = 0,577 A_∞ = 0,600

Plot of $\log \frac{A - A_o}{A_\infty - A}$ vs log(his)

slope = 1,06 (Sd = 0,04)

intercept = 1,93 (Sd = 0,08)

2. Histamine

a) pH 8,50 ; (hemin) = $90,5 \times 10^{-6}$M

$10^3(L)_T$, M	log(L) [b], (M)	A_{590}	$\log \frac{A-A_o}{A_\infty - A}$	log K,(M^{-1}) [a]
1,00	-3,00	0,402	-0,37	2,63
1,99	-2,70	0,410	0,00	2,70
2,98	-2,53	0,413	0,13	2,66
3,96	-2,40	0,415	0,22	2,62
5,91	-2,23	0,417	0,32	2,55
7,84	-2,11	0,419	0,45	2,56
11,65	-1,93	0,422	0,60	2,53
15,38	-1,81	0,424	0,75	2,56
22,63	-1,65	0,426	0,95	2,60

Av: 2,6 ± 0,1

A_o = 0,390 A_∞ = 0,430

Plot of $\log \frac{A - A_o}{A_\infty - A}$ vs log(L) :

slope = 0,91 (Sd = 0,04)

intercept = 2,40 (Sd = 0,08)

b) pH 10,0 ; (hemin) = $90,5 \times 10^{-6}$ M

10^3 $(L)_T$, M	$\log(L)^b$ (M)	A_{590}	$\log \frac{A-A_o}{A_\infty - A}$	$\log K_1^a$ (M^{-1})
1,00	-3,00	0,419	-0,36	2,65
1,99	-2,70	0,423	-0,03	2,67
3,96	-2,40	0,427	0,23	2,63
5,91	-2,23	0,431	0,54	2,77
7,84	-2,11	0,432	0,64	2,75
9,76	-2,01	0,433	0,76	2,77
11,65	-1,93	0,434	0,90	2,83

Av: 2,7 ± 0,1

A_o = 0,410 A_∞ = 0,437

Plot of $\frac{A-A_o}{A_\infty - A}$ vs log(L) :

slope = 1,16 (Sd = 0,05)

intercept = 3,11 (Sd = 0,11)

c) pH 11,0 ; (hemin) = $90,5 \times 10^{-6}$ M

10^3 $(L)_T$, M	log(L)[b] (M)	A_{590}	$\log \frac{A-A_o}{A_\infty - A}$	$\log K_1 (M^{-1})$ [a]
1,00	-3,00	0,416	-0,54	2,46
1,99	-2,70	0,419	-0,30	2,40
3,96	-2,40	0,423	-0,03	2,40
5,91	-2,23	0,425	0,10	2,33
7,84	-2,11	0,427	0,23	2,34
11,65	-1,93	0,429	0,33	2,26
15,38	-1,81	0,430	0,46	2,27
22,64	-1,65	0,432	0,64	2,29

Av: 2,4 ± 0,1

A_o = 0,410 A_∞ = 0,437

Plot of $\log \frac{A - A_o}{A_\infty - A}$ vs log(L) :

slope = 0,86 (Sd = 0,02)

intercept = 2,02 (Sd = 0,04)

3. Pilocarpate

a) pH 8,50 ; (hemin) = $90,5 \times 10^{-6}$M

$10^3(L)_T$, M	log(L) (M) [b]	A_{590}	$\log \frac{A-A_o}{A_\infty - A}$	$\log K_1 (M^{-1})$ [a]
0,50	-3,30	0,400	-1,10	2,20
1,00	-3,00	0,404	-0,76	2,24
1,98	-2,70	0,410	-0,46	2,24
2,96	-2,53	0,414	-0,30	2,23
3,92	-2,41	0,418	-0,16	2,25

Av: 2,23 ± 0,03

A_o = 0,396 A_∞ = 0,450

Plot of $\log \frac{A - A_o}{A_\infty - A}$ vs log(L) :

slope = 1,04 (Sd = 0,02)

intercept = 2,35 (Sd = 0,05)

b) pH 10,0 ; (hemin) = $90,5 \times 10^{-6}$ M

$10^3(L)_T$, M	log(L) (M)	[b] A_{590}	log $\frac{A-A_o}{A_\infty - A}$	log $K_1(M^{-1})$ [a]
0,50	-3,30	0,412	-1,46	1,84
1,00	-3,00	0,414	-1,15	1,85
1,98	-2,70	0,418	-0,81	1,89
2,60	-2,56	0,420	-0,70	1,86
3,92	-2,41	0,423	-0,56	1,85
5,83	-2,23	0,428	-0,37	1,86
7,69	-2,11	0,432	-0,24	1,87
9,52	-2,02	0,434	-0,18	1,84
13,08	-1,88	0,438	-0,06	1,82
16,51	-1,78	0,440	0	1,78
19,82	-1,70	0,442	0,04	1,74
23,01	-1,64	0,443	0,09	1,73

Av: 1,8 ± 0,1

A_o = 0,410 A_∞ = 0,470

Plot of log $\frac{A - A_o}{A_\infty - A}$ vs log(L) :

slope = 0,94 (Sd = 0,02)

intercept = 1,68 (Sd = 0,05)

c) pH 11,0 ; (hemin) = $90,5 \times 10^{-6}$ M

$10^3(L)_T$, M	log(L) (M) [b]	A_{590}	$\log \frac{A-A_o}{A_\infty - A}$	$\log K_1 (M^{-1})$ [a]
0,50	-3,30	0,428	-1,39	1,91
1,00	-3,00	0,430	-1,07	1,93
1,98	-2,70	0,432	-0,82	1,88
3,[illegible]	-2,41	0,436	-0,51	1,90
5	-2,23	0,439	-0,34	1,89
7,69	-2,11	0,441	-0,23	1,88
11,32	-1,95	0,446	0,00	1,95
14,81	-1,83	0,449	0,14	1,97
18,18	-1,75	0,451	0,23	1,98

Av: 1,9 ± 0,1

A_o = 0,427 A_∞ = 0,463

Plot of $\log \frac{A - A_o}{A_\infty - A}$ vs log(L) :

slope = 1,03 (Sd = 0,02)

intercept = 2,00 (Sd = 0,06)

[a] K_1 refers to the reaction $D + xL \rightleftharpoons D \cdots L_x$

[b] $\log(L)_{TOTAL} \approx \log(L)_{free}$ so the former is used.

B. Titrations at high ligand concentrations

i) Varying the ligand concentration

1. Histidine ; pH 9,0 (two duplicate experiments)

a) $(Fe)_{TOT} = 7,03 \times 10^{-6}$ M b) $(Fe)_{TOT} = 6,34 \times 10^{-6}$ M

$(L)_T$, M	A_{410}	$\log(L)_T$, M	$10^6(D)$, M	$10^6(ML_2)$, M	$\log \frac{(ML_2)^2}{(D)}$	$\log K_2$
a) 0,001	0,246	-3,00	3,292	0,446	-7,22	-1,22
0,02	0,302	-1,70	2,963	1,103	-6,39	-1,29
0,03	0,369	-1,52	2,570	1,890	-5,86	-1,30
0,04	0,452	-1,40	2,083	2,864	-5,40	-1,20
0,06	0,596	-1,22	1,238	4,554	-4,78	-1,12
0,08	0,669	-1,10	0,810	5,410	-4,14	-1,14
0,10	0,795	-1,00	0,458	6,115	-4,09	-1,09
0,15	0,776	-0,82	0,182	6,383	-3,61	-1,15

Av: -1,18 ± 0,12

$A_o = 0,208$ $A_\infty = 0,807$ (Plot of $\log \frac{(ML_2)^2}{(D)}$ vs $\log(L)$

n = 3,14 (Sd = 0,06)

I = -1,00 (Sd = 0,08)

	A_{413}					
b) 0,02	0,406	-1,70	2,667	1,006	-6,42	-1,32
0,04	0,409	-1,40	1,800	2,740	-5,38	-1,18
0,06	0,516	-1,22	1,152	4,037	-4,85	-1,19
0,08	0,608	-1,10	0,694	5,152	-4,35	-1,05
0,10	0,634	-1,00	0,436	5,467	-4,16	-1,16
0,20	0,692	-0,70	0,085	6,170	-3,35	-1,25

Av: -1,18 ± 0,14

$A_o = 0,183$ $A_\infty = 0,706$ (Plot of $\log \frac{(ML_2)^2}{(D)}$ vs $\log(L)$

$n = 3,09$ (Sd = 0,12)

$I = -1,08$ (Sd = 0,15)

Overall average of both experiments: $-1,2 \pm 0,1$

2. Histamine ; pH 9,0 $[(Fe)_{TOT} = 7,16 \times 10^{-6} M]$

$(L)_T$, M	$A_{408,5nm}$	$\log(L)_T$	$10^6(D)$, M	$10^6 ML_2$, M	$\log \frac{(ML_2)^2}{(D)}$	$\log K_2$
(0,01	0,257	-2,00	3,399	0,362	-7,41	-1,41)
0,02	0,277	-1,70	3,274	0,611	-6,94	-1,84
0,03	0,301	-1,52	3,125	0,911	-6,58	-2,02
0,04	0,330	-1,40	2,944	1,272	-6,26	-2,06
0,06	0,382	-1,22	2,620	1,921	-5,85	-2,19
0,08	0,448	-1,10	2,208	2,744	-5,47	-2,17
0,10	0,526	-1,00	1,721	3,717	-5,10	-2,10
0,15	0,584	-0,82	1,360	4,441	-4,84	-2,38
0,20	0,651	-0,70	0,942	5,276	-4,53	-2,43

Av: $-2,11 \pm 0,3$

$A_o = 0,228$ $A_\infty = 0,802$ (Plot of $\log \frac{(ML_2)^2}{(D)}$ vs $\log(L)$

$n = 2,32$ (Sd = 0,09)

$I = -2,93$ (Sd = 0,12)

3.) Pilocarpate ; pH 9,3 $[(Fe)_{TOT} = 7,25 \times 10^{-6} M]$

$10^3 \frac{(L)_T}{M}$,	A_{410}	$\log(L)_T$ (M)	$10^6 \frac{(D)}{M}$,	$10^6 \frac{(ML_2)}{M}$	$\log \frac{(ML_2)^2}{(D)}$	$\log K_2$
2,40	0,258	-2,62	3,358	0,534	-7,07	0,79
4,79	0,334	-2,32	2,896	1,457	-6,13	0,83
7,17	0,507	-2,14	1,846	3,558	-5,16	1,26
11,93	0,632	-1,92	1,087	5,076	-4,63	1,13
16,66	0,699	-1,78	0,680	5,890	-4,29	1,05
21,37	0,734	-1,67	0,480	6,291	-4,08	0,93
26,06	0,754	-1,58	0,346	6,558	-3,91	,83
30,72	0,770	-1,51	0,249	6,752	-3,74	0,79
35,36	0,785	-1,45	0,158	6,934	-3,52	0,83

Av: 0,97 ± 0,3

$A_o = 0,214$ $A_\infty = 0,811$ (Plot of $\log \frac{(ML_2)^2}{(D)}$ vs $\log(L)$

$n = 2,95$ (Sd = 0,16)

$I = 0,85$ (Sd = 0,31)

b) Pilocarpate ; pH 10,2 $[(Fe)_{TOT} = 7,46 \times 10^{-6} M]$

$10^3(L)_T$, M	A_{410}	$\log(L)_T$ (M)	$10^6(D)$ M	$10^6(ML_2)$, M	$\log \frac{(ML_2)^2}{(D)}$	$\log K_2$
7,97	0,272	-2,10	3,436	0,587	-6,99	-0,69
15,94	0,346	-1,80	2,984	1,492	-6,13	-0,73
23,72	0,432	-1,62	2,458	2,544	-5,58	-0,72
31,50	0,516	-1,50	1,944	3,571	-5,18	-0,68
39,22	0,577	-1,41	1,571	4,317	-4,93	-0,70
46,88	0,624	-1,33	1,284	4,892	-4,73	-0,74

Av: $-0,71 \pm 0,03$

$A_o = 0,224$ $A_\infty = 0,834$

Plot of $\log \frac{(ML_2)^2}{(D)}$ vs $\log(L)$

n = 2,98 (Sd = 0,04)

I = -0,75 (Sd = 0,07)

ii) Varying the hemin concentration (Shack and Clark dilution plots)

1. Histidine

used $\frac{\varepsilon_{D..L}}{2}$ = 26,4 ; ε_{1L_2} = 10,5 (both in mM^{-1} cm^{-1})

a) pH 8,5 ; $(histidine)_{TOTAL}$ = 0,05M

$10^6(Fe)_{TOTAL}$ M	A_{413}	α	$\log(Fe)_{TOT}\alpha$	$\log(Fe)_{TOT}(1-\alpha)$	$\log K_2$
2,97	0,290	0,824	-5,61	-6,28	-0,74
5,94	0,525	0,717	-5,37	-5,77	-0,77
8,91	0,729	0,641	-5,24	-5,49	-0,79
11,87	0,914	0,585	-5,16	-5,31	-0,81
14,84	1,080	0,537	-5,10	-5,16	-0,84
17,79	1,226	0,492	-5,06	-5,04	-0,88
20,74	1,366	0,456	-5,02	-4,95	-0,89
23,70	1,507	0,430	-4,99	-4,87	-0,91

Av: -0,82 ± 0,09

Plot of $\log (Fe)_{TOT}\alpha$ vs $\log (Fe)_{TOT}(1-\alpha)$

n = 0,44 (Sd = 0,01)

I = -2,84 (Sd = 0,05)

b) pH 9,0 ; $(histidine)_{TOTAL}$ = 0,05M

$10^6(Fe)_{TOTAL}$ M	A_{413}	α	$\log(Fe)_{TOTAL}\alpha$	$\log(Fe)_{TOTAL}(1-\alpha)$	$\log K_2$
2,56	0,237	0,765	-5,71	-6,22	-1,00
5,12	0,421	0,645	-5,48	-5,74	-1,02
7,67	0,575	0,561	-5,37	-5,47	-1,07
10,22	0,725	0,515	-5,28	-5,30	-1,06
12,76	0,860	0,474	-5,22	-5,17	-1,07
15,30	0,982	0,437	-5,18	-5,06	-1,10
20,37	1,206	0,379	-5,11	-4,90	-1,12

Av: -1,06 ± 0,06

Plot of $\log (Fe)_{TOT}\alpha$ vs $\log(Fe)_{TOT}(1-\alpha)$

n = 0,46 (Sd = 0,01)

I = -2,87 (Sd = 0,03)

c) pH 10,0 ; $(histidine)_{TOTAL}$ = 0.1 M

$10^6(Fe)_{TOTAL}$, M	A_{413}	α	$\log(Fe)_{TOT}\ \alpha$	$\log(Fe)_{TOT}(1-\alpha)$	$\log K_2$
1,60	0,169	0,916	-5,83	-6,87	-1,49
3,21	0,321	0,851	-5,56	-6,32	-1,50
4,81	0,467	0,817	-5,41	-6,06	-1,46
6,40	0,612	0,800	-5,29	-5,89	-1,39
8,00	0,746	0,773	-5,21	-5,74	-1,38
9,59	0,873	0,747	-5,14	-5,62	-1,36
11,19	0,991	0,719	-5,09	-5,50	-1,38
12,78	1,108	0,697	-5,05	-5,41	-1,39
14,38	1,222	0,677	-5,01	-5,33	-1,39
15,97	1,333	0,660	-4,98	-5,26	-1,40

Av: -1,41 ± 0,05

Plot $\log(Fe)_{TOT}\ \alpha$ vs $\log(Fe)_{TOT}(1-\alpha)$

n = 0,54 (Sd = 0,01)

I = -2,12 (Sd = 0,06)

d) pH 10,0 ; $(\text{Histidine})_{TOTAL}$ = 0,1M

$10^6(Fe)_{TOTAL}$,M	A_{413}		$\log(Fe)_{TOT}^{\alpha}$	$\log_R(Fe)_{TOT}(1-\alpha)$	$\log K_2$
(1,60	0,175	0,959	-5,81	-7,19	-1,13)
3,21	0,328	0,876	-5,55	-6,40	-1,40
4,81	0,468	0,820	-5,40	-6,06	-1,44
6,40	0,605	0,788	-5,30	-5,87	-1,43
8,00	0,729	0,748	-5,22	-5,70	-1,44
9,59	0,846	0,715	-5,16	-5,56	-1,46
11,19	0,963	0,692	-5,11	-5,46	-1,46
12,78	1,076	0,668	-5,07	-5,37	-1,47
14,38	1,185	0,647	-5,03	-5,30	-1,46
15,97	1,291	0,629	-5,00	-5,23	-1,47

Av: -1,45 ± 0,05

Plot of $\log (Fe)_T^{\alpha}$ vs $\log(Fe)_T(1-\alpha)$

n = 0,47 (Sd = 0,004)

I = -2,53 (Sd = 0,02)

Av $\log K_2$ for pH 10,0 = 1,43 ± 0,07

e) pH 11,0 ; $(histidine)_{TOTAL}$ = 0,05M

$10^6(Fe)_{TOTAL}$,M	A_{413}	α	$\log(Fe)_{TOT}\,\alpha$	$\log(Fe)_{TOT}(1-\alpha)$	$\log K_2$
2,52	0,103	0,167	-6,38	-5,68	-2,88
3,78	0,149	0,150	-6,24	-5,49	-2,79
5,03	0,203	0,161	-6,09	-5,37	-2,61
7,53	0,284	0,131	-6,01	-5,18	-2,64
10,04	0,361	0,110	-5,95	-5,05	-2,65
12,53	0,431	0,09[illegible]	-5,94	-4,94	-2,74
17,52	0,578	0,076	-5,87	-4,79	-2,74
22,49	0,718	0,064	-5,84	-4,68	-2,80
27,44	0,861	0,058	-5,80	-4,59	-2,81
32,38	1,001	0,052	-5,77	-4,51	-2,83
37,31	1,143	0,049	-5,74	-4,45	-2,83

Av: -2,75 ± 0,14

Plot of $\log (Fe)_T\alpha$ vs $\log (Fe)_T(1-\alpha)$

n = 0,47 (Sd = 0,03)

I = -3,61 (Sd = 0,17)

f) pH 11,5 ; (histidine)$_{TOTAL}$ = 0,2M

10^6(Fe)$_{TOTAL}$,M	A_{413}	α	log(Fe)$_{TOT}^{\alpha}$	log(Fe)$_{TOT}^{(1-\alpha)}$	log K_2
2,66	0,179	0,473	-5,90	-5,85	-3,55
5,32	0,307	0,362	-5,72	-5,47	-3,57
7,97	0,421	0,305	-5,61	-5,26	-3,56
10,62	0,522	0,263	-5,55	-5,11	-3,59
13,26	0,622	0,237	-5,50	-4,99	-3,61
15,90	0,722	0,220	-5,47	-4,91	-3,63
18,54	0,817	0,204	-5,42	-4,83	-3,61
21,17	0,911	0,192	-5,39	-4,77	-3,61
23,80	1,015	0,188	-5,35	-4,71	-3,59
26,42	1,108	0,180	-5,32	-4,66	-3,58

Av: -3,59 ± 0,04

Plot of log $(Fe)_T^{\alpha}$ vs log $(Fe)_T^{(1-\alpha)}$

n = 0,48 (Sd = 0,01)

I = -3,11 (Sd = 0,04)

g) pH 12,0 - $(histidine)_{TOTAL}$ = 0,2M

$10^6(Fe)_{TOTAL}$,M	A_{413}	α	$\log(Fe)_{TOT}\alpha$	$\log(Fe)_{TOT}(1-\alpha)$	$\log \beta_2$
(1,24	0,060	0,254	-6,50	-6,03	-4,57)
2,47	0,119	0,252	-6,21	-5,7[illegible]	-4,29
4,94	0,210	0,186	-6,04	-5,40	-4,28
7,40	0,295	0,156	-5,94	-5,20	-4,28
9,86	0,382	0,143	-5,85	-5,07	-4,23
12,31	0,465	0,131	-5,79	-4,97	-4,21
14,76	0,547	0,123	-5,74	-4,89	-4,19
17,21	0,627	0,116	-5,70	-4,82	-4,18
19,65	0,710	0,113	-5,66	-4,76	-4,16
22,09	0,789	0,108	-5,62	-4,71	-4,13
24,52	0,868	0,104	-5,59	-4,66	-4,12

Av: -4,20 ± 0,09

Plot of $\log(Fe)_T\alpha$ vs $\log(Fe)_T(1-\alpha)$

n = 0,58 (Sd = 0,01)

I = -2,88 (Sd = 0,06)

2. Histamine

used $\varepsilon_{\frac{D,L}{2}} = 31,9\ mM^{-1}\ cm^{-1}$; $\varepsilon_{ML_2} = 112\ mM^{-1}\ cm^{-1}$

a) pH 8,5 ; $(histamine)_{TOTAL} = 0,05M$

$10^6(Fe)_{TOTAL}$	$A_{408,5}$	α	$\log(Fe)_{TOT}\alpha$	$\log(Fe)_{TOT}(1-\alpha)$	$\log K_2$
1,58	0,135	0,670	-5,98	-6,28	-1,48
3,16	0,211	0,437	-5,86	-5,75	-1,77
4,74	0,277	0,334	-5,80	-5,50	-1,90
6,31	0,337	0,271	-5,77	-5,34	-2,00
7,89	0,403	0,242	-5,72	-5,22	-2,02
9,46	0,461	0,213	-5,70	-5,13	-2,07
1,58	0,139	0,701	-5,96	-6,32	-1,40

Av: $-1,73 \pm 0,34$

Plot of $\log(Fe)_T\alpha$ vs $\log(Fe)_T(1-\alpha)$

$n = 0,23$ (Sd = 0,01)

$I = -4,55$ (Sd = 0,07)

b) pH 9,0 ; $(histamine)_{TOT,L}$ = 0,05M

$10^6(Fe)_{TOTAL}$,M	$A_{408,5}$	α	$\log(Fe)_{TOT}^{\alpha}$	$\log(Fe)_{TOT}^{(1-\alpha)}$	$\log K_2$
2,03	0,139	0,457	-6,03	-5,96	-1,90
4,06	0,224	0,291	-5,93	-5,54	-2,12
6,08	0,310	0,238	-5,84	-5,33	-2,15
8,10	0,377	0,183	-5,83	-5,18	-2,28
10,12	0,454	0,162	-5,79	-5,07	-2,31
12,14	0,533	0,150	-5,74	-4,99	-2,29

Av: -2,15 ± 0,25

Plot of $\log (Fe)_T^{\alpha}$ vs $\log(Fe)_T^{(1-\alpha)}$

n = 0,29 (Sd = 0,02)

I = -4,33 (Sd = 0,12)

c) pH 10,0 ; $(histamine)_{TOTAL}$ = 0,1M

$10^6(Fe)_{TOT}$, M	$A_{408,5}$	α	$\log(Fe)_{TOT}\alpha$	$\log(Fe)_{TOT}(1-\alpha)$	$\log K_2$
2,08	0,218	0,910	-5,77	-6,73	-1,41
4,15	0,405	0,820	-5,47	-6,13	-1,51
5,19	0,461	0,711	-5,43	-5,82	-1,74
6,23	0,540	0,684	-5,37	-5,71	-1,73
6,23	0,526	0,656	-5,39	-5,67	-1,81
8,29	0,651	0,582	-5,32	-5,46	-1,88
9,39	0,701	0,534	-5,30	-5,36	-1,94
12,42	0,842	0,448	-5,25	-5,16	-2,04

Av: -1,71 ± 0,33

Plot of $\log (Fe)_T\alpha$ vs $\log (Fe)_T(1-\alpha)$

n = 0,29 (Sd = 0,01)

I = -3,73 (Sd = 0,11)

d) pH 10,0 ; $(histamine)_{TOTAL}$ = 0,1M

$10^6(Fe)_{TOT}$, M	$A_{408,5}$	α	$\log(Fe)_{TOT}\alpha$	$\log(Fe)_{TOT}(1-\alpha)$	log K_2
(1,57	0,173	0,977	-5,81	-7,45	-0,87)
3,14	0,319	0,870	-5,56	-5,40	-1,42
4,71	0,443	0,776	-5,44	-5,98	-1,60
6,26	0,547	0,693	-5,36	-5,72	-1,70
7,83	0,622	0,593	-5,33	-5,50	-1,86
9,39	0,711	0,547	-5,29	-5,37	-1,91

Av: -1,66 ± 0,25

Plot of $\log (Fe)_T\alpha$ vs $\log (Fe)_T(1-\alpha)$

n = 0,25 (S.D. = 0,01)

I = -3,93 (S.D. = 0,04)

Av log K_2 for pH 10,0 = -1,69 ± 0,15

a) pH 11,0 ; $(histamine)_{TOTAL}$ = 0,1M ; μ = 0,50

$10^6(Fe)_{TOTAL}$ M	$A_{408,5}$	α	$\log(Fe)_{TOT}\alpha$	$\log(Fe)_{TOT}(1-\alpha)$	$\log K_2$
1,58	0,146	0,756	-5,92	-6,41	-2,13
3,16	0,274	0,685	-5,66	-6,00	-2,02
4,74	0,380	0,604	-5,54	-5,73	-2,05
6,31	0,474	0,541	-5,47	-5,54	-2,10
7,89	0,561	0,491	-5,41	-5,40	-2,12
9,46	0,627	0,431	-5,39	-5,27	-2,21

Av: -2,10 ± 0,11

Plot of $\log (Fe)_T\alpha$ vs $\log (Fe)_T(1-\alpha)$

n = 0,47 (Sd = 0,04)

I = -2,89 (Sd = 0,21)

3. Pilocarpate

used $\varepsilon_{\frac{D..L}{2}}$ = 29,5 mM^{-1} cm^{-1} ; ε_{ML_2} = 111,8 mM^{-1} cm^{-1}

a) pH 8,5 ; (pilocarpate) = 0,005M

$10^6(Fe)_{TOT}$, M	A_{410}	α	$\log(Fe)_{TOT}\alpha$	$\log(Fe)_{TOT}(1-\alpha)$	$\log K_2$
1,5	0,147	0,794	-5,91	-6,50	1,88)
3,09	0,245	0,603	-5,73	-5,91	1,65
4,64	0,330	0,506	-5,63	-5,64	1,58
6,17	0,409	0,447	-5,56	-5,47	1,53
7,72	0,482	0,400	-5,51	-5,33	1,51
9,27	0,557	0,369	-5,47	-5,23	1,49
10,74	0,626	0,344	-5,43	-5,15	1,49
12	0,685	0,322	-5,40	-5,08	1,48
13,54	0,754	0,302	-5,38	-5,01	1,45
15,00	0,816	0,287	-5,35	-4,95	1,45
16,47	0,937	0,258	-5,32	-4,86	1,42
21,53	1,055	0,237	-5,29	-4,78	1,40

Av: 1,50 ± 0,10

Plot of $\log (Fe)_T\alpha$ vs $\log (Fe)_T(1-\alpha)$

n = 0,37 (Sd = 0,01)

I = -3,53 (Sd = 0,04)

b) pH 8,5 ; (pilocarpate) = 0,005M

$10^6(Fe)_{TOT}$, M	A_{410}	α	$\log(Fe)_{TOT}\alpha$	$\log(Fe)_{TOT}(1-\alpha)$	$\log K_2$
1,57	0,135	0,684	-5,97	-6,31	1,57
3,14	0,236	0,552	-5,76	-5,85	1,53
4,72	0,326	0,478	-5,65	-5,61	1,51
6,29	0,412	0,434	-5,56	-5,45	1,53
7,84	0,483	0,402	-5,50	-5,33	1,53
9,41	0,562	0,363	-5,47	-5,22	1,48
12,54	0,701	0,317	-5,40	-5,07	1,47
15,66	0,827	0,279	-5,36	-4,95	1,43
18,78	0,948	0,250	-5,33	-4,85	1,39
21,89	1,067	0,229	-5,30	-4,77	1,37
24,99	1,175	0,208	-5,28	-4,70	1,34

Av: 1,47 ± 0,13

Plot of $\log (Fe)_T\alpha$ vs $\log (Fe)_T(1-\alpha)$

n = 0,43 (Sd = 0,01)

I = -3,23 (Sd = 0,06)

c) pH 8,5 ; (pilocarpate) = 0,005M

$10^6(Fe)_{TOT}$, M	A_{410}	α	$\log(Fe)_{TOT}\alpha$	$\log(Fe)_{TOT}(1-\alpha)$	$\log K_2$
1,02	0,088	0,688	-6,15	-6,50	1,40
2,03	0,160	0,597	-5,92	-6,[illegible]	1,45
3,05	0,219	0,499	-5,82	-5,82	1,38
4,06	0,272	0,452	-5,74	-5,65	1,37
(6,08	0,321	0,279	-5,77	-5,36	1,02)
8,10	0,464	0,334	-5,57	-5,26	1,32
10,12	0,553	0,301	-5,52	-5,15	1,31
12,14	0,633	0,271	-5,48	-5,05	1,29
15,15	0,754	0,242	-5,44	-4,94	1,26
18,16	0,866	0,216	-5,41	-4,85	1,23
21,16	0,978	0,198	-5,38	-4,77	1,21
24,16	1,080	0,180	-5,36	-4,70	1,18
27,14	1,186	0,167	-5,34	-4,65	1,17

Av: 1,31 ± 0,14

Plot of log $(Fe)_T\alpha$ vs log $(Fe)_T(1-\alpha)$

n = 0,43 (Sd = 0,01)

I = -3,32 (Sd = 0,05)

Av log K_2 for pH 8,5 = 1,43 ± 0,12

d) pH 9,0 ; (pilocarpate) = 0,005M

$10^6(Fe)_{TOT}$, M	A_{410}	α	$\log(Fe)_{TOT}\alpha$	$\log(Fe)_{TOT}(1-\alpha)$	$\log K_2$
1,55	0,103	0,449	-6,16	-6,07	0,95
3,09	0,179	0,345	-5,97	-5,69	0,95
4,64	0,247	0,288	-5,87	-5,48	0,94
6,17	0,318	0,268	-5,78	-5,35	0,99
7,72	0,382	0,243	-5,73	-5,23	0,97
9,25	0,444	0,225	-5,68	-5,14	0,98
10,79	0,504	0,209	-5,65	-5,07	0,97
12,53	0,568	0,201	-5,61	-5,01	0,99
13,87	0,617	0,182	-5,60	-4,95	0,95
15,40	0,675	0,174	-5,57	-4,90	0,96
18,47	0,793	0,163	-5,57	-4,81	0,97
21,53	0,911	0,156	-5,47	-4,74	1,00

Av: 0,97 ± 0,03

Plot of $\log (Fe)_T\alpha$ vs $\log (Fe)_T(1-\alpha)$

n = 0,51 (Sd = 0,01)

I = -3,05 (Sd = 0,03)

e) pH 10,0 ; (pilocarpate) = 0,025M

$10^6(Fe)_{TOT}$, M	A_{410}	α	$\log(Fe)_{TOT}\alpha$	$\log(Fe)_{TOT}(1-\alpha)$	$\log K_2$
1,55	0,136	0,708	-5,96	-6,34	-0,47
3,09	0,243	0,597	-5,73	-5,90	-0,45
4,64	0,342	0,537	-5,60	-5,67	-0,42
6,17	0,434	0,496	-5,51	-5,51	-0,40
7,72	0,520	0,460	-5,45	-5,38	-0,41
9,25	0,601	0,431	-5,40	-5,23	-0,41
10,79	0,677	0,404	-5,36	-5,19	-0,42
12,33	0,752	0,383	-5,33	-5,12	-0,43
13,87	0,826	0,365	-5,30	-5,06	-0,43
15,40	0,893	0,346	-5,27	-5,00	-0,43
18,47	1,032	0,320	-5,23	-4,90	-0,43
21,53	1,163	0,298	-5,19	-4,82	-0,45

Av: -0,43 ± 0,04

Plot of $\log (Fe)_T\alpha$ vs $\log (Fe)_T(1-\alpha)$

$n = 0,51 \quad (Sd = 0,01)$

$I = -2,74 \quad (Sd = 0,04)$

f) pH 11,0 (pilocarpate) = 0,05M

$10^6(Fe)_{TOT}$, M	A_{410}	α	$\log(Fe)_{TOT}\alpha$	$\log(Fe)_{TOT}(1-\alpha)$	$\log K_2$
1,55	0,130	0,661	-5,99	-6,28	-1,50
3,09	0,242	0,593	-5,74	-5,90	-1,38
4,64	0,337	0,524	-5,61	-5,66	-1,36
6,17	0,425	0,479	-5,53	-5,49	-1,37
7,72	0,502	0,432	-5,48	-5,36	-1,40
9,25	0,581	0,405	-5,43	-5,26	-1,40
10,79	0,654	0,378	-5,39	-5,17	-1,41
12,33	0,727	0,358	-5,36	-5,10	-1,42
13,87	0,798	0,341	-5,33	-5,04	-1,42
15,40	0,864	0,323	-5,30	-4,98	-1,42
18,47	0,997	0,297	-5,26	-4,89	-1,43
21,53	1,117	0,272	-5,23	-4,80	-1,46

Av: -1,41 ± 0,09

Plot of $\log (Fe)_I\alpha$ vs $\log (Fe)_I(1-\alpha)$

n = 0,50 (Sd = 0,01)

I = -2,80 (Sd = 0,07)

g) pH 11,0 ; (pilocarpate) = 0,05M

$10^6(Fe)_{TOT}$, M	A_{410}	α	$\log(Fe)_{TOT}\alpha$	$\log(Fe)_{TOT}(1-\alpha)$	$\log K_2$
2,72	0,207	0,566	-5,81	-5,93	-1,49
5,44	0,350	0,446	-5,62	-5,52	-1,52
8,16	0,495	0,379	-5,51	-5,29	-1,53
10,89	0,624	0,338	-5,43	-5,14	-1,52
13,56	0,744	0,308	-5,38	-5,03	-1,53
16,27	0,866	0,288	-5,33	-4,94	-1,52
18,98	0,985	0,272	-5,29	-4,86	-1,52
21,68	1,099	0,257	-5,25	-4,79	-1,51
24,38	1,214	0,247	-5,22	-4,78	-1,50
27,08	1,324	0,236	-5,20	-4,68	-1,52

Av: -1,52 ± 0,03

Plot of $\log (Fe)_T\alpha$ vs $\log (Fe)_T(1-\alpha)$

n = 0,50 (Sd = 0,01)

I = -2,88 (Sd = 0,03)

h) pH 11,0 ; (pilocarpate) = 0,05M

$10^6(Fe)_{TOTAL}$, M	A_{510}	α	$\log(Fe)_{TOT}\alpha$	$\log(Fe)_{TOT}(1-\alpha)$	$\log K_2$
2,72	0,234	0,687	-5,73	-6,07	-1,19
5,44	0,408	0,553	-5,52	-5,61	-1,23
8,16	0,569	0,489	-5,40	-5,38	-1,22
10,89	0,697	0,419	-5,34	-5,20	-1,28
13,56	0,828	0,383	-5,28	-5,08	-1,28
16,27	0,957	0,356	-5,24	-4,98	-1,30
18,98	1,079	0,332	-5,20	-4,90	-1,30
21,68	1,198	0,313	-5,17	-4,83	-1,31
24,38	1,311	0,295	-5,14	-4,76	-1,32
27,08	1,421	0,279	-5,12	-4,71	-1,33

Av: -1,27 ± 0,08

Plot of $\log (Fe)_T\alpha$ vs $\log (Fe)_T(1-\alpha)$

$$n = 0,45 \quad (Sd = 0,01)$$
$$I = -3,01 \quad (Sd = 0,03)$$

Overall Av $\log K_2$ for pH 11,0 = -1,4 ± 0,1

APPENDIX 5 : CORRECTION OF THE BINDING CONSTANTS OF HISTIDINE, HISTAMINE AND PILOCARPATE FOR THE PKAS OF THE FREE AND COORDINATED LIGANDS

(Chapter 5)

It is known that coordination of histamine to B_{12a} reduced the pKa of NH_2 from 9,7 to 4,7 on coordination.[119] In this analysis, it will be assumed that the pKa of $-NH_2$ in histamine and histidine is reduced to less than 8 on coordination, while the pKa of -OH in pilocarpate is reduced to about 10 (from ~15).[98]

In all cases, the overall binding constant will be used ($K_1 K_2$), which refers to equation (1).

$$(FeOH)_2 + 4L \rightleftharpoons 2FeL_2 + 2OH^- \qquad (1)$$

The corrected binding constants are given in table 5.5.

a) Histidine, histamine

$$(OH)_2 Fe + 4L \rightleftharpoons 2FeL_2 + 2OH^- \qquad K_{obs} = K_1 K_2$$

$$K_{obs} = \frac{(FeL_2)^2 (OH^-)^2}{((OHFe)_2)\ (L)^4}$$

now

$$Fe(RNH_3^+)_2 \rightleftharpoons Fe(RNH_2)_2 + 2H^+ \qquad K_a(Fe\text{-}L_2)$$

where $Fe(RNH_3^+)$ and $Fe(RNH_2)_2$ refers to the coordinated ligands with the amine protonated and unprotonated respectively

$$\therefore \quad Ka(Fe\text{-}L) = \frac{(Fe(RNH_2)_2)\ (H^+)^2}{(Fe(RNH_3^+)_2)}$$

and

$$(FeL_2) = (Fe(RNH_2)) + (Fe(RNH_3^+)_2)$$

$$= Fe(RNH_2)_2 \quad (1 + \frac{(H^+)^2}{Ka(Fe\text{-}L_2}$$

$\approx (Fe(RNH_2)_2)$ if $(H^+)^2 \ll Ka(Fe\text{-}L_2)$

also

$$RNH_3^+ \rightleftharpoons RNH_2 + H^+ \qquad Ka_L$$

where RNH_3^+ and RNH_2 refer to the free ligands with the amine protonated and unprotonated respectively.

$$Ka_L = \frac{(RNH_2)(H^+)}{(RNH_3^+)}$$

and

$$(L) = (RNH_2) + (RNH_3^+)$$

$$= (RNH_2)\left(1 + \frac{(H^+)}{Ka_L}\right)$$

$$\therefore K_{obs} = \frac{(Fe(RNH_2)_2)^2 (OH^-)^2}{(FeOH)_2)^2 (RNH_2)^4 (1 + \frac{(H^+)}{Ka_L})^4}$$

If K_3 refers to the reaction

$$(FeOH)_2 + 4RNH_2 \rightleftharpoons 2Fe(RNH_2)_2 + 2OH^-$$

then $$K_{obs} = K_3 \frac{1}{1 + (H^+)/Ka_L}$$

$$\therefore K_3 = K_{obs}\left(1 + \frac{(H^+)}{Ka_L}\right)^4$$

$$\therefore \log K_3 = \log K_{obs} + 4 \log \left(1 + \frac{(H^+)}{Ka_L}\right)$$

b) Pilocarpate

The pKa of -OH of uncoordinated pilocarpate would be about 15 * and will thus be ignored.

* which is the approximate pKa expected for an alcohol,[98]

$(FeOH)_2 + 4L \rightleftharpoons 2FeL_2 + 2OH^- \quad K_1K_2 = K_{obs}$

$$\therefore K_{obs} = \frac{(FeL_2)^2(OH^-)^2}{((FeOH)_2)(L)^4}$$

now $Fe(ROH)_2 \rightleftharpoons Fe(ROH)(RO^-) + H^+ \quad Ka(Fe\text{-}L)$

where ROH refers to pilocarpate with an undissociated hydroxyl group.

$$\therefore Ka(FeL) = \frac{(Fe(ROH)(RO^-))(H^+)}{(Fe(ROH)_2)}$$

and $(FeL_2) = (Fe(ROH)_2) + (Fe(ROH)(RO^-))$

$$= (Fe(ROH)_2)\left(1 + \frac{Ka(Fe\text{-}L)}{(H^+)}\right)$$

$$\therefore K_{obs} = \frac{(Fe(ROH)_2)^2\left(1 + \frac{KaFeL}{(H^+)}\right)^2(OH^-)^2}{((OHFe)_2)(L)^4}$$

If K_3 refers to the equilibrium

$(OHFe)_2 + 4L \rightleftharpoons 2Fe(ROH)_2 + 2OH^-$

then $K_{obs} = K_3\left(1 + \frac{KaFe\text{-}L}{(H^+)}\right)^2$

$$\therefore \log K_3 = \log K_{obs} - 2 \log \left(1 + \frac{KaFe\text{-}L}{(H^+)}\right)$$

APPENDIX 6 : TABLES OF DATA FOR THE KINETIC STUDY OF THE REDUCTION OF BIS-HISTIDINE HEMIN BY DITHIOTHREITOL (Chapter 7)

Table 1 : Variation of k_{obs} with dithiothreitol concentration; pH 10,0 ; 0,4M histidine; $30x10^{-6}$M hemin; μ = 0,5

(dtt), M	$10^2\ k_{obs}$, s^{-1}	(dtt), M	$10^2\ k_{obs}$, s^{-1}
$2x10^{-4}$	2,19; 2,12	$6,4x10^{-3}$	6,30
$3x10^{-4}$	3,40; 3,41	$1,0x10^{-2}$	5,86
$3,5x10^{-4}$	3,76	$2,0x10^{-2}$	5,15
$4,0x10^{-4}$	3,86	$3,0x10^{-2}$	3,77
$8,0x10^{-4}$	5,40	$5,0x10^{-2}$	3,21
$1,6x10^{-3}$	6,72	$7,5x10^{-2}$	3,03
$2,4x10^{-3}$	6,75	$1,0x10^{-1}$	3,01
$3,2x10^{-3}$	6,72	$1,0x10^{-1}$	2,91

Table 2 : Variation of k_{obs} with histidine concentration; at pH 10,0 ; $30x10^{-6}$M hemin, μ = 0,5

(histidine), M	$10^2\ k_{obs}$, s^{-1}	
	low (dithiothreitol) ($3x10^{-4}$M)	high (dithiothreitol) (0,1 M)
0,205	7,70	2,60
0,250	6,77	3,05
0,300	5,36	2,85 ; 3,05
0,350	5,32	3,15 ; 2,96
0,380	4,60	3,07 ; 2,85
0,400	4,16	3,01 ; 2,91

Table 3 : Variation of k_{obs} with pH; $3x10^{-5}$M hemin ; 0,4M histidine ; $4x10^{-4}$M dtt ; μ = 0,5 ; 25°C

pH	$10^2 k_{obs}$, s^{-1}	f Fe(III)(histidine)$_2$ [a]	$10^2 k_{corr}$, s^{-1} [b]
8,0	6,14	0,999	6,15
8,5	6,96;7,23	0,994	7,00;7,27
9,0	6,78	0,992	6,83
9,5	6,19	0,983	6,30
10,0	4,73	0,975	4,85
11,0	2,10	0,721	2,91

[a] f Fe(III)(histidine)$_2$ is the fraction the bis-histidine hemin present (calculated from data in chapter 5)

[b] $k_{corr} = k_{obs}$/f Fe(III)(histidine)$_2$

APPENDIX 7 : DERIVATION OF THE RATE EQUATION FOR THE REDUCTION OF BIS-HISTIDINE HEMIN BY DITHIOTHREITOL (DISCUSSED IN CHAPTER 7)

The kinetic results for the above reaction were fitted to a rate law derived by Fleck's method.[112] The derivation is given below.

$a + b \underset{k_{-1}}{\overset{k_1}{\rightleftharpoons}} c + d$ (where a = dtt; b = $Fe^{III}L_2$; c = $Fe^{III}(L)(RS)$

$c \xrightarrow{k_2} p + f$ d = L ; p = $Fe^{II}L_2$; f = dtt

$c + a \underset{k_{-3}}{\overset{k_3}{\rightleftharpoons}} g$ g = $Fe^{III}(L)(HS)\cdots\cdot(RS)$

$g \xrightarrow{k_4} p + f$

Assuming that both (a) and (d) are large compared to (b) such that

(a) = $(a)_o$ and (d) = $(d)_o$ ($(\ )_o$ = initial concentrations)

i.e. pseudo first order conditions. Then

$$\frac{d}{dt}(b) = k_{-1}(d)(d)_o - k_1(a)_o\, b$$

$$\frac{d}{dt}(c) = k_1(a)_o(b) + k_{-3}(g) - c\,(k_2 + k_{-1}(d)_o + k_3(a)_o)$$

$$\frac{d}{dt}(g) = k_3(c)(a)_o - (g)(k_{-3} + k_4)$$

$$\frac{d}{dt}(p) = k_2(c) + k_4(g)$$

assuming that $(b) = be^{-mt} \Longrightarrow \frac{d}{dt}(b) = -mbe^{-mt}$

$(c) = ce^{-mt} \Longrightarrow \frac{d}{dt}(c) = -mce^{-mt}$

$(g) = ge^{-mt} \Longrightarrow \frac{d}{dt}(g) = -mge^{-mt}$

$(p) = pe^{-mt} \Longrightarrow \frac{d}{dt}(p) = -mpe^{-mt}$

Then

$-mbe^{-mt} = k_{-1}(d)_o\, ce^{-mt} - k_1(a)_o\, be^{-mt}$

$\Longrightarrow o = k_{-1}(d)_o c + (m - k_1(\cdot)_o)b$ (1)

$-mce^{-mt} = k_1(a)_o\, be^{-mt} + k_{-3}\, ge^{-mt} - ce^{-mt}(k_2 + k_{-1}(d)_o + k_3(a)_o)$

$$\Longrightarrow 0 = \left[m - (k_2+k_{-1}(d)_o+k_3(a)_o\right] c + k_1(a)_o b + k_{-3} \quad g \qquad (2)$$

$$-mge^{-mt} \approx k_3(a)_o ce^{-mt} - (k_{-3} \quad +k_4)\ ge^{-mt}$$

$$\Longrightarrow 0 = \left[m-(k_{-3} \quad +k_4)\right]g + k_3(a)_o c \qquad (3)$$

$$-mpe^{-mt} \approx k_2 ce^{-mt} + k_4\ ge^{-mt}$$

$$\Longrightarrow 0 = mp + k_2 c + k_4 g \qquad (4)$$

$$\begin{vmatrix} m-k_1(a)_o & k_{-1}(d)_o & 0 & 0 \\ k_1(a)_o & m-(k_2+k_{-1}(d)_o+k_3(a)_o & k_{-3} & 0 \\ 0 & k_3(a)_o & m-(k_{-3} \quad +k_4) & 0 \\ 0 & k_2 & k_4 & m \end{vmatrix} = 0$$

$$\left(m-k_1(a)_o\right)\begin{vmatrix} m-(k_2+k_{-1}(d)_o+k_3(a)_o & k_{-3} & 0 \\ k_3(a)_o & m-(k_{-3} \quad +k_4) & 0 \\ k_2 & k_4 & m \end{vmatrix}$$

$$-\ k_{-1}(d)_o \begin{vmatrix} k_1(a)_o & k_{-3} & 0 \\ 0 & m-(k_{-3} \quad +k_4) & 0 \\ 0 & k_4 & m \end{vmatrix} = 0$$

$$\therefore (m-k_1(a)_o)\left[m-(k_2+k_{-1}(d)_o+k_3(a)_o\right] \begin{vmatrix} m-(k_{-3} \quad +k_4) & 0 \\ k_4 & m \end{vmatrix}$$

$$-(m-k_1(a)_o)(k_{-3}) \begin{vmatrix} k_3(a)_o & 0 \\ k_2 & m \end{vmatrix}$$

$$-(k_{-1}(d)_o(k_1(a)_o) \begin{vmatrix} m-(k_{-3} \quad +k_4) & 0 \\ k_4 & m \end{vmatrix}$$

$$+(k_{-1}(d)_o(k_{-3}(d)_o \quad \begin{vmatrix} 0 & 0 \\ 0 & m \end{vmatrix} = 0$$

$\therefore$ $[m-k_1(a)_o][m-(k_2+k_{-1}(d)_o+k_3(a)_o)][m-(k_{-3}+k_4)]m$

$-[m-k_1(a)_o](k_{-3})[k_3(a)_o]m$

$-(k_{-1}(d)_o(k_1(a)_o)[m-(k_{-3}+k_4)]m = 0$

(Note: Flack does not cancel these m's but instead finds that one of the roots is zero; cancelling the m's gives the same results with all roots non-zero.)

$\therefore$ $[m-k_1(a)_o][m^2-(k_2+k_{-1}(d)_o+k_3(a)_o)m+(k_2+k_{-1}(d)_o+k_3(a)_o)$
$(k_{-3}+k_4)]$

$(-m(k_{-3})(k_3(a)_o) + k_1(a)_o(k_{-3})k_3(a)_o$

$-m(k_{-1}(d)_o k_1(a)_o) + k_{-1}(d)_o k_1(a)_o(k_{-3}+k_4)) = 0$

$\therefore$ $m^3-m^2(k_2+k_{-1}(d)_o+k_3(a)_o+k_{-3}+k_4)$

$+m(k_2+k_{-1}(d)_o+k_3(a)_o)(k_{-3}+k_4)$

$-k_1(a)_o m^2 + m\,k_1(a)_o(k_2+k_{-1}(d)_o+k_3(a)_o+k_{-3}+k_4)$

$-(k_1(a)_o)(k_2+(k_{-1})(d)_o+k_3(s)_o)(k_{-3}+k_4)$

$-m(k_{-3}k_3(a)_o+k_{-1}(d)_o k_1(a)_o+k_1(a)_o(k_{-3}k_3(a)_o+k_{-1}(d)\ )(k_{-3}+k_4) = 0$

i.e. coefficient of $\frac{m^2}{m} = 1$

$$= -(k_1(a)_o+k_2+k_{-1}(d)_o+k_3(a)_o+k_{-3}+k_4)$$

$k_2k_{-3}+k_2k_4+k_{-1}(d)_o k_{-3}+k_{-1}(d)_o k_4+k_3(a)_o k_{-3}$

$+k_3(a)_o k_4 + k_4(a)_o k_2 + k_1(a)_o k_{-1}(d)_o+k_1{}^n3(a)_o{}^2$

$+k_1(a)_o k_{-3}+k_1(a)_o k_4 - k_{-3}k_3(a)_o$

$-k_{-1}(d)_o k_1(a)_o$

$$= k_2(k_{-3}+k_4) + k_{-1}(d)_o(k_{-3}+k_4)$$

$$+ (a)_o(k_3k_4+k_1k_2 + k_1k_3(a)_o+k_1k_{-3}+k_1k_4)$$

$$= [k_2+k_{-1}(d)_o][k_{-3}+k_4] + (a)_o\ [k_3k_4+k_1k_2+k_1k_4+k_1k_{-3}+k_1k_3(a)_o]$$

$$\underline{m^o}$$

$$k_1(a)_ok_{-3}k_3(a)_o + k_{-1}(d)_ok_1(a)_ok_{-3}$$

$$+ k_{-1}(d)_ok_1(a)_ok_4 - k_1(a)_ok_2(k_{-3}+k_4)$$

$$-k_1(a)_ok_{-1}(d)_o(k_{-3}+k_4) - k_1(a)_ok_3(a)_o(k_{-3}+k_4)$$

$$= \underline{k_1(a)_ok_{-3}k_3(a)_o}+k_{-1}(d)_ok_1(a)_ok_{-3}+k_{-1}(d)_ok_1(a)_ok_4$$

$$-k_1(a)_ok_2k_{-3} - k_1(a)_ok_2k_4$$

$$-k_1(a)_ok_{-1}(d)_ok_{-3} - k_1(a)_ok_{-1}(d)_ok_4$$

$$-k_1(a)_ok_3(a)_ok_{-3} \qquad - k_1(a)_ok_3(a)_ok_4$$

$$= -k_1(a)_o[k_2(k_{-3}+k_4) + k_3(a)_ok_4]$$

Now if the three roots of the cubic equation are m_o, m_1, m_2 then

$$[m-m_o][m-m_1][m-m_2] = 0$$

$$\Longrightarrow [m-m_o][m^2-(m_1+m_2)m + m_1m_2] = 0$$

$$\Longrightarrow m^3 -(m_1+m_2)m^2 + (m_1m_2)m - (m_o)m^2 + (m_1+m_2)m_o\ m - m_om_1m_2 = 0$$

$$\Longrightarrow m^3 - m^2(m_o+m_1+m_2) + (m_om_1+m_om_2+m_1m_2)m-m_om_1m_2 = 0$$

Equating coefficients of m^3, m^2, m^1, m^o:

$$m_o+m_1+m_2 = k_1(a)_o+k_2+k_{-1}(d)_o+k_3(a)_o+k_{-3}+k_4$$

$$m_om_1m_2 = k_1(a)_o[k_2(k_{-3}+k_4) + k_3(a)_ok_4]$$

$$m_om_1+m_om_2+m_1m_2 = [k_2+k_{-1}(d)_o][k_{-3}+k_4]$$

$$+ (a)_o\ [k_3k_4+k_1k_2+k_1k_4+k_1k_{-3}+k_1k_3(a)_o]$$

if $m_2 \ll m_o$, m_1 (as reaction is monophasic)

(i.e. m_o and m_1 are associated with rapid equilibration)

then $m_o m_1 + m_o m_2 + m_1 m_2 \approx m_o m_1$

(and $m_o + m_1 \approx k_1(a)_o + k_{-1}(d)_o + k_3(a)_o + k_{-3} \quad + k_2 + k_4$

$\approx k_1(a)_o + k_{-1}(d)_o + k_3(a)_o + k_{-3}$ if k_2, k_4 small)

$$\therefore m_2 = \frac{m_o m_1 m_2}{m_1 m_2}$$

$$\approx \frac{k_1(a)_o[k_2(k_{-3}+k_4) + k_3(a)_o k_4]}{[k_2+k_{-1}(d)_o][k_{-3}+k_4]+(a)_o[k_3k_4+k_1(k_2+k_4)]+(a)_o^2 k_1 k_3}$$

$$\text{i.e. } m_2 \approx \frac{x(a)_o + y(a)_o^2}{z + v(a)_o + w(a)_o^2} \qquad (5)$$

where $x = k_1k_2\ (k_{-3} + k_4)$ (6)

$y = k_1k_3k_4$ (7)

$z = (k_2+k_{-1}(d)_o)(k_{-3}+k_4)$ (8)

$v = (k_3k_4+k_1k_2+k_1k_4+k_1\ k_{-3})$ (9)

$w = k_1k_3$ (10)

Equations (5) - (10) with symbols as defined at the start will be used in the text (chapter 7).

APPENDIX 8 : TABLES OF DATA FOR THE AUTOXIDATIONS OF THIOLS CATALYSED BY COBALT CORRINOIDS (DISCUSSED IN CHAPTER 8)

All experiments carried out at 25°C in solutions with an ionic strength of 0,1.

Table 1 : The effect of pH on the rate of O_2 uptake by B_{12a} + cysteine; $2x10^{-2}$M cysteine; $1x10^{-5}$M B_{12a};O_2 saturated buffers.

pH	initial rate - B_{12a} ($\mu MO_2\ s^{-1}$)	initial rate + B_{12a} ($\mu MO_2\ s^{-1}$)
4,0	0,01	0,02
6,0	0,03	0,07
8,0	0,03	0,11
8,5	0,15	0,92
9,0	0,17	1,52
9,5	0,14	1,61
10,0	0,15	1,73
10,5	0,14	1,52
11,0	0,20	1,34

Table 2 : Effect of the B_{12a} concentration on the rate of O_2 uptake by B_{12a} + cysteine in air saturated solutions containing $2x10^{-3}$M EDTA; pH 10,0; $5x10^{-3}$M cysteine

$10^5(B_{12a})$, M	rate, $\mu MO_2\ s^{-1}$
0,78	0,737
1,94	1,22
3,88	2,27
5,82	3,11
7,76	4,08

Table 3 : Effect of the cysteine concentration on both the rate of reduction of B_{12a} under N_2 and the rate of O_2 uptake in air saturated solutions at pH 10,0; $1{,}94\times10^{-5}$M B_{12a}; 25°C; μ = 0,1; 2×10^{-3}M EDTA

10^3 (cysteine), M	initial rate of O_2 uptake, $\mu MO_2\ s^{-1}$	$10^1\ k_{obs}$ for O_2 uptake, s^{-1} [a]	$10^2\ k_{obs}$ for reduction, s^{-1} [b]
2,5	0,688	0,35	
5,0	1,22	0,63	
7,5	1,66	0,86	
10,0	1,93	0,99	0,48
15,0	2,30	1,19	
20,0	2,91	1,50	
30,0	3,07	1,58	
40,0	3,55	1,83	
50,0	3,90	2,01	1,7
60,0	4,05	2,09	
80,0	4,22	2,18	3,0
100,0	4,40	2,27	3,6

[a] k_{obs} for O_2 uptake $= \dfrac{\text{initial rate of } O_2 \text{ uptake}}{(B_{12a})}$

[b] derived from the slope of the semilog plot (see chapter 6)

Table 4 : Effect of pH on the rate of O_2 uptake in the presence of B_{12a} and dithiothreitol; $1{,}94 \times 10^{-5}$M B_{12a}; 1×10^{-3}M dithiothreitol

pH	initial rate/μMO_2 s^{-1}
2,0	0,161
4,0	0,207
6,0	0,368
7,0	0,653
8,0	1,19
8,5	1,43
9,0	1,64
9,5	1,96
10,0	1,52
11,0	1,04
12,0	0,603 ; 0,575

Table 5 : Effect of the dithiothreitol concentration on the rate of O_2 uptake in the presence of B_{12a} and dithiothreitol; $1{,}94 \times 10^{-5}$M B_{12a}; pH 10,0; air saturated solutions.

10^3 (dithiothreitol), M	initial rate, $\mu M O_2\ s^{-1}$
0,5	0,667
1,0	1,29
2,0	1,95
4,0	3,35
6,0	4,33
10,0	6,03 ; 6,21
15,0	8,15
20,0	10,6 ; 10,7

Table 6 : Effect of the B_{12a} concentration on the rate of O_2 uptake in the presence of B_{12a} and dithiothreitol in air saturated solutions at pH 10,0

10^5 (B_{12a}), M	initial rate, $\mu MO_2\ s^{-1}$	
	1×10^{-3}M dithiothreitol	2×10^{-2}M dithiothreitol
0	0,143	-
0,388	0,465	4,42
0,776	-	6,04
1,94	1,52	10,8
2,91	-	14,3
3,88	2,62	19,0
7,76	4,65	-
11,6	6,75	-
15,5	9,02	-

Table 7 : The effect of pH on the rate of O_2 uptake by diaquocobinamide + thiols in O_2 saturated buffers; $1x10^{-7}$M diaquocobinamide; $2x10^{-2}$M thiol ; 25°C

pH	initial rate/μMO_2 s^{-1}					
	Ethanethiol		Mercaptoethanol		Cysteine	
	-Co	+Co	-Co	+Co	-Co	+Co
4	0,91	0,55	-	-	0,01	0,02
5	-	-	0,06	0,08	0,01	0,02
6	-	-	0,11	0,12	0,02	0,03
7	1,16	1,87	0,50	1,09;1,21	0,02	0,23
8	1,65	2,64	0,55	2,34	0,11	0,74
9,0	0,61	6.11	0,55	3,24	0,39	1,33
9,5	1,10	12,3	0,55	4,00	0,11	1,72
10,0	1,38	14,9	0,44	4,06	0,17	1,91
10,5	1,43	12,1	0,55	3,90	0,11	1,25
11,0	0,83	6,9	0,44	2,34	0,11	0,78

Table 8 : The effect of the diaquocobinamide concentration on the rate of O_2 uptake by diaquocobinamide + thiols in O_2 saturated buffers at the optimum pH; 2×10^{-2}M thiol; 25°C

	Rate, $\mu MO_2\ s^{-1}$						
10^7(DAC), M	Ethanethiol (pH 10)		Mercaptoethanol (pH 9,5)			Cysteine (pH 10)	
	initial -Co	initial +Co	initial -Co	initial +Co	max +Co	initial -Co	initial +Co
0,11	-	-	-	-	-	0,14	0,41
0,14	-	-	0,44	1,21	1,83	-	-
0,21	0,35	5,54	-	-	-	0,14	0,57
0,28	-	-	0,44	1,79	2,85	-	-
0,43	-	-	-	-	-	0,14	0,86
0,57	-	-	0,44;0,99	2,42	4,56	-	-
0,64	1,10	11,7	-	-	-	0,18	1,22
0,85	-	-	0,50	3,12	7,02	-	-
0,86	-	-	-	-	-	0,14	1,51
1,07	1,38	14,8	-	-	-	0,23	1,94
1,14	-	-	0,44	3,51	8,50	-	-
1,42	-	-	0,44	4,68	8,97	-	-
1,50	1,05	21,4	-	-	-	-	-
2,14	0,94;1,27	29,0;28,5	-	-	-	-	-

Table 4 : The effect of the thiol concentration on the rate of O_2 uptake by diaquocobinamide + thiols at the pH optimum in O_2 saturated buffers; 1×10^{-7} M diaquocobinamide

10^3(thiol) M	Rate, $\mu MO_2\ s^{-1}$							
	Ethanethiol (pH 10)			Mercaptoethanol (pH 9,5)			Cysteine (pH 10)	
	initial -Co	initial +Co	max +Co	initial -Co	initial +Co	max + Co	initial -Co	initial +Co
2,0	-	-	-	0,04	0,92	2,00	0,01	0,27
4,0	-	-	-	0,07	2,69	3,47	0,02	0,39
5,0	0,22	7,66	13,31	-	-	-	-	-
6,0	-	-	-	-	-	-	0,04	0,86
7,0	-	-	-	0,11	3,57	5,84	-	-
8,0	-	-	-	-	-	-	0,04	1,17
10,0	0,55	12,96	2,20	0,18	4,66	7,22	0,16	1,83
12,0	-	-	-	-	-	-	0,09	1,91
14,0	-	-	-	-	-	-	0,16	1,95
15,0	-	-	-	0,32;3,28	4,66;4,81	7,33	-	-
16,0	-	-	-	-	-	-	0,14	1,99
20,0	1,10	15,97	-	0,55	4,45	9,66	0,18	1,87
30,0	1,98	21,21	-	-	-	-	-	-
40,0	3,30	23,56	-	-	-	-	-	-
50,0	2,42	23,09	-	-	-	-	-	-
60,0	1,65	22,81	-	-	-	-	-	-
69,6	1,60	22,44	43,0	-	-	-	-	-
79,2	1,82	21,5	-	-	-	-	-	-
90,0	1,65	23,38	-	-	-	-	-	-
100,0	1,76	23,09	-	-	-	-	-	-

APPENDIX 9 : TABLES OF DATA FOR THE AUTOXIDATION OF DITHIOTHREITOL CATALYSED BY BIS-HISTIDINE HEMIN (DISCUSSED IN CHAPTER 9)

All experiments carried out in air saturated solutions with $\mu = 0,5$ at 25°C

Table 1 : The effect of dithiothreitol concentration on the rate of O_2 uptake catalysed by hemin + histidine; 6×10^{-6}M hemin; 0,4M histidine; pH 10,0.

10^3 (dithiothreitol), M	rate (initial), μ MO_2 s^{-1}
0,05	0,414
0,1	0,[illegible]
0,25	0,[illegible]
0,5	1,04 ; 1,01
0,75	0,897
1,00	0,722
3,05	0,621
5,00	0,543
10,0	0,520 ; 0,552
20,0	0,529

Table 2 : The effect of the hemin concentration on the rate of O_2 uptake catalysed by hemin + histidine at pH 10,0 in 0,4M histidine

10^6 (hemin) M	initial rate, $\mu MO_2\ s^{-1}$	
	low (dithiothreitol) ($3x10^{-4}$M)	high (dithiothreitol) ($5x10^{-3}$M)
0	0,561	0,299
2,52	1,02	-
3,02	1,06	-
4,05	-	0,405
6,04	1,12	-
8,10	-	0,507
12,1	1,62	0,888
16,2	-	1,15
18,1	2,08	-
20,25	-	1,51
20,66	-	1,82
24,16	2,42	-
28,36	-	1,93 (max 2,94)
30,20	3,06	-
34,44	-	1,96 (max 3,46)
40,52	-	2,11 (max 4,24)

Table 3 : The effect of the histidine concentration on the rate of O_2 uptake in the presence of hemin + histidine at low dithiothreitol concentration; ($3x10^{-4}$M); $26,3x10^{-6}$M hemin; pH 10,0

(histidine) M	initial rate (with hemin), $\mu MO_2\ s^{-1}$	initial rate(- hemin), $\mu MO_2\ s^{-1}$
0,20	2,17	0,515
0,30	2,34	0,639
0,40	2,20 ; 2,70	0,453 ; 0,561

REFERENCES

1. M. Hughes, 'The Inorganic Chemistry of Biological Processes', Wiley, London (1972).

2. J.M. Pratt, 'Techniques and Topics in Bioinorganic Chemistry', ed. C.A. McAuliffe, MacMillan, London (1975).

3. G.L. Eichhorn (ed) 'Inorganic Biochemistry' Vol. 2, 795. Elsevier, Amsterdam (1973).

4. P. Argos, F.S. Matthews, J. Biol. Chem., 250, 747 (1975).

5. F.R. Salemme, Ann. Rev. Biochem., 46, 299 (1977).

6. M.F. Perutz, Brit. Med. Bull., 32, 195 (1976).

7. T.L. Poulos, S.T. Freer, R.A. Alden, N.H. Xuong, S.L. Edwards, R.C. Hamlin, J. Kraut, J. Biol. Chem., 253, 3730 (1978).

8. R.E. White, M.J. Coon, Ann. Rev. Biochem., 49, 315 (1980).

9. J.M. Pratt, 'Inorganic Chemistry of Vitamin B_{12}', Academic Press, London (1972).

10. J. Shack, W. Clark, J. Biol. Chem., 171, 143 (1947).

11. D. Keilin, Proc. Roy. Soc., B100, 129 (1926),(footnote p.136).

12. W. Gallagher, W. Elliott, Biochem. J., 105, 461 (1967).

13. J. Simplicio, Biochem., 11, 2525 (1972).

14. J. Simplicio, K. Schwenzer, Biochem., 12, 1923 (1973).

15. P. Hambright, P.B. Chock, J. Inorg. Nucl. Chem., 37, 2363 (1975).

16. W. Gallagher, W. Elliott, Biochem. J., 108, 131 (1968).

17. S. Brown, P. Jones, A. Suggett, J. Chem. Soc. Faraday Trans., 64, 986 (1964).

18a B.M. Hoffman, D.H. Petering, Proc. Nat. Acad. Sci., U.S.A., 67, 637 (1970).

b G.C. Hsu, C.A. Spillburg, C. Bull, B. Hoffman, Proc. Nat. Acad. Sci. U.S.A., 69, 2122 (1972).

19. J.H. Bayston, N.K. King, F.D. Looney, M.E. Winfield, J. Amer. Chem. Soc., 91, 2775 (1969).

20. K. Smith (ed) 'Porphyrins and metalloporphyrins', Elsevier, Amsterdam (1975).

21. F.A. Cotton, G. Wilkinson, 'Advanced Inorganic Chemistry', 3rd ed., Wiley, London (1972).

22a M. Kastner, W. Scheidt, T. Mashiko, C. Reed, J. Amer. Chem. Soc., 100, 666 (1978).

b T. Mashiko, M. Kastner, K. Spartalian, W. Scheidt, C. Reed, J. Amer. Chem. Soc., 100, 6354 (1978).

23. M. Zobrist, G.N. La Mar, J. Amer. Chem. Soc., 100, 1945 (1978).

24. W. White in 'The Porphyrins', ed. D. Dolphin, Academic Press, New York (1978), vol. V, chapter 7.

25. R. Lemberg, J. Legge, 'Hematin Compounds and Bile Pigments', Wiley, New York (1949).

26. D.H. O'Keefe, C.H. Barlow, G.A. Smythe, W.H. Fuchsman, T.H. Moss, H. Lilienthal, W.S. Caughey, Bioinorg. Chem., 5, 125 (1975).

27. T.H. Moss, A. Bearden, W.S. Caughey, J. Chem. Phys., 51, 2624 (1969).

28. H. Goff, L. Morgan, Inorg. Chem., 15, 3180 (1976).

29. J. Fuhrhop, Angew. Chem. Int. Ed., 88, 704 (1976).

30a R. Foster, 'Organic Charge Transfer Complexes', Academic Press, New York (1969).

30b M. Slifkin, 'Charge Transfer Interactions of Biomolecules', Academic Press, New York (1971).

31a S. Brown, T. Dean, P. Jones, Biochem. J., 117, 733 (1970).

31b S. Brown, H. Hatzikonstantinou, Biochim. Biophys. Acta, 539, 352 (1978).

31c S. Brown, H. Hatzikonstantinou, D. Harries, Biochim. Biophys. Acta, 539, 338 (1978).

31d P. Jones, K. Prudhoe, S. Brown, J. Chem. Soc. Dalton Trans., 911 (1974).

31e S. Brown, H. Hatzikonstantinou, Biochem. Biophys. Acta, 544, 407 (1978).

31f S. Brown, H. Hatzikonstantinou, Biochem. Biophys. Acta, 585, 143 (1979).

32a G. Kams, W. Gallagher, W. Elliott, Bio-org. Chem., 8, 69 (1979).

32b S. Brown, M. Shillock, P. Jones, Biochem. J., 153, 279 (1976).

33a G.N. La Mar, D. Viscio, J. Amer. Chem. Soc., 96, 7354 (1974).

33b G.N. La Mar, D. Viscio, K. Smith, W.S. Caughey, M. Smith, J. Amer. Chem. Soc., 100, 8085 (1978).

33c D. Viscio, G.N. La Mar, J. Amer. Chem. Soc., 100, 8092, (1978).

33d D. Viscio, G. La Mar, J. Amer. Chem. Soc., 100, 8096 (1978).

33e D. Budd, G. La Mar, K. Langry, K. Smith, R. Mayyir-Mazhir, J. Amer. Chem. Soc., 101, 6091 (1979).

34. G. Blauer, H. Rottenberg, Acta. Chem. Scand., 17, 5216, (1963).

35. G. Blauer, A. Ehrenberg, Biochim. Biophys. Acta, 112, 496 (1966).

36. G. Blauer, B. Zvilichovsky, Arch. Biochem. Biophys., 127, 749 (1968).

37. D. Mauzerall, Biochem., 4, 1801 (1965).

38. J. Heathcote, G. Hill, P. Rothwell, M. Slifkin, Biochim. Biophys. Acta, 153, 13 (1968).

39a J. Cann, Biochem., 6, 3435 (1967).

39b J. Cann, Biochem., 8, 4036 (1969).

40. J. Keilin, Biochem. J., 37, (1943) 281.

41. C. Barry, H. Hill, P. Sadler, R. Williams, Proc. Roy. Soc. London Ser. A, 334, 493 (1973).

42. T. Yoshimura, T. Ozaki, Bull. Chem. Soc. Jpn., 52, 2268, (1979).

43. J. Wang, H. Yeh, D. Johnson, J. Amer. Chem. Soc., 100, 2400 (1978).

44a W. Scheler, P. Mohr, K. Pommerening, J. Behlke, Eur. J. Biochem., 13, 77 (1970).

44b H. Ollcott, A. Lukton, Arch. Biochem. Biophys., 93, 666 (1961).

44c J. Akoyunoglou, H. Ollcott, W. Brown, Biochem., 2, 1033 (1963).

44c R.J. Porra, E.A. Irving, A. Tennick, Arch. Biochem. Biophys., 148, 37 (1972).

45. P. Adams, D.Baldwin, C. Hepner, J. Pratt, Bioinorg. Chem., 9, 479 (1978).

46. B.B. Hasinoff, H.B. Dunford,D.G.Horne, Can. J. Chem., 47, 3225 (1969).

47. T.H. Davies, Biochim. Biophys. Acta, 329, 108 (1973).

48. J. Simplicio, K. Schwenzer, F. Maenpa, J. Amer. Chem. Soc., 97, 2319 (1975).

49. W. Hinze, J. Fendler, J. Chem. Soc. Dalton Trans., 15, 1469 (1976).

50. R. Little, K. Dymock, J. Ibers, J. Amer. Chem. Soc., 97, 4532 (1975).

51. T. Ozaki, T. Yoshimura, Inorg. Chim. Acta, 36, L421 (1979).

52a H. Goff, J. Amer. Chem. Soc., 102, 3252 (1980).

52b C.K. Chang, T.G. Traylor, Proc. Nat. Acad. Sci. U.S.A., 70, 2647 (1973).

52c M. Momenteau, M. Rougee, B. Loock, Eur. J. Biochem., 71, 63 (1976).

52d M. Momenteau, B. Loock, Biochim. Biophys. Acta, 343, 535 (1974).

52e P. Warme, L. Hager, Biochem., 9, 1606 (1970).

52f C.E. Castro, 4, 45 (1974).

53. A. Balch, J. Watkins, D. Doonan, Inorg. Chem., 18, 1228 (1979).

54. M. Momenteau, J. Mispelter, D. Lexa, Biochim. Biophys. Acta, 323, 652 (1973).

55. T. Yoshimura, T. Ozaki, Y. Shintani, H. Watanabe, J. Inorg. Nucl. Chem., B38, 1879 (1976).

56. G.N. La Mar, J.D. Satterlee, R.F. Snyde, J. Amer. Chem. Soc., 96, 7137 (1974).

57. C.E. Castro in 'The Porphyrins', ed. D. Dolphin, Academic Press, New York (1978), vol. V, chapter 1.

58. B.B. Wayland, J.C. Swartz, Inorg. Chim. Acta, 23, 221 (1977).

59a H. Ruf, P. Wende, V. Ullrich, J. Inorg. Biochem., 11, 189 (1979).

59b V. Ullrich, H. Sakurai, H. Ruf, Acta. Biol. Med. Ger., 38, 287 (1979).

59c H. Ruf, P. Wende, J. Amer. Chem. Soc., 99, 5499 (1977).

60. S. Tang, S. Koch, G.C. Papaefthymiou, S. Foner, R. Frankel, J. Ibers, R. Holm, J.Amer. Chem. Soc., 98, 2414 (1976).

61. H. Sakurai, S. Shimomura, K. Ishizu, Chem. Pharm. Bull., 25, 199 (1977).

62. P. Adams, M.Berman, D. Baldwin, J. Chem. Soc. Chem. Comm., 856 (1979).

63a H. Sakurai, S. Ogawa, Chem. Pharm. Bull., 27, 2171 (1979).

63b H. Sakurai, S. Shimomura, Y. Sugiura, K. Ishizu, Chem. Pharm. Bull., 27, 3022 (1979).

64. F. Nome, J. Fendler, J. Chem. Soc. Dalton Trans., 1212 (1976).

65. S. Patai (ed.), 'The Chemistry of the Thiol Group', Wiley, London (1974).

66. E. Loechler, T. Hollocher, J. Amer. Chem. Soc., 97, 3235 (1975).

67. D. Nelson, R. Peterson, M. Symons, J. Chem. Soc. Perkin II, 2005 (1977).

68. P.Chan, H.Bielski, J. Amer. Chem. Soc., 95, 5504 (1973).

69. B. James in 'The Porphyrins', ed. D. Dolphin, Academic Press, New York (1978), vol. V, Chapter 6.

70. E. Abel, J. Pratt, R. Whelen, P.J. Wilkinson, J. Amer. Chem. Soc., 96, 7119 (1974).

71. J.L. Peel, Biochem. J., 88, 296 (1963).

72a D.J. Cookson, T.D. Smith, J.F. Boas, P.R. Hicks, J.R. Pilbrow, J. Chem. Soc. Dalton Trans., 109 (1977).

72b J. Dvlansky, D.M. Wagnerova, J. Veprek-Siska, Collect. Czech. Chem. Commun., 41, 2326 (1976).

73. R. Jameson, A. Masters, J. Philp, Abstract no. 86, XXI international conference on coordination chemistry, Toulouse, France (1980).

74. P. George in 'Oxidases and Related Redox Systems', ed. T.E. King, H.Mason, M. Morrison, Wiley, New York (1965).

75. D. Behar, G. Czapski, J. Rabani, L. Dorfman, H. Schwartz, J. Phys. Chem., 74, 3209 (1970).

76. 'Handbook of Chemistry and Physics', Weast (ed), 55th edition, Chemical Rubber Co. Press (1974 - 1975).

77a D. Chin, J. Del Gaudio, G. La Mar, A. Balch, J. Amer. Chem. Soc., 99, 5486 (1977).

77b D. Chin, G. La Mar, A. Balch, J. Amer. Chem. Soc., 102, 4344 (1980).

78. D. Chin, A. Balch, G. La Mar, J. Amer. Chem. Soc., 102, 1446 (1980).

79. H. Sigel, B. Prijs, F. Rapp, F. Dinglinger, J. Inorg. Nucl. Chem., 39, 179 (1977).

80. M. Berman, C. Adnams, K. Ivanetich, J. Kench, Biochem. J., 157, 237 (1976).

81. L. Meites, T. Meites, Anal. Chem., 20, 984 (1948).

82. 'Biochemists' Handbook', C. Long (ed), E. & F.N. Spon Ltd., London (1971).

83a A. Albert, 'Heterocyclic Chemistry', Athlone Press, University of London (1959).

83b R. Robins, 'Heterocyclic Compounds', ed. Elderfield, Wiley, New York (1967), vol. 8, pp 244, 387.

84. M.V. George, V. Bhat, Chem. Revs., 79, 447 (1979).

85. W. Cowgill, W. Clark, J. Biol. Chem., 198, 33 (1952).

86. W. Rawlinson, Austr. J. Expt. Biol. Med. Sci., 18, 185 (1940).

87. D. Smith, R. Williams in 'Structure and Bonding', Springer-Verlag, Berlin, 7, 1 (1970).

88. B. Nair, W. Elliott, Bio-org. Chem., 4, 326 (1975).

89. P.Mohr, W. Scheler, Eur. J. Biochem., 8, 444 (1969).

90. A.B. Scott, H.V. Tartar, J. Amer. Chem. Soc., 65, 692 (1943).

91. S.B. Brown, I.R. Lantzke, Biochem. J., 115, 279 (1969).

92. G. Collier, J. Pratt, C. de Wet, C. Tshabalala, Biochem. J., 179, 281 (1979).

93. P. George, J. Beetlestone, J. Griffith, Rev. Mod. Phys., 36, 441 (1964).

94. K. Murray, Coord. Chem. Rev., 12, 1 (1974).

95. H. Polet, J. Steinhardt, Biochem., 8, 857 (1969).

96. A. Maehly, A. Åkeson, Acta. Chem.Scand., 12, 1259 (1958).

97. Y. Inada, K. Shibata, Biochem. Biophys. Res. Comm., 9, 323 (1962).

98. N. Allinger, M. Cava, D. de Jongh, C. Johnson, N. Lebel, C. Stevens, 'Organic Chemistry', Worth, New York (1971).

99. A. Maehly, Acta. Chem. Scand., 12, 1247 (1958).

100. T. Spiro, J. Strong, P. Stein, J. Amer. Chem. Soc., 101, 2648 (1979).

101. D. Lexa, J. Savéant, J. Zickler, J.Amer. Chem. Soc., 99, 2786 (1977).

102. R.G. Thorp, D. Phil. Thesis, Oxford (1967).

103. C.F.Bernasconi, 'Relaxation Kinetics', Academic Press, New York (1976) Chapter 9.

104. D. Thusius, J. Amer. Chem. Soc., 93, 2629 (1971).

105. D. Cavallini, R. Scandurra, E. Barboni, M. Marcucci, FEBS lett., 1, 272 (1968).

106. R. Birke, G. Brydon, M. Boyle, Electroanal. Interfac. Electrochem., 52, 237 (1974).

107. H. Rüdiger, Eur. J. Biochem., 21, 264 (1974).

108. D.A. Baldwin, V.M. Campbell, L.A. Carleo, H.M. Marques, J.M. Pratt, J. Amer. Chem. Soc., in press.

109. H. Goff, L.Morgan, Inorg. Chem., 15, 2069 (1976).

110. P. Birker, H. Freeman, J. Amer. Chem. Soc., 99, 6890 (1977).

111. J. Martinsen, M. Miller, D. Trogan, D.Sweigart, Inorg. Chem., 19, 2162 (1980).

112. G.M. Fleck, 'Chemical reaction mechanisms', Holt, Rinehart and Winston Inc., New York (1971).

113. R. Lemberg, J. Barrett, 'Cytochromes', Academic Press, London (1973).

114. R.F. Jameson, N.J. Blackburn, J. Chem. Soc. Dalton Trans., 6, 534 (1976).

114b R.F. Jameson, N.J. Blackburn, J. Chem. Soc. Dalton Trans., 16, 1596 (1976).

115. O. Farver, I. Pecht in 'The Copper Proteins', ed. T. Spiro, Wiley, New York, in press.

116a W. Wallace, W. Caughey, Biochem. Biophys. Res. Comm., 62, 561 (1975).

116b D. Eaton, K. Wilson, J. Inorg. Biochem., 10, 195 (1979).

117. J. French, C. Winterbourn, R. Carrell, Biochem. J., 173, 19 (1978).

118. E. Antonini, M. Brunori, 'Hemoglobin and myoglobin in their reactions with ligands', North Holland Publishing Co., Amsterdam (1971) Chapter 4.

119. G. Hanania, D. Irvine, M. Irvine, J. Chem. Soc. (A), 296 (1966).